Progress in Neurobiology Vol. 35, pp. 85 to 133, 1990
Printed in Great Britain.

0301-0082/90/$0.00 + 0.50

STOCHASTIC APPROACHES TO THE STUDY OF SYNAPTIC FUNCTION

RICCARDO FESCE

Bruno Ceccarelli Center for the Study of Peripheral Neuropathies and Neuromuscular Diseases—C.N.R. Center of Cytopharmacology, Department of Pharmacology, University of Milano, Milano, Italy

(*Received* 15 *January* 1990)

CONTENTS

1. INTRODUCTION

Many processes studied by neurobiologists display an apparently continuous and deterministic nature, but are actually generated by the summation of small elementary events. Sodium currents in the nerve axon, endplate potentials at the neuromuscular junction and receptor potentials in the photoreceptor are typical examples. Processes like these are more correctly regarded as discrete (quantal) in nature.

Furthermore, the elementary events do not occur deterministically, but rather at random, although their probability of occurrence may be constant or may vary with time, under different experimental conditions, in a deterministic way.

If the student wishes to go beyond a merely descriptive analysis of such processes, he must turn to a stochastic approach, which may disclose important clues as to the underlying mechanisms. The purpose of this work is to review some important contributions which have come from this kind of approach to our current knowledge of the mechanisms of synaptic transmission.

The processes and mechanisms involved in the transmission of signals between neurons have long been studied using the neuromuscular junction as a model synapse.

In their early studies, del Castillo, Katz and Fatt (Fatt and Katz, 1950, 1951, 1952; del Castillo and Katz, 1954a,b,c, 1956) recorded the membrane potential at the endplate, and demonstrated the spontaneous, random occurrence of small transient deflections in the endplate potential, reasonably uniform in amplitude at single neuromuscular junctions. These events were called miniature endplate potentials (MEPPs), because they were very similar to the endplate potential (EPP), i.e. the depolarization produced by the acetylcholine (ACh) secreted when the action potential invades the nerve terminal. Indeed, the amplitude of the endplate potential itself can be reduced under particular experimental conditions (e.g. low Ca^{2+} concentration) to values few times greater than the amplitude of the single MEPP. Under these circumstances the amplitudes of successive EPPs cluster around values which are multiples of the mean amplitude of MEPPs (Fig. 1). This indicates a "quantal" nature of the EPP, which is constituted by relatively uniform MEPPs occurring synchronously (del Castillo and Katz, 1954b; Boyd and Martin, 1956; Liley, 1956b; Dudel and Kuffler, 1961).

The asynchronous, spontaneous occurrence of MEPPs, as well as the synchronous, evoked release producing the EPPs, can be studied thoroughly by recording the membrane potential at the endplate. Both processes are profitably analyzed by employing stochastic approaches since they arise either from the *random occurrence* of unitary events (MEPPs) or from the synchronous occurrence of a *random number* of such events (EPPs).

The miniature endplate potential is produced by a depolarizing current (miniature endplate current, MEPC) flowing through the ion channels contained in the ACh-Receptor molecules (AChR), located on the endplate membrane. The relatively constant amplitude of the MEPP is due to the fact that ACh is released by the presynaptic terminal in multimolecular "packets" of relatively constant size, which in turn activate a relatively constant number of ACh receptors. The kinetics and conductance of the single AChR channel can be studied, and have been intensely examined, using the stochastic procedures known as noise analysis, or fluctuation analysis. This approach has yielded reliable estimates of the conductance of the AChR channel, of its kinetics of activation, opening, closing and inactivation, and of the number of ACh molecules which constitute a quantum. Furthermore, molecular leakage of ACh has been evidenced and measured through similar approaches.

In this review, the stochastic approach to the study of evoked quantal release will be dealt with first (Section 2) for historical reasons. However, noise analysis will be the main topic of the paper. Section 4 will be dedicated to the study of molecular transmitter–receptor–channel interactions by stochastic approaches and in Section 5 the application of stochastic principles to the analysis of asynchronous quantal release (either spontaneous or experimentally enhanced) will be reviewed at some length. Since many biologists, and among them some neurobiologists as well, are rather frightened by the statistical and mathematical complexities of a stochastic approach, an appendix has been included to review, in part unrigorously but I hope in a way that can be grasped by the profane, the basic theoretical principles involved.

2. RELEASE OF NEUROTRANSMITTER EVOKED BY NERVE STIMULATION

2.1. QUANTAL NATURE OF ACETYLCHOLINE RELEASE AT THE ENDPLATE

The classical studies of Katz, Fatt and del Castillo in the 1950s demonstrated the occurrence of small transient changes in the membrane potential at the endplate. As these transients resembled the much higher deflections produced by the stimulation of the nerve and which give rise to the postsynaptic spike, they called these events miniature endplate potentials (MEPPs). MEPPs were interpreted as arising from

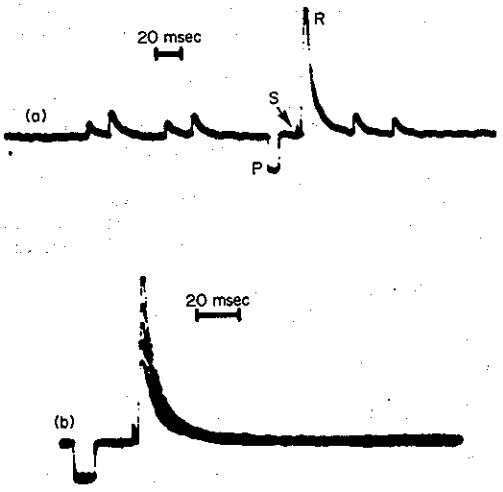

FIG. 1. Intracellular recordings of EPPs and MEPPs at a frog neuromuscular junction. Trace (a) shows several MEPPs and an EPP (R) in response to a stimulus delivered to the nerve (S = artifact due to the stimulus). The calibration pulse (P) is 1 mV · 10 ms. In (b), five EPPs from the same junction are superimposed, to emphasize the stepwise changes in their amplitude, with a size of the steps comparable to the amplitude of MEPPs in (a).

the spontaneous release of neurotransmitter from the resting motor nerve endings. Detailed studies of their amplitude, in the frog by del Castillo and Katz (1954b), in mammals by Boyd and Martin (1956) and Liley (1956a), and in crayfish by Dudel and Kuffler (1961), showed that they constituted elementary events with rather uniform amplitudes, and that the summation of a certain number of such events gave rise to the endplate potential (EPP). This theory was named quantal theory of neurotransmitter secretion and it was further substantiated by many statistical studies of the amplitude of endplate and postsynaptic potentials in many preparations. Basically, the idea was that if an EPP is constituted by a certain number of quanta (MEPPs), then the amplitudes of successive EPPs should cluster around integer multiples of the MEPP amplitude. Since in reality MEPP amplitudes do not have a fixed value but are distributed continuously about a mean value, the distribution of EPP amplitudes is not expected to be discrete; rather, it will be multimodal, with the various peaks located at values which equal integer multiples of MEPP mean amplitude. This was in fact the observed distribution (del Castillo and Katz, 1954b; Boyd and Martin, 1956). The statistical demonstration of the quantal nature of the EPP became so classic that the picture shown in Fig. 2, which illustrates the good fit of a statistically calculated distribution of EPP amplitudes to the experimental data, can be found in many textbooks as a neat demonstration of the theory.

2.2. STATISTICAL MODELS OF QUANTAL SECRETION

The purpose of this section is not to review in detail the published data on statistics of quantal release, as several excellent reviews are available on this topic (Katz, 1962, 1966, 1969; Martin, 1966; Vere-Jones, 1966; Hubbard, 1973; Krnjević, 1974; Ginsborg and Jenkinson, 1976; McLachlan, 1978); rather, the models employed to describe and interpret the statistics of evoked quantal release will be recalled and discussed with the main object of evaluating their consistency with experimental data and their capability of yielding information on the process and disclosing the cellular mechanisms involved.

2.2.1. *Poisson statistics*

The first statistical fits to the data of evoked quantal secretion were in agreement with Poisson statistics (see Appendix), i.e. they suggested the existence of a great many release sites (or releasable quanta), each with a very low probability of release. They were obtained under experimental conditions where the probability of release of quanta during the nerve response to an electrical stimulus was kept very low by lowering the extracellular concentration of Ca^{2+} and elevating the Mg^{2+} concentration.

The consistency of the Poisson statistical model could be assessed by estimating the mean number of quanta in the EPPs by two different approaches. In fact Poisson statistics predict that the proportion of failures, i.e. zero quanta in an EPP, will be e^{-m}, where **m** is the average number of events in a large series of trials; thus **m** can be computed from the logarithm of the ratio between number of trials and number of failures. The average number of events can be on the other hand estimated directly by counting the number of quanta constituting each EPP. This can be done sometimes rather easily, for very low values of **m**, when the stepwise changes in endplate potential amplitude are rather clear, but it can always be done, based on the additivity of the mean (Appendix) by taking the ratio between the average amplitude of the EPP and the mean MEPP amplitude. Good consistency was always obtained, for low quantal contents, between these approaches, and with the results of the "variance method" described below (del Castillo and Katz, 1954b). As illustrated in Fig. 2, the whole distribution of EPP amplitudes could be well fit by the theoretical distribution predicted by the single parameter **m** and the coefficient of variation of MEPP amplitudes.

2.2.2. *The binomial model of quantal release*

Poisson statistics represent a particular case of the more general binomial statistics (see Appendix), and it is obtained when the probability of release becomes very low, approaching zero. With more elevated probability of release, binomial statistics, based on the assumption of a finite number of release sites (or releasable quanta), **n**, each with the same probability of release, **p**, should be used to describe the distribution of endplate potentials. From this kind of analysis, interpretations of physiological relevance were proposed. In fact the number of possible events, **n**, resulted as being always rather low ($\lesssim 1000$). In the original interpretation it was thought that the Poisson model could reflect the existence of a very high number of release sites (del Castillo and Katz, 1954b), or releasable quanta, possibly associated with the very numerous synaptic vesicles (De Robertis and Bennet, 1954) that could be seen in the presynaptic terminal, each having a very low probability of being released (del Castillo and Katz, 1956). However, this number lower than 1000 is more consistent with the idea of a limited number of release sites, or of a small fraction of the quanta constituting a population of readily releasable quanta (Liley and North, 1953). The number of a few hundred in the frog neuromuscular junction, in particular, could be related to the number of active zones (in the order of 600 per terminal in the frog), the specialized membrane areas where the fusion of vesicles generally occurs (Birks *et al.*, 1960; Couteaux and Pécot-Déchavassine, 1970), so that neurotransmitter is released directly opposite to the postjunctional folds whose shoulders have the highest concentration of acetylcholine receptors (Salpeter and Eldefrawi, 1973). Thus the binomial parameters **n** may represent the few hundred active spots which could release a quantum of neurotransmitter in response to the nerve action potential; Poisson statistics would still be obtained for very low probabilities of release. The idea that **n** and **p** may have precise correlates in nerve terminal cellular physiology, however, is far from assessed.

The binomial model appeared particularly sensible as it could explain the effect of different Ca^{2+} concen-

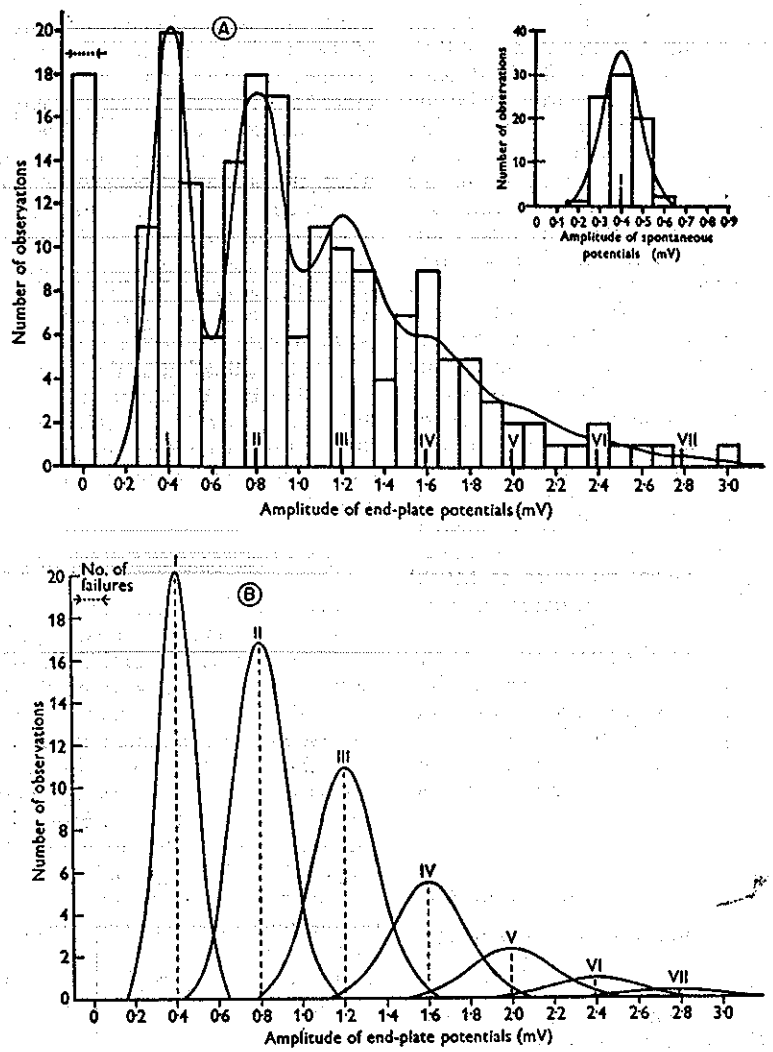

FIG. 2. A: Distribution of endplate potential amplitudes at mammalian neuromuscular junction blocked with Mg^{2+}. Peaks occur at multiples (I, II, III, etc.) of mean miniature potential amplitude (inset). First bar is number of failures. Smooth curve is theoretically expected distribution; arrows indicate expected number of failures. B: Method of construction of theoretical distribution in (A). m is estimated from mean [EPP]/mean[MEPP] = M/q and used in the Poisson equation to calculate expected number of failures (n_0), single responses (n_1), and multiple responses (n_2, n_3, etc.). These are then distributed normally around mean amplitudes q, $2 \cdot q$, $3 \cdot q$ with variances σ^2, $2 \cdot \sigma^2$, $3 \cdot \sigma^2$ (where σ^2 = variance of MEPP amplitude) and summed to produce smooth curve in (A). From Boyd and Martin (1956).

trations on evoked quantal release in terms of probability of release, the number of release sites remaining unchanged (del Castillo and Katz, 1954a; Katz and Miledi, 1965; Dodge and Rahamimoff, 1967; for reviews, see Silinsky, 1985; Cohen and Van der Kloot, 1985; Parnas and Segel, 1989). However, if **n** represents the releasable quanta, or the release sites occupied by a releasable quantum, there is no reason to assume that it must remain constant under various conditions and especially during repetitive stimulation (Zucker, 1973; Vere-Jones, 1966). A series of problems arise in attempting this kind of correlation, in particular when quantal content is not kept artificially low. The first such problem stems from the nonlinearity of the conductance–voltage relation at the endplate.

Nonlinearity

As the depolarization of the endplate reduces the driving force across the AChR channel, the voltage change produced by a fixed change in conductance is different at different membrane potentials, and contributions of additional steps in conductance are smaller when they add to a greater initial conductance. This produces a nonlinear relation between EPP amplitude and the underlying change in conductance. A very simple DC membrane model can be devised to predict the nonlinearity of the conductance–voltage relation and to recover the value of the conductance change from the voltage measurements (see Fig. 13). This approach was followed by Martin (1955), who proposed a correction factor for nonlin-

earity that became classic and was widely applied in many experimental studies. However, Martin's correction factor turned out not to be sufficiently accurate, due to the effect of membrane capacitance. In fact, the EPP is rather fast with respect to the time constant of the endplate membrane, so that the EPP peak amplitude is not solely determined by the change in conductance; it is also partly dependent on the charging of the membrane capacitance, which tends to reduce nonlinearity in the conductance–voltage relation. In other words, Martin's correction over-corrects for nonlinearity, and this was realized by Martin himself (1976), who proposed a modified correction factor, considering also the effects of capacitance; this correction appeared to be more accurate, and could be tailored to the particular synapse where one wishes to study the EPP amplitude: in particular it was studied for the mammal and frog endplate (McLachlan and Martin, 1981).

All these problems could in principle be bypassed by working on current measurements, under conditions of voltage clamp. Still, after all corrections or under voltage clamp, it appeared that binomial statistics might not constitute an adequate description of the distributions of EPP amplitudes obtained under various conditions.

Binomial fitting

The main criteria for fitting a binomial distribution to the EPP amplitude distribution are as follows: if each release site has probability $\mathbf{p}$ of releasing a quantum, then in the long run it will release an average of $\mathbf{p}$ quanta per trial, with a variance $\mathbf{p}\cdot(1-\mathbf{p})$ (see Appendix). If the release sites are independent, then a basic principle of the theory of probability predicts that the mean value and the variance of the sum of the outputs of $\mathbf{n}$ release sites will be $\mathbf{n}$ times the mean and variance of the output of a single site, i.e. $\mathbf{n}\cdot\mathbf{p}$ and $\mathbf{n}\cdot\mathbf{p}\cdot(1-\mathbf{p})$, respectively. Therefore, the ratio between variance and mean of EPP quantal content should give $(1-p)$, and

$$\mathbf{p} = 1 - \text{variance/mean}, \tag{1}$$

which is the classical equation of del Castillo and Katz (1954b). Rather strong limitations affect this simple model: the quantal content rather than the amplitude of the EPPs must be measured, and the experimental data are bound to depart from the ideal model if the release sites are not independent, if the probability of releasing a quantum is not the same for all sites or varies from trial to trial, and if the number of available quanta or release site changes with time. Furthermore, for low values of $\mathbf{p}$ the estimates of $\mathbf{n}$ become erratic, and only the single parameter $\mathbf{m}$ can be estimated (by assuming Poisson statistics), which makes systematic analysis of the parameters $\mathbf{n}$ and $\mathbf{p}$ problematic.

Estimating quantal content

The problem of estimating the quantal content in each EPP is not particularly hard at low quantal contents, when EPP amplitudes cluster around integer multiples of MEPP amplitude, and in general when MEPP amplitude can be measured. In this case, assuming that nonlinearities can be accurately corrected for, the quantal content, $\mathbf{m}$, equals the ratio between EPP and MEPP amplitudes. Estimating $\mathbf{m}$ becomes more complex when the amplitude of the MEPP cannot be measured, as is the case when EPPs with high quantal content (and amplitude) are examined in the presence of neuromuscular blocking drugs (curare). Under these conditions various approaches have been followed.

The pharmacological approach consists in deriving from a dose effect curve what is the fractional reduction in EPP amplitude produced by a fixed concentration of the blocking drug, and deducing the amplitude of the unmeasurable MEPP in the presence of curare from the MEPP amplitude measured before applying the drug (Ceccarelli *et al.*, 1973). Although the experimental error affecting this procedure may be acceptable in estimating the mean quantal content (and the approach was used to this purpose by Ceccarelli and colleagues), it would probably affect to different extents the estimates of the mean quantal content, and of its variance, so yielding unreliable information on the parameters and the adequacy of a specific statistical model.

The statistical approach consists of the so-called method of the variance (del Castillo and Katz, 1954b). In a Poisson system, with mean value $\langle m\rangle$, the variance in $\mathbf{m}$ is again $\langle m\rangle$ (see Appendix); the variance of the EPP, which is given by the sum of a variable number of MEPPs ($\mathbf{m}$, with average $\langle m\rangle$), apart from the variance of the recording noise, var[noise], equals $\langle m\rangle$ times the mean square value of the MEPP amplitude (see Appendix). Thus, indicating by q the mean quantal amplitude and by σ^2 its variance, we have:

$$\text{mean[EPP]} = \langle m\rangle\cdot q, \tag{2}$$

$$\text{var[EPP]} - \text{var[noise]} = \langle m\rangle\cdot(q^2+\sigma^2) = (\text{mean[EPP]})^2\cdot(1+\sigma^2/q^2)/\langle m\rangle \tag{3}$$

and

$$\langle m\rangle = (\text{mean[EPP]})^2 \times (1+cv^2)/(\text{var [EPP]} - \text{var[noise]}) \tag{4}$$

where $cv^2 = \sigma^2/q^2$ is the coefficient of variation of MEPP amplitudes.

This approach permits neglecting the absolute value of MEPP amplitude, q, and can be used in the presence of neuromuscular blockers. However, it suffers from two main drawbacks: it loses accuracy when the recording noise becomes significant with respect to the amplitude of MEPPs (as is the case with curare) and it is based on the assumption of Poisson statistics, which makes it unsuitable for testing a different statistical model. The approach was extended to binomial statistics by Kuno (1964): as the variance for a binomial process equals $n\cdot p\cdot(1-p) = \langle m\rangle\cdot(1-p)$ (see below and Section 8.2), Eqn 4 yields $m_1 = \langle m\rangle/(1-p)$; on the other hand the estimate of m from the logarithm of the ratio of the number of trials to the number of failures yields, for a binomial process, $m_2 = -\mathbf{n}\cdot\log(1-p)$.

Therefore the ratio m_1/m_2 equals $-p/(1-p)/\log(1-p)$; this yields **p**; $\langle m \rangle$ is then computed as $m_1 \cdot (1-p)$.

2.2.3. *"Generalized" binomial statistics*

Even in the particularly lucky conditions where the quantal content of the EPPs can be measured with accuracy, as mentioned above, the ideal binomial model will yield grossly biased estimates of **p** and **n** in the presence of correlation among release sites, or if the probability of releasing a quantum is not the same for all sites (nonuniform release) or varies from trial to trial (nonstationary release), or if the number of available release sites changes with time (Brown *et al.*, 1976; Barton and Cohen, 1977). Perkel and Feldman (1979) examined a series of possibilities and obtained equations for deriving the bias error in estimates of **p** in a generalized binomial model, taking into consideration spatial variance in **p** (different probability of release from different sites, or classes of sites), temporal variance in **p** (different probability from trial to trial) and variance in **n** (the number of sites or classes of sites). A more elementary derivation was reported by Miyamoto (1986) considering only spatial variance among sites, and a similar derivation for both spatial and temporal variance in **p** (unpublished results) is reported in the Appendix.

The main results for a generalized binomial model are as follows: the variance in **p** *reduces* the variance of quantal content, **m**, by a factor $n \cdot \mathrm{var}[p]$ with respect to a system with fixed **p** for all sites; however, temporal variance in **p** introduces a variance in the expected value of **m** among different trials, equal to $n^2 \cdot \mathrm{var}_t[p]$ so that, if $\mathrm{var}[p]$ is decomposed into spatial and temporal components, $\mathrm{var}[m]$ is increased by $\mathbf{n} \cdot (\mathbf{n}-1) \cdot \mathrm{var}_t[p] - \mathbf{n} \cdot \mathrm{var}_s[p]$; a variance in the number of sites, **n**, with time, also contributes variance to the expected value of **m** in different trials, so further increasing the variance (Perkel and Feldman, 1979).

From these observations it is clear that the use of the classical equation to derive **p**, $p = 1 - \mathrm{var}[m]/\langle m \rangle$, yields biased estimates of **p**; in particular **p** will be *overestimated* in the presence of *spatial variance alone*, but it will generally be *underestimated* in the presence of *temporal variance* in **p** and/or **n**. In fact, the bias factors linked to temporal variations are of higher order of magnitude than the one linked to $\mathrm{var}_s[p]$, if $\mathbf{n} \gg 1$, as is usually the case. Actually, even negative values were often obtained for **p** by the use of Eqn 1.

Due to this series of problems, the binomial nature of evoked quantal release is still under debate, and certainly we are far from being able to attribute a precise functional or structural meaning to the parameters **n** and **p** of the statistical model.

False consistency for wrong models

It may be useful here to consider what would happen in the presence of variance of **p** and **n** capable of reducing the value of **p**, as estimated by the binomial model (Eqn 1), to values much lower than the true one.

Let us call "extravariance", EV, the contribution of variance in **p** and **n** to the variance of quantal content. The measured variance will be $\mathrm{var} = \mathbf{n} \cdot \mathbf{p} \cdot (1-\mathbf{p}) + \mathrm{EV}$. Now suppose $\mathbf{p} = 0.5$ ($\mathrm{mean} = \mathbf{n} \cdot \mathbf{p} = 0.5 \cdot \mathbf{n}$), and $\mathrm{EV} = 0.4 \cdot \mathbf{n} \cdot \mathbf{p}$, so that **p**, as estimated by Eqn 1, will be $\hat{p} = 1 - \mathrm{var}/\mathrm{mean} = 1 - 0.9(np/np) = 0.1$. Small relative changes in the extravariance may easily bring $\hat{p}$ to 0.05 or 0.15, or even to zero or negative values. The consequent estimates of $\mathbf{n} = \mathbf{m}/\mathbf{p}$ will be, respectively, 1000% or 333% of the true value, or even infinity or negative. As $\hat{p}$ looks small and estimated **n** is erratic, the experimenter will turn to Poisson statistics, to find that $\mathrm{var} = 0.9 \cdot \mathrm{mean} \cong \mathrm{mean}$, in accord with Poisson statistics. The number of observed failures will probably be lower than the one predicted by Poisson law, as $(1-p)^n = 0.5^n < e^{-m} = e^{-n \cdot p} = (e^{-0.5})^n$, but the difference might not be astonishing and the distribution of EPP amplitudes probably will not contradict the Poisson hypothesis, unless a very high number of observations have been gathered. It is therefore possible that a binomial process contaminated by overlooked variance be interpreted as a Poisson process.

Under conditions where it seems that the binomial model can be maintained (estimated **p** not very small and, consequently, estimates of **n** not too erratic), estimates of **p** and **n** may be in substantial error, due to nonuniformity and/or nonstationarity of release. In a computer simulation study, Brown and colleagues (1976) pointed out that even in the presence of such substantial errors in the estimated parameters, the simple binomial model (with the wrong parameters) would still fit very well (no significant inconsistency by chi-squared tests) the experimental data under many conditions, so that errors due to nonuniform/nonstationary release would not be detected by comparing experimental and analytical histograms.

Use of higher moments

A very interesting approach to the whole question, which was not followed by many authors, was proposed by Courtney (1978), who extended the analysis to higher cumulants of the distribution. As it is the case for the mean and the variance, the values of other parameters of the distribution of EPP amplitudes can be measured and compared to the values predicted by the chosen statistical model, in order to check for its validity; conversely, if a particular statistical model is assumed to be valid, the knowledge of further parameters of the distribution allows the indirect derivation of more unknowns in the model. The skewness of the distribution, that is the average cubed departure from the mean, can for example be measured, and the knowledge of this parameter will allow determining not only **p** and **n**, but also the mean quantal amplitude when it cannot be measured, or the bias factor, due to variance in **p** and **n** in the estimate of **p** from the generalized binomial model. This approach was used by Miyamoto (1986) to derive unbiased estimates of **p** in a binomial model where spatial variance of **p** is included. In the Appendix the same procedure is developed, allowing also for *temporal* variance in **p**, which is presumably more effective in biasing the estimates of **p**.

Studies under repetitive stimulation

The study of quantal responses during repetitive stimulation of release offers the opportunity of investigating to greater depth and precision the statistical model of quantal release, although this approach implies more complex and apparently less direct analyses.

The decrease of the second EPP amplitude with respect to the first EPP, in response to pairs of stimuli delivered with short intervals ("depression"), was taken as an indication of partial depletion of the pool of readily releasable quanta (**n** in the binomial model) by the first response (Liley and North, 1953; Thies, 1965), which directly yields an estimate of the fraction of quanta released by the first stimulus (i.e. an estimate of **p** in the binomial model). Elmqvist and Quastel (1965) extended the analysis to the first few EPPs in response to high-frequency trains of stimuli and estimated **p** as the slope of quantal content versus the total number of quanta released by previous stimuli (assuming that **p** did not change during the train), and **n** as the ratio of the first quantal content to **p**, $n_0 = m_0/p$.

Although this approach seemed self-evident, several assumptions (including the assumed binomial model) are implicit in it; one basic assumption is that changes in **p** between the stimuli can be neglected; this is in contrast with the demonstration of facilitation of quantal release following stimulation, though this phenomenon was mainly observed at low levels of quantal release (Mallart and Martin, 1967) and its magnitude decreases at high calcium concentrations (see Parnas and Segel, 1989); furthermore, this assumption was directly disproved by Betz (1970) and Christensen and Martin (1970). Betz (1970) showed that the decrease in the second EPP amplitude is not linearly related to the amplitude of the first EPP (as expected if only the number of releasable quanta were reduced), but the relation is rather a quadratic one, suggesting that **p** is decreased about to the same extent as **n** (and $\mathbf{m} = \mathbf{n} \cdot \mathbf{p}$ is therefore reduced like n^2) as a consequence of release in response to the first stimulus. The author suggested that different quanta may have different probability of release and the most likely to be released are lost preferentially after the first EPP, thereby reducing the average **p** for subsequent stimuli. Christensen and Martin (1970) confirmed Betz's conclusions by measuring quantal content and estimating the parameters **n** and **p**, separately for the first and second EPP, in pairs of trials at different Ca^{2+} concentrations, on the assumption that this changed **p** but not **n**.

The regression of quantal content on total past release (Elmqvist and Quastel, 1965) can be combined with reduction of fluctuations by ensemble averaging over several trains of stimuli (Mallart and Martin, 1967). Although a procedure of this kind is more complicated, it permits neglecting the variance in quantal content, so overcoming problems of nonuniform probability of release; furthermore, it can be applied directly to EPP amplitudes rather than quantal contents, to investigate time-dependent changes in **n** (in relative terms) and **p**, during release at normal levels of Ca^{2+}.

2.3. QUANTAL RELEASE AT OTHER SYNAPSES

Early investigations of the quantal nature of neurotransmitter release in invertebrate ganglia were reviewed by Tauc (1967), and in central and ganglionic synapses of vertebrates by Kuno (1971). A general feature of central and ganglionic synapses is that several presynaptic fibres converge onto the same neuron. Whereas at the neuromuscular junction many quanta are released by a single terminal in response to electrical stimulation of the nerve, at central and ganglionic synapses activation of single presynaptic fibres usually produces small EPSPs and failures are very frequent. In these preparations release from single fibres generally follows Poisson statistics with low quantal content (Katz and Miledi, 1963; Kuno, 1964, 1971; Sacchi and Perri, 1971). However, when the electrical stimulation activates several afferent fibres, departures from Poisson statistics were sometimes observed in motor-neurons (Kuno, 1964), although this procedure should increase **n** but not **p**, and therefore should not shift the system from Poisson to binomial statistics. Martin (1966) suggested that this phenomenon might arise from some kind of interaction among presynaptic fibres. The alternative possibility existed that nonuniformity and/or nonstationarinity be responsible for departures from simple theoretical models (see above).

Specific difficulties arise in studying evoked release at central synapses, among which the difficulty in recognizing a unitary response from background synaptic activity in a cell that receives numerous distributed inputs, and the relevance of noise from various sources. Several procedures for extracting significant information from histograms of postsynaptic responses have been developed, and important advances have been achieved in this field since the introduction of the teleost Mauthner cell as a particularly suitable system for both pre- and postsynaptic intracellular recording. These aspects were reviewed in detail by Korn and Faber (1987). In that review article the experimental evidence, in favour of or against the binomial model of synaptic transmission, is discussed. Contrary to previous reports indicating that simple binomial statistics are inadequate for central transmission, and nonuniform probability of release for different sites is a more adequate model (e.g. Walmsley *et al.*, 1987), Korn and Faber reach the conclusion that the appropriate mathematical treatment of the noisy histograms of evoked response (by means of maximum likelihood procedures aimed at testing the adequacy of various statistical models) is consistent with binomial release. In particular, the binomial parameter **n** corresponds to the number of synaptic "boutons" where the presynaptic fibre contacts the postsynaptic neuron, as good consistency is observed between the statistically computed value of **n** and the histologically defined number of boutons. This would imply that each bouton is activated in an all-or-none fashion to release the content of one synaptic vesicle, so that **n** is by definition constant for a certain synapse, and **p**, the probability of release from each bouton, is the only factor that may change under different conditions (e.g. different frequencies of stimulation) in order to send the

postsynaptic neuron a particular message. Departures are observed from pure binomial behaviour, in that responses close to the average value are more frequent than predicted by binomial statistics; this phenomenon can be accounted for by a negative interaction among boutons which are located in close vicinity to each other, and in fact it is less prominent for synapses where boutons are more widely dispersed (Korn and Faber, 1987).

2.4. Conclusive Remarks on Evoked Release Models

The basic interpretation of the quantal nature of evoked neurotransmitter release, initially proposed by del Castillo and Katz (1954b) appeared self-evident, so that refinements in the model were introduced only when the possibility of nonuniform probability of release or of time-dependent changes in probability or number of release sites was explicitly taken into consideration (Vere-Jones, 1966; Zucker, 1973; Hatt and Smith, 1976; Brown *et al.*, 1976). It is now clear that many assumptions, implicit in the binomial model, may be (and in some instances actually are) incorrect. In spite of this, apparently meaningful estimates of the binomial parameters **n** and **p** are often obtained; these estimates may be in error of even orders of magnitude and still the inadequacy of the assumptions of the model may not become evident on inspection or estimation of the goodness of the fit (Brown *et al.*, 1976; Barton and Cohen, 1977). Thus, with the possible exception of the most recent procedures of analysis that consider the whole distribution, by maximum-likelihood approaches (Korn and Faber, 1987), or higher moments of the distribution and/or independent estimates of spatial and temporal variation in the binomial parameters (Perkel and Feldman, 1979; Miyamoto, 1986; see also in Appendix, Section 8.2), most of these approaches, so popular because apparently direct, are not "robust", i.e. they are very sensitive to explicit and implicit assumptions, to the point that no physiological meaning can be reliably attributed to the estimated parameters of the model.

Notwithstanding the complexity of the problem, the possibility of describing by a statistical model the process of evoked quantal release is still extremely attractive, because it may help in clarifying the mechanims underlying the Ca^{2+}-dependence of quantal release (Katz and Miledi, 1965; Dodge and Rahamimoff, 1967; for a review see Cohen and Van der Kloot, 1985), and in understanding regulatory processes in synaptic activity, like facilitation, depression and post-tetanic potentiation; though these phenomena have been intensely studied with various approaches (see for reviews Hubbard, 1973; Magleby, 1979) their mechanisms are still quite obscure, with the possible exception of the fast component of facilitation, presumably due to calcium that entered the nerve terminal during the previous action potential and has not been removed yet ("residual calcium", see e.g. Parnas and Segel, 1989).

3. NOISE ANALYSIS: BASIC PRINCIPLES AND CONSTRAINTS

One central concept of the theory of probability is the additivity of certain parameters of the distribution of independent random variables (quantities that may take on any one of a certain range of values, each with a certain probability). As it is more extensively discussed in the Appendix (Section 8.1) the mean and variance (and other statistics known as semi-invariants or cumulants) of the sum of several independent random variables are equal to the sums of the means and variances (and further cumulants), respectively, of the single random variables. The usefulness of this relation in the analysis of random processes was pointed out by Campbell (1909), who first demonstrated that several parameters of the elementary events giving rise to a noisy signal can be inferred from the mean and variance of the noise. He studied the electrical signal produced by the emission of electrons from radioactive material and showed that, if an average of N events occur in a period of time, T (i.e. the events occur with mean rate $r = N/T$), and the single event (shot) produces a transient bump with amplitude h and waveform $w(t)$, i.e. with area

$$A_1 = (h) \cdot \int w(t)\,dt,$$

then the mean value of each shot, A_1/T, will add up to yield the mean value of the composite signal,

$$M = N \cdot A_1/T = (N/T) \cdot h \cdot \int w(t)\,dt = r \cdot h \cdot I_1, \quad (5)$$

where I_1 is the duration of a square pulse, of amplitude h, equivalent to a single shot (equivalent duration of the shot).

Similarly, the variance of each shot (mean square value minus square of mean value) equals $A_2/T - (A_1/T)^2$, where

$$A_2 = h_2 \int w^2(t)\,dt$$

is the area under the square of a single shot, and the variances of all shots add up to yield the variance of the noise,

$$V = N \cdot [A_2/T - (A_1/T)^2] = (N/T) \cdot h^2 \cdot \left(\int w^2(t)\,dt - (1/T) \cdot \left[\int w(t)\,dt \right]^2 \right)$$
$$= r \cdot h^2 \cdot (I_2 - I_1 \cdot I_1/T). \quad (6)$$

I_2 is the "equivalent duration" of the square of the shot. Now, if we assume the frequency of the events, r, to be stationary, we can theoretically extend the time of observation to infinity. As T becomes much greater than shot duration I_1, (I_1/T) approaches zero, and the second term in the right hand side of Eqn (6) becomes null. For a stationary process we therefore have:

$$M = r \cdot h \cdot \int w(t)\,dt = r \cdot h \cdot I_1$$

$$V = r \cdot h^2 \cdot \int w^2(t)\,dt = r \cdot h^2 \cdot I_2. \quad (7)$$

Knowing $w(t)$, and therefore its integrals I_1 and I_2, it is easily deduced that

$$h = (V/I_2)/(M/I_1) \quad (8)$$

and

$$r = (M/I_1)^2/(V/I_2). \quad (9)$$

This derivation is known as Campbell's theorem (Campbell, 1909; for a more rigorous demonstration, see Rice, 1944), and it has been applied to a number of noisy signals, mainly in physical applications initially, and, during the last decades, in other fields and in biology as well. A stochastic process must obey some clearcut constraints to be amenable to noise analysis following Campbell's theorem. The main constraints are as follows: the shots must occur *at random* and at a *stationary mean rate*; they must sum up *linearly*; they must be *homogeneous* in amplitude and time course; they must *not be correlated.*

Rice (1944) extended Campbell's theorem to higher cumulants, demonstrating the general equation:

$$C_n = r \cdot h^n \cdot \int w^n(t)\,dt \quad (10)$$

where C_n is the n^{th} semi-invariant or cumulant (C_1 = mean, C_2 = variance, C_3 = skew, C_4 = kurtosis, etc.). He also extended the theorem to processes where the amplitude of the events is not uniform. In this case we have:

$$C_n = r \cdot \langle h^n \rangle \cdot \int w^n(t)\,dt \quad (11)$$

where $\langle h^n \rangle$ indicates the average value of h^n. Furthermore, he suggested that in cases where the expected frequency of occurrence of the shots changes with time, and many recordings of the same process are available, then averaging can be performed over the ensemble of records at each particular value of time. Thus time varying estimates of mean and variance can be obtained (Rice, 1944), and, if the frequency of occurrence changes slowly enough to be considered nearly constant during the time course of a single event, then Campbell's theorem can be applied to yield estimates of shot amplitude, $h(t)$, and rate of occurrence, $r(t)$, at each value of time (Sigworth, 1980, 1981a,b; Conti *et al.*, 1980, 1984).

Noise analysis can therefore be applied to signals generated by slowly nonstationary processes and where the shot amplitudes are not uniform. Nonlinear summation of the shots can be corrected for before the analysis (Martin, 1955) or alternatively the effect of nonlinearity on the measured statistics can be calculated and compensated for a posteriori (Katz and Miledi, 1972; Wong and Knight, 1980; Fesce *et al.*, 1986a,b). The procedure can be applied even when the mean signal drifts or is not reliable for any other reasons, as is often the case, thanks to Rice's (1944) extension of Campbell's theorem to higher cumulants (Segal *et al.*, 1985; Fesce *et al.*, 1986a,b; Rossi *et al.*, 1989). As described below in more detail, even fast nonstationarities and correlations in the process can be dealt with (Heiden, 1969; Schick, 1974; Wong and Knight, 1980; Fesce *et al.*, 1986a,b; Rossi *et al.*, 1989; Grzywacz *et al.*, 1988) in most cases. Thus, noise analysis has become a versatile tool for the study of processes in neurobiology that cannot be studied by any other approach.

3.1. THE SHOT WAVEFORM

Campbell's theorem, and its extensions to higher cumulants and nonideal situations, are often insufficient to extract useful information on stochastic processes. In most cases, in fact, the waveform of the single event is not known, because single shots cannot be seen in isolation, or there is reason to believe that their waveform may change during the process under study. It can be shown that the autocovariance of the noise shares the additive property of the cumulants. For any possible time interval (τ), the autocovariance $R(\tau)$ of a signal can be defined as the average value of the product (after subtraction of the mean) of a pair of measurements of the signal, taken τ seconds apart (see below the discussion of autocovariance of single channel noise). For $\tau = 0$, the autocovariance, $R(0)$, equals the variance of the signal and, for a single shot, it equals the integral of the square of $w(t)$. For τ greater than the duration of the single shot, the autocovariance for the single shot is zero (as at least one of the two values, τ sec apart, will be zero); thus, provided that the shots are independent and uncorrelated, the autocovariance of the signal will also be zero. For τ shorter than the duration of the shot, the autocovariance for a single shot with unit amplitude is a defined function of τ, in particular

$$R_s(\tau) = \int w(t) \cdot w(t+\tau)\,dt$$

and, for independent shots, the autocovariance of the signal will be the sum of the autocovariances contributed by each shot, yielding:

$$R(\tau) = r \cdot h^2 \cdot R_s(\tau) = r \cdot h^2 \cdot \int w(t) \cdot w(t+\tau)\,dt. \quad (12)$$

The shape of $R(\tau)$ is therefore the same as that of $R_s(\tau)$; thus, $w(t)$ can in general be derived from $R(\tau)$. In certain cases the same autocovariance function can be obtained from two or more different waveforms of the single event (for example, a square wave with random duration and mean duration τ has the same autocovariance as an exponential waveform with decay time constant, τ; however, there are usually reasonable criteria for choosing between the two possibilities (see also Section 8.5).

4. NOISE ANALYSIS AND THE STUDY OF ION CHANNELS

A major improvement has revolutionized, during the last decade, our approach to, and knowledge of, the electrical properties of excitable membranes; the development of the patch clamp technique (Neher and Sakmann, 1976a), which made possible the recording of ionic currents flowing across single ion channels located in a small patch of cell membrane ($\approx 1\,\mu m^2$). By this approach the conductance of an ion channel can be measured directly from the step changes which occur in the recorded current

when the ion channel opens; the selectivity of the channel can be investigated quite directly; the kinetics of the pore opening and closing can also be examined, and the molecular pharmacology of ion channels precisely defined in terms of the effect of drugs on conductance, probability of opening and closing, open channel lifetime, and state of activation.

Many of the pieces of information yielded by single channel recording can be obtained, and in fact some were obtained, at least for a few channels, before this technique became available, by the less direct approach of noise analysis.

4.1. General Principles and Applications

Under conditions of classical voltage clamp, the current flowing through all the ion channels in the cell membrane is recorded. As the ion channels continuously open and close independently in random sequence, the current can be considered as random noise, and the parameters of the channels are deduced from the statistics of the "noise". Two kinds of parameters are generally considered: descriptors of the probability distribution of the noise (the simplest are the mean value and the variance) and descriptors of temporal correlations or frequency composition of the noise (autocovariance function and power spectrum). As long as the events that generate the noisy signal are independent and randomly occurring, the parameters cited above are endowed with the property of additivity, so that the mean, variance and autocovariance of the noise will equal the sum of the corresponding parameters of the single events. It should be observed, however, that independence of the events implies that the possible events (in this case the number of channels that can be open) are so numerous that the opening of a few of them does not change the probability of further channel openings. This will occur only when many channels are present in the cell and a small percentage of them is open at any time, so that the probability of occurrence of one opening is always the same (i.e. the process is Poissonian). If the number of channels is limited, or the probability of being open is high for each channel, then the probability of further openings will depend on the number of channels already open; under these conditions one should turn to the more general binomial statistics, where two parameters (n = number of channels, and p = probability of being open for each channel) determine the expected number of open channels, $m = n \cdot p$.

The probability distribution

In particular, the probability distribution of the recorded noise will behave as follows:

(A) For many channels and small probability of being open. A single opening of the channel generates a unitary current i with a certain mean lifetime τ (i.e. an average total current, $i \cdot \tau$); the mean value of the current noise will be $I = r \cdot i \cdot \tau$ where r is the number of openings per unit time; similarly, the square of the current through a single channel during one opening is $i^2 \cdot \tau$, so that the variance of the current noise will be $\sigma^2 = r \cdot i^2 \cdot \tau$ (Katz and Miledi, 1972). These observations hold if the number of channel openings per second (r) behaves as a Poisson random variable. In this case,

$$\text{var/mean} = \sigma^2/I = r \cdot i^2 \cdot \tau/(r \cdot i \cdot \tau) = i \qquad (13)$$

and

$$\text{mean}^2/\text{var} = I^2/\sigma^2 = r^2 \cdot i^2 \cdot \tau^2/(r \cdot i^2 \cdot \tau) = r \cdot \tau, \qquad (14)$$

i.e. the single channel current is easily computed, and the number of openings per second can be measured, from $r \cdot \tau$ (which is the mean number of open channels at any time), if τ is known (see below).

(B) For high p. If the number of channels (n) in the cell (or patch) is low, and/or the mean number of channels open ($r \cdot \tau$) is a relevant fraction of n, then r will not behave according to Poisson, but rather to binomial statistics. In this case the probability of being open, for any channel, p, can be equated to the ratio $r \cdot \tau/n$ (mean number of open channels divided by the total number of channels) and binomial statistics predict:

$$\text{mean current } I = (n \cdot p) \cdot i = r \cdot \tau \cdot i$$

and

$$\text{variance } \sigma^2 = n \cdot p \cdot (1-p) \cdot i^2 = r \cdot \tau \cdot (1 - r \cdot \tau/n) \cdot i^2.$$

The Eqns (13) and (14) directly follow from these as a particular case for $p \ll 1$, i.e. $r \cdot \tau \ll n$. From these equations a parabolic relation between current variance and mean current follows (Fig. 3):

$$\sigma^2 = I \cdot i - I^2/n = I \cdot i \cdot (1 - r \cdot \tau/n). \qquad (15)$$

When the channels are shut most of the time ($r \cdot \tau \ll n$) the curve approaches a straight line ($\sigma^2 \cong I \cdot i$) with slope $\sigma^2/I = i$:

$$i = \mathrm{d}\sigma^2/\mathrm{d}I \; \{I \to 0\}; \qquad (16)$$

when the channels are open half the time ($r \cdot \tau = n/2$), I has half its maximum possible value, $I_{1/2} = n \cdot i/2$, σ^2 has its maximum value, $\sigma^2_{max} = n \cdot i^2/4$, and the ratio $(I_2)^2/\sigma^2_{max} = (n^2 \cdot i^2/4)/(n \cdot i^2/4) = n$ yields the total number of channels; **n** is also obtained directly by rearranging Eqn 15:

$$n = I^2/(I \cdot i - \sigma^2); \qquad (15b)$$

finally σ^2 tends towards zero for $r \cdot \tau$ approaching n, and I approaching its maximum theoretical value $I_{max} = n \cdot i$, from which n can also be computed, knowing i. An important parameter for this system is the average fraction of channels open at any time, i.e. the probability for each channel of being open: $r \cdot \tau/n = 1 - \sigma^2/(I \cdot i)$.

This mathematical treatment of ion channel noise was developed by Sigworth (1980) who pointed out that consistency of data with the parabolic relation (15) can be considered as an indication that the ion channels under study have only two primary levels of conductance, corresponding to "open" and "shut" state.

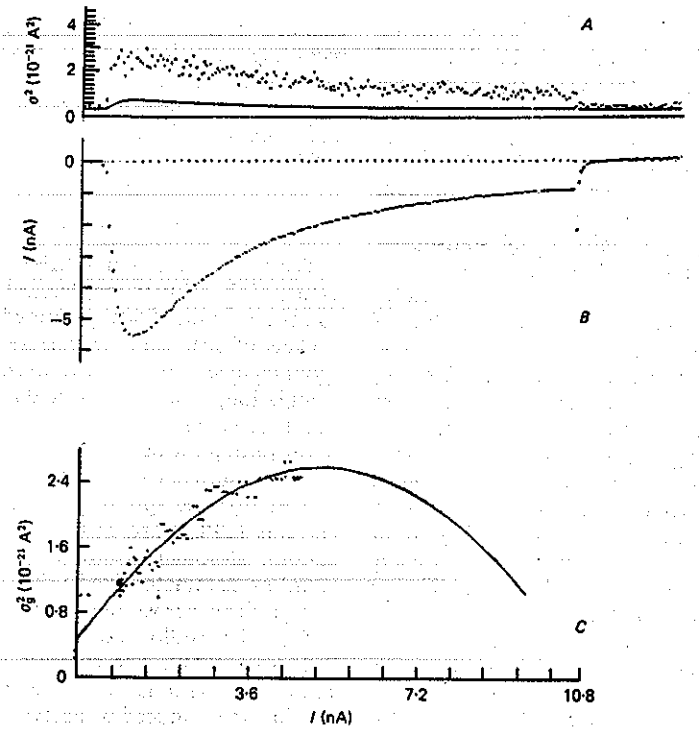

FIG. 3. Variance and mean sodium current in nodes of Ranvier. A: Variance calculated at each sample point (solid line represents background thermal noise variance). B: Time course of the mean current. C: Scatter plot of variance vs mean (each plotted point is the average of four samples). Solid curve is Eqn 15 (text) with $i = -0.55$ pA and $n = 20{,}400$. Scales are such that an initial slope of unity corresponds to conductance of 5 pS. From Sigworth (1980).

The autocovariance

The time dependence of the fluctuations in current also yields useful information. If conductances at two different times, separated by an interval Θ, are considered, the probability of finding one channel open at the time $t + \Theta$, given it was open at time t, will be maximum for very small values of Θ, will decay for increasing Θ (exponentially, with a time constant τ = mean lifetime of the channel) and will settle about a steady level, equal to the absolute probability of finding the channel open, for $\Theta \gg \tau$. The function describing this phenomenon is the autocovariance, $R(\Theta)$, computed as the expected value of the product (after subtraction of the mean) of two measurements of the signal separated by an interval, Θ. The autocovariance function of the single channel will be shared also by the composite noise, apart from a scaling factor again equal to the rate of the elementary events (openings of the channels), for Poissonian behaviour, or to $(1 - r \cdot \tau/n) \cdot r$, when many channels are open at any time. The mean lifetime, τ, of the channel responsible for a noisy conductance (or current) signal can therefore be deduced from the shape of the autocovariance function. The frequency of openings can then be deduced, from the mean of the noise, I, the unitary conductance, i, and the mean lifetime, τ:

$$r = I/(i \cdot \tau). \qquad (17)$$

When the binomial model is used, a further parameter can be estimated:

$$r/n = (1 - \sigma^2/Ii)/\tau \qquad (18)$$

which represents the frequency of openings of a single channel (opening rate constant).

The approach outlined above for the Poisson model was employed first by Katz and Miledi (1972), though in a slightly more complicated form as they recorded voltage rather than current, and by Anderson and Stevens (1973), who studied the features of the elementary events underlying the electrical noise produced by ACh at the endplate. The approach has become a standard since then, and has yielded plenty of information on many ion channel types (see, for reviews, Conti and Wanke, 1975; De Felice, 1977; Neher and Stevens, 1977; Hille, 1984; Ruff, 1986).

Violation of constraints

Interestingly, noise analysis is based on a series of constraints which can seldom be verified and are often grossly violated by the noisy biological processes under study. The central assumption is that noise is produced by the summation of events which are uniform and occur independently, at random, at a stationary rate.

Independence and random occurrence cannot be neatly demonstrated, in general, and the absence of noticeable correlations together with good adherence to the theoretical expectations is usually considered as a heuristic counterproof that the process is Poissonian in nature. It should be observed that this is not incorrect, in principle, as correlations or nonrandom features in the noise, that are not detected by statistical approaches are, by definition, not statistically significant, which means that they are not able to influence the process to such an extent that it deviates *detectably* from purely random behaviour. In fact, if significant correlations occur, they must be detectable at least in the power spectrum (see, e.g. Heiden, 1969). The assumption of stationarity can be, and has often been, bypassed thanks to the availability of ensembles of recordings with the same time course of the process (Sigworth, 1980; Conti *et al.*, 1980). The question of uniformity of the events is probably the more difficult to deal with: openings may result from different states of the ion channel so producing different classes of conductance and/or mean lifetime of the open state. All equations derived above for ion channels noise hold on the assumption that the channels exist only in 2 possible states: open with fixed conductance, and shut with zero conductance. This has been shown not to be the case for most channels, and this aspect has been clarified in many instances by single channel recording (see below).

4.2. Ligand Gated Channels: The Nicotinic Acetylcholine Receptor

As in this review we are concerned with the study of synaptic function, the next sections will be dedicated to channels implied in synaptic transmission (mainly the acetylcholine receptor, AChR). In the study of these channels the limitations of noise analysis are rather severe. In fact the existence of several shut states for the channel (at least unbound and ligand-bound) is to be assumed for these channels, and a behaviour like the one schematically represented in Fig. 4 is to be expected (Colquhoun and Hawkes, 1977, 1981; Milne *et al.*, 1986).

A bursting behaviour, with rapid closures within a burst and longer gaps between bursts, has in fact been described for AChR (Sakmann *et al.*, 1980; Colquhoun and Sakmann, 1981, 1985; Auerbach and Sachs, 1983) and other ligand gated channels (see Ruff, 1986). Under these conditions the noise is dominated by the bursts, rather than by the single openings, which yields to incorrect results of noise analysis: the "elementary conductance" and "lifetime" of the single channel and the number of openings, as estimated from the statistics and the power spectrum (or autocovariance) of the noise, will actually represent the average conductance during a burst of openings of a single channel (an underestimate of the true conductance as the channel is not open during the whole burst duration), and the average duration and the number of bursts, rather than of single openings (Colquhoun and Hawkes, 1977, 1981).

Due to these drawbacks, noise analysis has been somewhat abandoned by students of ligand gated channels in favour of the analysis of single channel recordings, which has much evolved, meanwhile, so that it can be performed not only on single cells in culture, but also on preparations freshly isolated and even on whole tissue slices (Edwards *et al.*, 1989).

4.2.1. *Acetylcholine molecular noise*

The early description of MEPPs and of the quantal nature of the EPP, in the classical studies of Katz and coworkers in the 1950s, generated the hypothesis that packets of acetylcholine, released either at random, spontaneously, or synchronously, following nerve stimulation, interacted with the postsynaptic membrane producing the transient opening of aqueous pores through which ions could cross the membrane and generate a current. Voltage clamp studies demonstrated that the spontaneous (MEPCs) and evoked currents (EPCs) are carried rather unselectively by cations, although inward flux of sodium (and calcium) predominates due to the relevant electrochemical gradient across the membrane (Fatt and Katz, 1951; del Castillo and Katz, 1954c; Takeuchi and Takeuchi, 1960). The currents display an exponentially decaying time course, suggesting that either the conductance induced by acetylcholine is initially high and then declines with time, or, much more reasonably, many channels are opened by the ACh pulse and they close at different times (Katz and Miledi, 1972), while ACh leaves the receptor and is removed from the synaptic cleft by hydrolysis by acetylcholinesterase (AChE). The exponential decay would then reflect an exponential distribution of channel lifetimes, in accord with simple Poisson kinetics where the channel, once opened, has a fixed probability of closing. An alternative possibility could still be hypothesized, i.e. the channel remains open as long as ACh is bound, and a first order kinetic in ACh unbinding (and/or hydrolysis) is responsible for the exponential decay in the current.

A neat approach to this question was proposed by Katz and Miledi (1970, 1972) who applied noise analysis to intracellular recordings of potential, and focal extracellular recordings of current, during applications of ACh to frog endplates. They calculated that ACh opens membrane channels with conductance $\approx 10^{-10}\ \Omega^{-1}$, and a mean lifetime well in accord with the decay time constant of the EPCs ($\approx$ 1 msec at 20°C). They also showed that curare has little or no effect on the characteristics of the elementary events, whereas carbachol produces considerably briefer, and therefore less effective, current pulses than ACh. The same authors (Katz and Miledi, 1973a,b) studied the elementary events produced by ACh agonists like acetylthiocholine (producing 0.12 msec openings), decamethonium and suberyldicholine (1.65 msec openings) and showed that in the presence of prostigmine (to block ACh hydrolysis) the kinetics of channel gating by ACh appear unaffected though quantal changes are much prolonged, suggesting that either ACh binding/unbinding or the gating kinetics, but not ACh hydrolysis, determine the "open lifetime" of the channel. In the presence of a cholinesterase inhibitor the action of ACh was prolonged even more than expected from the

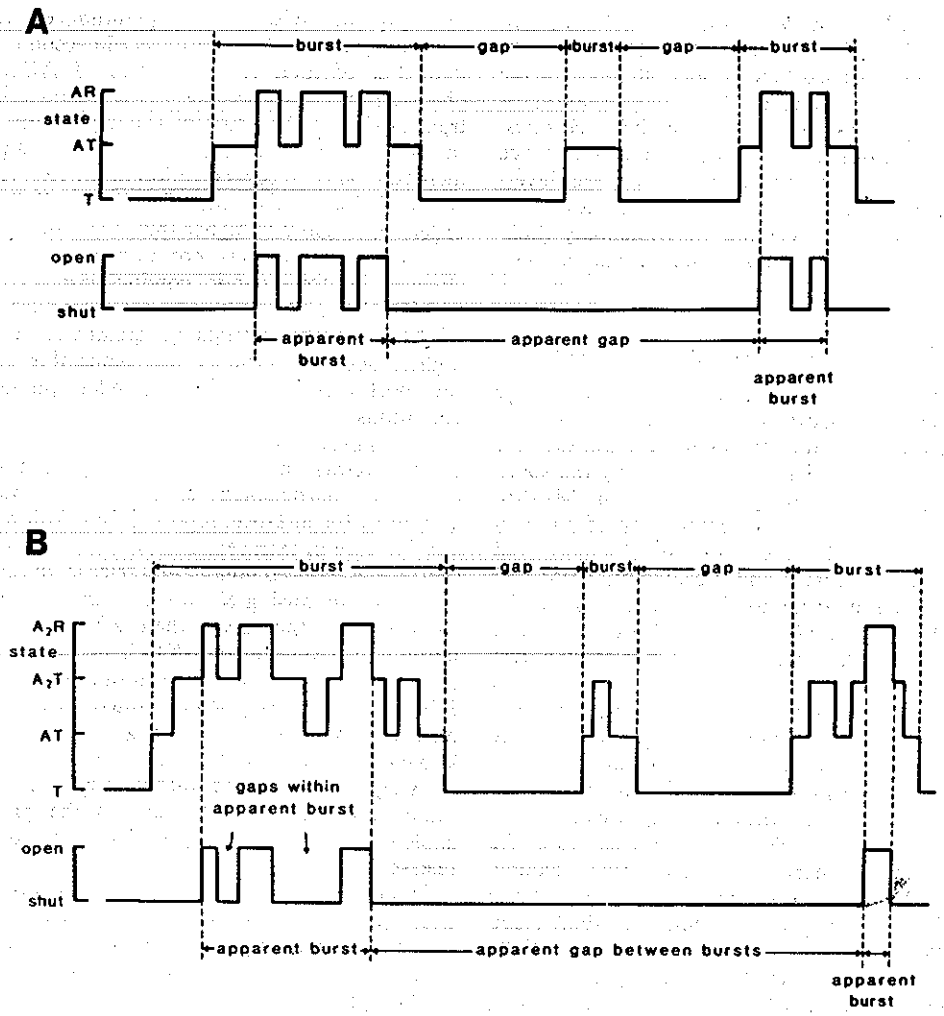

FIG. 4. A: Diagrammatic representation of possible behaviour of single channel, based on the scheme $R \rightleftharpoons AR \rightleftharpoons AR^*$ where A = agonist, R = receptor and * means activation (opening) of receptor–channel. B: Same as (A), based on scheme $R \rightleftharpoons AR \rightleftharpoons A_2R \rightleftharpoons A_2R^*$. In each panel the upper part shows the actual behaviour of the system; the lower part shows the corresponding appearance of single channel current. From Colquhoun and Hawkes (1981).

estimated kinetics of ACh diffusion out of the synaptic cleft, possibly due to ACh binding to the receptor and, under conditions of extracellular recording, to an apparent compression artifact which obstructs outward diffusion of the transmitter.

Several studies have been performed since, using this or similar approaches. Among the most important was the study by Anderson and Stevens (1973) who recorded frog endplate noise under voltage clamp and were able to corroborate by more direct evidence the conclusion that ACh noise arises from statistical fluctuations of conductance generated by ion channel gating; furthermore, they showed that single channels have a conductance of ≈ 30 pS and are characterized by a time constant equal to the decay time constant of the EPC (and MEPC), and equally dependent on membrane potential (the time constant increases exponentially with hyperpolarization). This study appeared to corroborate the suggestion that EPC decay time constant reflects the mean open lifetime of the channel (Magleby and Stevens, 1972a,b), which would indicate that channel gating kinetics dominate ACh noise, and therefore ligand binding, unbinding and hydrolysis must be fast with respect to channel opening and closing, the latter being the rate limiting process (Anderson and Stevens, 1973). This study soon became a classic, and the procedure of measuring EPC and noise time constants became the standard approach for studying the physiology and the pharmacology of the endplate AChR (Katz and Miledi, 1973a,b, 1978; Colquhoun *et al.*, 1975, 1977; Magleby and Terrar, 1975; Dreyer *et al.*, 1976; Ruff, 1977; Adams, 1977; Dionne and Ruff, 1977; Mallart and Molgo, 1978; Gibb and Marshall, 1984). The same procedure was applied at other synapses, like sympathetic and parasympathetic ganglia (Derkach *et al.*, 1983; Connor and Parsons, 1983) and glutamatergic or GABAergic neuromuscular junctions (Crawford and McBurney, 1976; Anderson *et al.*, 1976; Cull-Candy, 1986; Finger and

Stettmeier, 1981). However, with the development of the single channel recording technique, it became clear that the so-called "mean open lifetime" of the AChR channel is actually the mean duration of bursts of openings, interrupted by brief closures, either complete or incomplete, i.e. to subconductance levels (see below). This phenomenon has been investigated theoretically (Colquhoun and Hawkes, 1977, 1981; Milne *et al.*, 1986) and experimentally (Sakmann *et al.*, 1980; Colquhoun and Sakmann, 1981, 1985).

4.2.2. *Nonquantal release of acetylcholine*

Mitchell and Silver (1963) pointed out that a large discrepancy exists between the total amount of ACh released from innervated resting muscle and the very much smaller quantities accounted for by the spontaneous quantal discharge resulting in MEPPs. Estimates of the molecular composition of an ACh quantum are in the order of 10^4 (Fletcher and Forrester, 1975; Kuffler and Yoshikami, 1975) and quantal secretion accounts for about 2% of the resting release of ACh (Fletcher and Forrester, 1975). It was suggested that most of the ACh released at rest came from tissue other than the nerve terminal (Fletcher and Forrester, 1975). However, Katz and Miledi (1977) pointed out that a possible steady leakage of ACh from the nerve terminal could well exceed spontaneous quantal secretion by more than one order of magnitude without giving rise to electrophysiologically noticeable signals. Furthermore, the ACh contained in nerve terminals, which accounts for ≈65–80% of the total content in nerve–muscle preparations (Bhatnagar and MacIntosh, 1960; Hebb *et al.*, 1964; Miledi *et al.*, 1982), is only partially confined to synaptic vesicles, generally thought to constitute the quantum "container" (Zimmermann, 1979; Ceccarelli and Hurlbut, 1980a); 10–70% of it has been estimated to be free in the cytoplasm (Israel *et al.*, 1970; Whittaker *et al.*, 1972; Gorio *et al.*, 1978; Katz and Miledi, 1977; Miledi *et al.*, 1982). The possibility that ACh molecular leakage (nonquantal release) from the nerve terminal accounted for the discrepancy between total and quantal release at rest was directly addressed by Katz and Miledi (1977) with an electrophysiological approach and by Gorio *et al.* (1978) by intracellular recording combined with ACh bioassay. Both groups concluded that nonquantal release can exceed by about two orders of magnitude resting quantal release. In particular Gorio *et al.* (1978) estimated that quantal release of ACh contributes only ≈4% of total release from resting nerve terminals, but it is rather selectively increased by high K^+-stimulation; in 25 mM K^+ it accounts for ≈50% of total release. The approach used by Katz and Miledi (1977) was exclusively electrophysiological. They applied massive doses of curare iontophoretically to endplates treated with anti-esterase and recorded a small hyperpolarization (≈40 μV), corresponding to the hyperpolarization produced by the presence of about 10^{-8} M ACh in the synaptic cleft. From this value and the calculated parameters of diffusion of ACh out of the cleft, the authors estimated a molecular leakage rate of nearly 10^6 molecules/sec per endplate, as opposed to a typical resting quantal release of ≈1 quantum/sec ≈5×10^3 molecules/sec, which therefore would account for less than 1% of total resting release of ACh. These observations emphasize the phasic characteristics of transmission at the neuromuscular junction. In fact the release of a quantum of ACh temporarily increases the ACh concentration in the cleft to values ≈3×10^{-4} M (Kuffler and Yoshikami, 1975), i.e. 4 orders of magnitude higher than the estimated leakage concentration; this produces easily detectable changes in postsynaptic conductance (giving rise to MEPCs and MEPPs) whereas molecular leakage of ACh, which amounts to quantities ≈100-fold higher, does not produce any detectable effect on the postsynaptic membrane under physiological conditions.

The approach described above to measure nonquantal release has been extensively used since to define the pharmacology of the process. Vyskocil *et al.* (1983), for instance, reported that both reduction and increase in extracellular Ca^{2+} from normal concentrations reduced nonquantal release; the latter was unaffected by raising K^+ up to 13 mM and electrical stimulation of the nerve, whereas it was blocked by botulinum toxin and by SKF-525A, a drug known to increase AChR desensitization. More recently, Edwards *et al.* (1985) demonstrated that nonquantal release is blocked by the drug AH5183, which is known to inhibit the ACh transport system present in synaptic vesicles; the authors suggested that this same molecule, when present on the presynaptic axolemma, may be responsible for nonquantal release.

In all these studies the mean hyperpolarization over great numbers of endplates was considered, rather than applying Campbell's theorem in its full form by measuring the reduction in variance as well as the hyperpolarization produced by curare in the same fiber. Although the changes in variance may be too slight to be reliable, the latter approach would constitute a self-consistency test and yield information on the elementary conductance responsible for the hyperpolarization effect of curare. Available data, however, tend to confirm that activation of the normal AChR, by ACh which escapes in molecular form from the nerve terminal, is involved (Vyskocil *et al.*, 1983).

4.2.3. *Structure and function of the acetylcholine receptor channel*

Biochemical data indicate that the nicotinic acetylcholine receptor at the neuromuscular junction is constituted by five subunits, two of which (α subunits) are identical. The five subunits all span the cell membrane to constitute an ion channel which transiently opens in response to binding of two ACh molecules with specific sites located on the extracellular portion of the α subunits (see, e.g. Sakmann *et al.*, 1985; Changeux *et al.*, 1987, and the book edited by Maelicke, 1986).

The composition of the endplate receptor was thought to be $\alpha_2\beta\gamma\delta$, until the recent work of Mishina *et al.* (1986), who clarified that subunit ε is actually present in place of subunit γ in the endplate receptor, whereas subunit γ is present in the receptors of

embryonic and noninnervated muscle fibers (where they are not confined to the endplate region). The possibility that two different forms of the receptor were present in normal and noninnervated muscles had been suggested by a number of studies: starting from the observation of Katz and Miledi (1972) that in noninnervated muscles the mean "open lifetime" of the AChR channel is much longer, the properties of the different AChR channel were investigated by several groups by means of fluctuation analysis and single channel recording. The AChR channel in noninnervated muscle was shown to have a lower open-state conductance ($\approx 2/3$) and a 3–4 times longer "open lifetime" (Katz and Miledi, 1972; Neher and Sakmann, 1976b). Sakmann and Brenner (1978) demonstrated that a change in gating behaviour takes place during postnatal development and suggested that a fetal type of receptor becomes replaced by the adult-type during synaptogenesis. It is now generally accepted that the fetal form is the same form which predominates in noninnervated muscle (Schuetze and Role, 1987).

The adult-type AChR itself displays different channel gating kinetics and even different open-state conductances depending on the agonist that activates it (see, e.g. Colquhoun *et al.*, 1987). Detailed studies of the kinetics of AChR channel at the frog neuromuscular junction in response to ACh and various analogues (Sakmann *et al.*, 1980; Colquhoun and Sakmann, 1981, 1985) showed that the activation of the channel gives rise to bursts of openings separated by short closed periods (gaps).

This kind of behaviour had been predicted and investigated theoretically by Colquhoun and Hawkes (1977, 1981). Colquhoun and Sakmann (1985) showed that the mean burst duration depends on the agonist used (Fig. 5) and on membrane potential, and is equivalent to the previously so called "mean open lifetime" of the channel (Katz and Miledi, 1972; Anderson and Stevens, 1973). Gaps within bursts are several hundred-fold briefer than gaps between burst, on average; they were classified by Colquhoun and Sakmann (1985) as short and intermediate gaps. Both classes of gaps within bursts have mean duration that depend on the agonist used, but not on its concentration, or on membrane potential.

The bursting kinetics and the distribution of gap lengths led the authors to conclude that gaps originate from multiple openings of the doubly occupied channel, before dissociation occurs; this would imply opening (β) and dissociation (K_{-2}) rate constants consistent with the relative potencies of different agonists and with results at high agonist concentration, but inconsistent with the hypothesis that binding is much faster than channel opening; the estimated value for β was 36,000 sec^{-1} and that for $K_{-2} \approx$ was 8150 sec^{-1}, with a ratio opening/closing rate constant, $\beta/\alpha = 29$–43 depending on the agonist. Though the latter ratio is in agreement with direct estimates obtained by measuring the maximum frac-

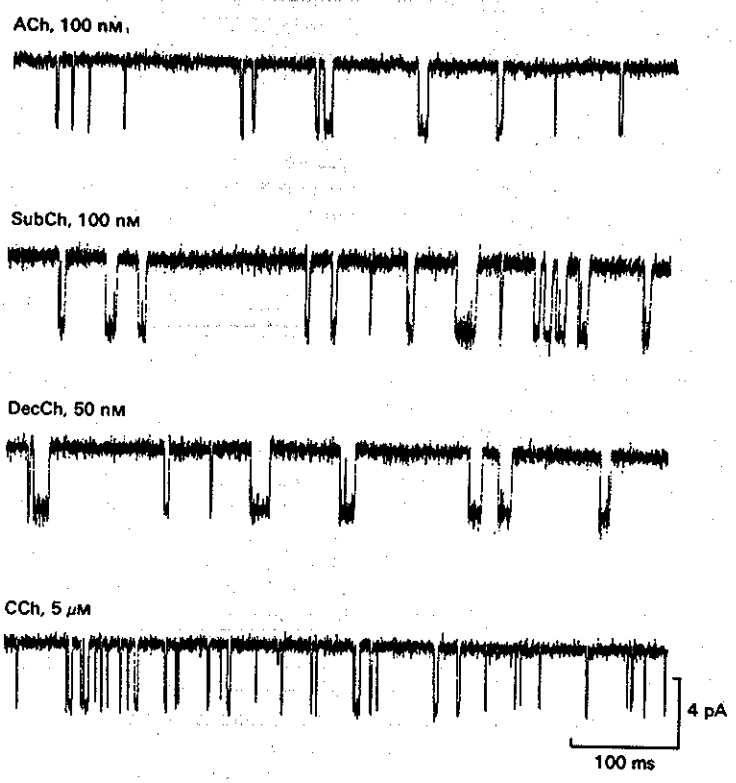

FIG. 5. Elementary currents activated by ACh and its analogues at the endplate, showing the differences in average duration of elementary bursts. Mean burst durations were: 4.2 ms for ACh, 7.4 ms for suberyldicholine (SubCh), 12 ms for decan-1,10-dicarboxylic acid dicholine ester (DecCh), 1.8 ms for carbachol (CCh). Membrane potential −120/−130. 9–10°C. From Colquhoun and Sakmann (1985).

tion of time spent in the open state in response to ACh, apart from desensitization (e.g. Sakmann *et al.*, 1980), much controversy still remains on the estimate of β, for which values ranging from 300 to 40,000 sec^{-1} have been reported (see Madsen and Edeson, 1988), using methods ranging from the quench-flow technique to measurement of MEPC rising phase and single channel recording. Overviews on the kinetic properties of the AChR channel can be found in Colquhoun and Ogden (1986) and Colquhoun *et al.* (1987).

Fine pharmacology

The different actions of acetylcholine-like drugs on the various aspects of the nicotinic receptor function generate a complex pharmacology for this receptor (Karlin *et al.*, 1986; Changeux *et al.*, 1987). In fact drugs can compete with different affinity for the ACh binding site and block the channel in the shut state, or favour its opening by modifying to a variable extent the rate constants for conformational changes (Katz and Miledi, 1973a) or even open the channel and then "plug" it. Drugs may also bind to high-affinity sites involved in AChR desensitization (Changeux *et al.*, 1987). Pure antagonism may follow, or more complex effects, which, depending also on the presence of the endogenous agonist, may consist in activation of the receptor, partial activation (the opening probability is increased less by the drug than by ACh, or the open time is decreased) with reduced response to ACh, or initial activation (opening of the channel) followed by block due to desensitization or to the drug entering the ion channel and plugging it. These aspects were reviewed by Colquhoun and colleagues (1987). The block of the channel (which is in general voltage-dependent) has been described for all agonists tested (even for ACh, though to the least extent), for a series of unrelated drugs like local anaesthetics (Ruff, 1977; Neher and Steinbach, 1978), and for many "pure" antagonists like gallamine and tubocurarine (see e.g. Katz and Miledi, 1978). The channel blocking capability of decamethonium is so high in certain muscles that it is not clear whether its apparently "partial" agonist action is due to genuine low ability of opening the channel or to this self-blocking action (Adams and Sakmann, 1978). The ion channel block by depolarizing agents may help explain the "dual" block induced by these drugs; this consists of initial depolarizing block of the receptor, not relieved by increased ACh release or by anticholinesterases but (partly) by curare, followed by apparently pure antagonistic block, relieved by increased ACh and anticholinesterases but worsened by curare (Zeimis, 1953).

The clinical pharmacology of nicotinic agonists and blockers is further complicated by the presence of presynaptic ACh receptors, both nicotinic and muscarinic, which appear to be able to regulate neurotransmitter release (see, for a recent review, Wessler, 1989).

Neuronal acetylcholine receptors

Most properties of the endplate acetylcholine receptors are not shared by nicotinic AChRs located on different structures. Since the work of Paton and Zaimis (1952) on the pharmacological differentiation of muscular and neuronal (ganglionic) nicotinic AChR, a huge amount of evidence has accumulated, especially during the last few years, on the pharmacological, structural and functional properties of neuronal AChRs. Most recent evidence is reviewed in the book edited by Clementi *et al.* (1988).

4.3. Other Ligand Gated Channels

The properties of many ligand gated ion channels were reviewed by Ruff (1986b). In recent years a good deal of information has accumulated on the structure, function and possible multiplicity of the $GABA_A$ receptor/channel complex (Stephenson, 1987; Schwartz, 1988; Olsen *et al.*, 1988; Sieghart, 1989). Its structural and sequence similarities with the AChRs have led to the notion of "ligand gated receptor superfamily" (Schofield *et al.*, 1987). This idea has been strengthened by the observation of conserved quaternary structure in the postsynaptic glycine receptor (Langosch *et al.*, 1988). The numerous noise-analysis and single-channel studies published recently on the electrophysiological properties of the subtypes of glutamate, of $GABA_A$ and of glycine receptor channels will not be reviewed here, as a systematic description of ion channels is not the object of this section.

The number of neurotransmitters that are recognized to activate directly ligand gated ion channels is increasing; the existence of receptor-operated calcium channels, which had long been postulated, was demonstrated in smooth muscle by Benham and Tsien (1987), who showed such a channel activated by ATP; furthermore, a histamine-activated chloride channel was recently described at arthropode photoreceptor synapses (Hardie, 1989), and the serotonin receptor, 5-HT_3, on neurons of the enteric plexus of mammals, has also been shown to be coupled to an ion channel (Derkach *et al.*, 1989).

5. NOISE ANALYSIS APPLIED TO THE ASYNCHRONOUS OCCURRENCE OF QUANTAL EVENTS AT HIGH FREQUENCY

The transmission of electrical signals across chemical synapses involves the release of relevant amounts of neurotransmitters, which interact with ligand gated ion channels with different specificities on the postsynaptic membrane, or with receptors capable of initiating biochemical cascades, generally by activating G proteins. However, as discussed above, transmitters are not generally released as single molecules, but rather in multimolecular packets (quanta). When the effect of a quantum of neurotransmitter can be detected, e.g. by a transient change in postsynaptic membrane potential, the study of the amplitude, frequency and pattern of occurrence of these elementary events yields useful information on presynaptic processes. In particular, the kinetics of quantal release, processes of facilitation, inhibition and modulation of release, and the mechanisms of generation and storage of the quanta of neurotrans-

mitter can be investigated, especially when quantal secretion is intense and prolonged. Under these conditions the effects of single quanta are generally superimposed, and the individual events cannot be recognized, counted or examined in isolation; noise analysis provides the means for studying their amplitude, time course and rate of occurrence.

The application of noise analysis to these kinds of processes will be reviewed with particular attention to three fields where the approach has provided new insights: (1) the study of photoreceptor potentials in arthropods, where the quantal events are transitory increases in membrane conductance (Fuortes and Yeandle, 1964; Adolph, 1964) generated by isomerization of the photopigment following the absorption of photons; this gives rise to depolarizing "bumps", whose summation constitutes the generator potential (Rushton, 1961); (2) quantal release of ACh at the neuromuscular junction; (3) quantal release at the labyrinthine cytoneural junction between the hair cell and the first afferent neuron.

The approaches employed in these studies are based on Campbell's theorem and spectral analysis, but important extensions and generalizations of noise analysis have derived from these applications.

5.1. General Principles

Campbell's theorem states that the mean and variance of a noisy signal generated by the summation of homogeneous shots occurring at random are linearly related to the mean rate of occurrence of the shots, r, and in particular are given by (Eqns 5 and 8):

$$M = r \cdot h \cdot \int w(t)\,dt = r \cdot h \cdot I_1$$

$$V = r \cdot h^2 \cdot \int w^2(t)\,dt = r \cdot h^2 \cdot I_2,$$

where h is shot height and $w(t)$ is the shot waveform. The integrals I_1 and I_2 have physical dimension of time and correspond to the "equivalent duration" of the shot and of its square, i.e. the duration of a square wave with height h (or h^2) and area equal to that under the shot (or under its square).

As was discussed in Section 3.1, these equations yield the values of r and h if the waveform $w(t)$ is known. Spectral analysis is used in these applications to extract information on $w(t)$ from the noise. It is based on the analogous principle that the autocovariance of the noise has the same shape as the autocovariance of the shot (see Sections 3.1 and 4.1), so that the power spectrum, which is a linear (Fourier) transform of the autocovariance function, also shares this property. Information on the waveform of the single shot can therefore be extracted from the power spectrum of the noise. A simple interpretation of power spectral analysis can be envisioned. The noise can be fed through a band-pass filter which eliminates all frequency components outside a narrow range (like the tuning of a radio receiver); the resulting noise is equivalent to the noise that would be generated by the process under study if the shots had a different waveform, $w_b(t)$, equal to $w(t)$ after filtering through the same band-pass filter. This implies that Campbell's theorem must hold for band-passed noise as well, i.e. the variance of the band-pass filtered noise is given by:

$$V_b = r \cdot h^2 \cdot \int w_b^2(t)\,dt = r \cdot h^2 \cdot W_b. \qquad (19)$$

But V_b is properly the part of the variance of the noise due to frequency components comprised within the pass-band of the filter, and for a narrow-band filter centered on the frequency f (with pass-band $= \Delta f$), $V_b/\Delta f = S(f)$ is the spectral density of the variance at frequency f; similarly, $W_b/\Delta f = W(f)$ is the energy spectral density of $w(t)$ at the frequency f, so that we may rewrite:

$$S(f) = r \cdot h^2 \cdot W(f). \qquad (20)$$

Equation 20 implies that the power spectrum of the noise, $S(f)$, must have the same shape as the energy spectral density of the single shot, $W(f)$, scaled up by the factor, $r \cdot h_2$, as was shown to be the case for the autocovariance (Eqn 12).

If the shot rate is not stationary, this will introduce further variance, and $S(f) \geq r \cdot h^2 \cdot W(f)$. It may be noticed that if r changes slowly with time its contribution to the variance will be confined to the low frequency range, leaving the high frequency region of the spectrum possibly unaffected (Schick, 1974; Sigworth, 1981b; Fesce *et al.*, 1986a,b). When ensembles of records of the same process are available, then the contribution of nonstationary r and/or h to the power spectrum can be virtually eliminated, by computing the spectrum on the difference between the value of each record and the ensemble average value at each time point (Sigworth, 1981b; Grzywacz *et al.*, 1988).

If correlations are present among the events, these may produce either increased (positive correlation) or reduced variance (negative correlation), and again correlations over long time periods will affect mainly the low-frequency region of the spectrum (Heiden, 1969; Wong and Knight, 1980).

Under these nonideal conditions the waveform of the shot cannot be deduced straightforwardly from the shape of the noise power spectrum; still, important information may be extracted, provided that the general features of $w(t)$ are known, so that fitting just a limited region of the spectrum may be sufficient (Wong and Knight, 1980; Fesce *et al.*, 1986a,b; Rossi *et al.*, 1989).

5.2. The Photoreceptor Potential

Depolarizing bumps observed in *Limulus* photoreceptors are thought to arise from isomerization of photopigment following the absorption of single photons (Fuortes and Yeandle, 1964; Borsellino and Fuortes, 1968). Single bumps can be observed in the dark, when cells are very dark-adapted; in very dim light their rate of occurrence increases proportionally to light intensity (Fuortes and Yeandle, 1964; Adolph, 1964). In response to higher light intensities a noisy depolarizing response is observed. Its main features are (Fig. 6): (i) the initial peak is followed by a plateau, (ii) the amplitude of the response is not linear with light intensity, but rather with its logarithm, and (iii) the amplitude of the noise at the

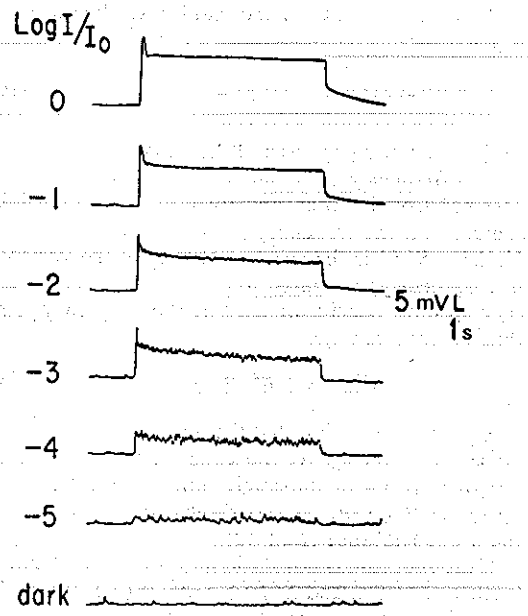

FIG. 6. Records obtained from an eccentric cell of *Limulus* showing the responses of a photoreceptor to light of various intensities (I_0 = intensity of the light emitted by light source without attenuation). The lowest trace shows spontaneous bumps occurring in a very dark-adapted cell. Under very dim steady illumination the response appears to be generated by summation of bumps. At higher light intensity bumps cannot be observed individually. Note the initial transient, the proportionality of the plateau response with the logarithm on intensity, the decreased noise at higher light intensities (at difference with the prediction of Campbell's theorem for uncorrelated noise), and the apparent silence (absence of bumps) after the cessation of bright light. From Wong and Knight (1980); reproduced from *Journal of General Physiology* (1980) **76**, 539–557, by copyright permission of the Rockefeller University Press.

plateau decreases with increasing stimulus intensity (Dodge *et al.*, 1968). These observations suggested that the response to bright light is the sum of bumps with smaller average size than those occurring in the dark. As smaller bumps are also evoked by dim light after bright light (Dodge *et al.*, 1968), it was concluded that the average size of bumps decreases with light intensity, and this is the major mechanism of light adaptation ("adapting bump model").

5.2.1. *The adapting bump model: example of correlated noise*

In order to demonstrate these hypotheses, one should be able to monitor bump size and frequency during the response to various light intensities. Noise analysis, and Campbell's theorem in particular, appeared particularly suitable to this purpose, since it is properly devised to extract size/frequency information from noise generated by the superposition of independent bumps ("Poisson shot noise"). However, the hypothesis of size adaptation implies correlation among the events (the height of any event is reduced by the occurrence of previous events), so that the noise cannot be dealt with directly as if it were Poissonian. A very interesting approach was developed by Wong and Knight (1980). The theoretical aspects involved are briefly summarized below.

If the noise is generated by uncorrelated events, we know that (Eqns 5 and 7):

$$M = r \cdot h \cdot \int w(t)\,\mathrm{d}t = r \cdot h \cdot I_1$$

$$V_u = r \cdot h^2 \cdot \int w^2(t)\,\mathrm{d}t = r \cdot h^2 \cdot I_2 \qquad (21)$$

where the subscript "u" indicates uncorrelated events, r is bump rate of occurrence (sec^{-1}), h is bump height and I_1 and I_2 have dimension of time (sec). In the presence of correlation among the events, the variance must still be proportional to the square bump duration, I_2, and amplitude, h^2, and to bump rate, r. Therefore:

$$V = r \cdot h^2 \cdot \Phi \cdot I_2, \qquad (22)$$

where Φ is a real number, without physical dimension, characteristic of the correlations in the process underlying the noise.

If Φ could be estimated, as well as I_1 and I_2, by analyzing the noise, then h and r could still be obtained by equations very similar to Eqns 8 and 9:

$$h = (\mathrm{VAR}/I_2/\Phi)/(\mathrm{MEAN}/I_1), \qquad (23)$$

and

$$r = (\mathrm{MEAN}/I_1)^2/(\mathrm{VAR}/I_2/\Phi). \qquad (24)$$

The factor Φ can be estimated from comparative spectral analysis of records obtained either in the absence or in the presence of correlations among bumps. At very low light intensities, the waveforms of single bumps can be studied on the average of several isolated events, and fitted by a suitable analytical function, in this case a gamma distribution function of the form

$$\tau \cdot \Gamma(t;n,\tau) = (t/\tau)^n \cdot \exp(-t/\tau)/n!$$

A rather accurate reconstruction of the low-light bump can also be obtained directly from the noise power spectrum, based on the sole assumption that a "minimum phase" function describes its time-course (see Appendix, Section 8.5).

Estimate of correlation from the power spectrum

In response to a brief flash of bright light the generator potential displays a peak and an undershoot before returning to the resting value (Fig. 7). This occurs over a much longer time than the duration of a single bump, suggesting that it is not due to the superposition of biphasic bumps but rather to a discharge of bumps whose amplitude decreases with time, so that when their rate falls back to the spontaneous resting value the generator potential becomes negative, and then slowly recovers to the resting level as the bump amplitude increases back to normal. If this interpretation is correct, then a reduction in the variance of the noise must occur, due to this form of correlation of the bumps (adaptation), which implies reduction in bump height. It directly

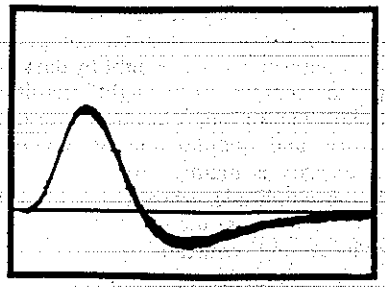

FIG. 7. Oscilloscope record of the eccentric cell's voltage response to a brief (40 ms) flash superimposed upon a bright, steady light. The sweep duration is 0.5 s, and the response amplitude is ≅5 mV. The generator potential amplitude is 16 mV. Reproduced from Dodge *et al.*, *Science* (1968) **160**, 88–90, copyright 1968 by the American Association for the Advancement of Science.

follows from the definition of power spectrum that the variance of the noise equals the area under the power spectrum, and the area under the spectrum of correlated bumps at high light intensity must therefore be reduced by adaptation. As the correlation occurs over a time scale (hundreds of milliseconds) longer than the individual bump duration, the reduction in the area under the power spectrum must affect mainly the low frequency region. This is actually observed at high light intensity (Fig. 8); furthermore, if the bright-light power spectrum is fit by the analytical curve derived from bumps observed in the dark, then good agreement is obtained in the high frequency region of the spectrum, and the decrease in the area due to correlation can be estimated (Fig. 8b). This reduction equals the ratio $VAR/VAR_u = \Phi$. Knowing Φ, Eqns 23 and 24 can be used to compute r and h.

By this approach, Wong and Knight (1980) were able to demonstrate that: (1) the generator potential in response to bright light is produced by the summation of bumps with the same general waveform of those seen in isolation in the dark; (2) the decline in the generator potential and noise in bright light (adaptation) is due to correlation among the bumps, and in particular to a reduction in bump amplitude following intense activity; (3) the bump rate increases proportionally to light intensity up to $\cong 500/s^{-1}$ and then it increases less than linearly; (4) the bump height decreases with increasing light intensity and the duration decreases down to about half the dark value; (5) the adaptation factor departs from the value in the dark ($\Phi = 1$, no correlation) at 10^2 times the threshold light brightness and falls to 0.3 at 10^5 times the threshold.

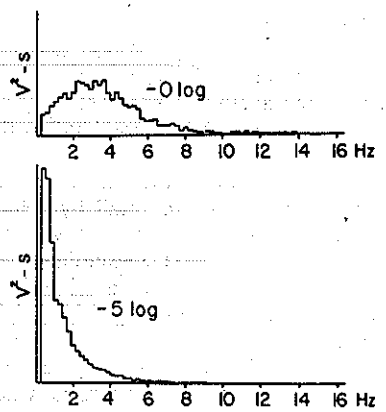

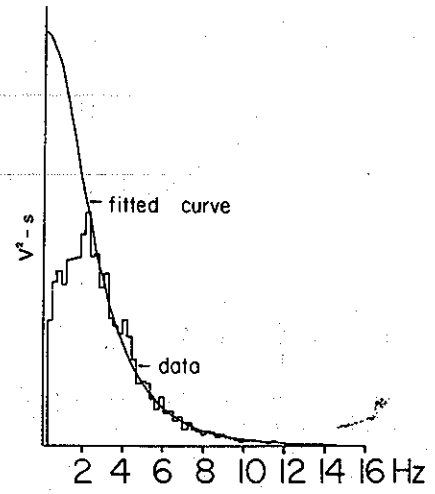

FIG. 8. A: Power spectra calculated on transmembrane voltage of *Limulus* retinular or eccentric cells obtained at low light intensity (−5 log) and at high light intensity (0 log). The horizontal axis is frequency and the scale is 0.234 Hz per bin. The vertical scale is in arbitrary units. The areas under the two curves are normalized. The shapes of the two curves are very different: for low light intensity, the power spectrum is represented by a monotonic curve, whereas for high light intensity, the power spectrum shows a low frequency cutoff due to "adaptation". B: The procedure for estimating the duration of the bumps and the adaptation factor Φ at high light intensity. The analytical curve is matched to the data at frequencies above 2 Hz. The areas of the two curves in this range are normalized. The parameters of the best fitting curve were used to calculate bump waveform. The ratio of the areas under the two curves gives an estimation for Φ (0.6 in this case). From Wong and Knight (1980); reproduced from *Journal of General Physiology* (1980) **76**, 539–557, by copyright permission of the Rockefeller University Press.

5.2.2. *Analysis of noise transients*

Further information on quantal discharge at the *Limulus* photoreceptor has recently come from a more sophisticated approach to shot noise transients (Grzywacz *et al.*, 1988). Here rapid changes in bump rate and amplitude were considered, during the transient response to a flash of weak light. Rapid changes in shot rate were treated by Rice (1944), who showed that the time-varying mean, $M(t)$, and variance, $V(t)$, of the noise, taken on an ensemble of records of the same process, are:

$$M(t) = \int_{-\infty}^{t} h \cdot r(t') \cdot w(t - t')\, dt' \qquad (25)$$

$$V(t) = \int_{-\infty}^{t} h^2 \cdot r(t') \cdot w^2(t - t')\, dt'. \qquad (26)$$

For a pictorial representation of this kind of integral (convolution) see Fig. 20. Notice that for distributed bump amplitudes, h indicates the average value, $\langle h \rangle$, and h^2 the average square value, $\langle h^2 \rangle$. This problem will be dealt with in more detail in the next sections.

The properties of the power spectrum of nonstationary shot noise were studied in detail by Schick (1974), Sigworth (1981), and Fesce *et al.* (1986a,b). Grzywacz and coworkers (1988) reexamined the question with a novel approach with more general applicability. They pointed out that Eqns 25 and 26 as well as the corresponding equations for time varying h, where $h(t')$ and $h^2(t')$ take the place of h and h^2, constitute a set of integral equations which may be easily solved for $r(t)$ and $h(t)$, at least for several simple forms of $w(t)$. As an example, for $w(t) = (1/\tau) \cdot \exp(-t/\tau)$,

$$M(t) + \tau \cdot \frac{d}{dt} M(t) = \int_{-\infty}^{t} r(t') \cdot h(t') \cdot [w(t - t') + \tau \cdot \frac{d}{dt} w(t - t')] dt'$$

$$= \int_{-\infty}^{t} r(t') \cdot h(t') \cdot \delta(t - t')\, dt'$$

$$= r(t) \cdot h(t);$$

similarly,

$$2 \cdot V(t) + \tau \cdot \frac{d}{dt} V(t) = r(t) \cdot h^2(t).$$

This procedure is related to autoregressive analysis (Appendix, Section 8.5) and is easily performed for low-order autoregressive waveforms.

By this method, the mean and variance of the shot noise are computed, for each value of time, over an ensemble of records of the response, and $r(t)$ and $h(t)$ are derived from relations like Eqns 9 and 10. However, this procedure requires that $w(t)$ be known, so information on $w(t)$ must be extracted from the power spectrum. As mentioned above, nonstationarity introduces extra variance, which must show up in an increase of the values of power spectral components. It is directly perceivable that the variance contributed by nonstationarity (either in r or in h) constitutes the time variance of the record obtained by averaging all records over the ensemble obtained by repeating the test many times; in fact, the average record will be purged of random noise, and its variance will be the variance generated by deterministic changes in rate and amplitude of the shot which occur synchronously in all records. If the power spectrum of the average record is subtracted from the power spectrum of each single record, the "decompound power spectrum" for the single record is obtained. This procedure is performed on all records, and the resulting spectra are averaged so to yield a purged spectrum which is identical in shape to that of a time-homogeneous shot noise generated by bumps of the same shape as those generating the response under study, i.e. it has the same shape as the power spectral density function of the single shot. Information on $w(t)$ is extracted from this decompound power spectrum in the usual way.

The approach just described was used by Grzywacz *et al.* (1988) to study the quantal composition of transient responses to flashes of light by dark adapted *Limulus* photoreceptors. At low light intensities these responses show marked supralinearity with respect to light intensity, and quantal analysis demonstrated that supralinearity is mainly due to an increase in average bump amplitude, whereas the total number of bumps in the response increases linearly with light intensity, indicating constant quantum efficiency (number of quanta generated per photon), and bump time courses are not markedly altered.

5.3. Intense Quantal Release of Acetylcholine at the Frog Endplate

The neuromuscular junction is a system particularly well studied as a simple model synapse. A particularly favourable feature of the nerve–muscle preparation is that single junctions can be identified and their function studied under various experimental conditions, to investigate the kinetic and regulatory properties of the machinery for neurotransmitter secretion. Furthermore, biochemical and cell-fractionation data can be obtained on the electroplaque of electrical fish, which is a homogenous tissue constituted by a great many cholinergic synapses, strictly related to the neuromuscular junction under both structural and functional aspects. The correlation between electrophysiological, morphological and biochemical results in these systems has yielded plenty of information on the role of synaptic vesicles in quantal secretion of ACh (see, e.g. Zimmermann, 1979; Ceccarelli and Hurlbut, 1980a) and on the relationship between synaptic vesicle-recycling and quantal turnover, i.e. synthesis, compartmentalization and release of neurotransmitter in relatively constant-sized packets (Ceccarelli *et al.*, 1972, 1973; Heuser and Reese, 1973; Heuser *et al.*, 1979; Ceccarelli and Hurlbut, 1980a; Hurlbut *et al.*, 1990).

Quantal secretion at the neuromuscular junction is traditionally studied by measuring the amplitudes of indirectly evoked endplate potentials (EPPs) or currents (Section 2) and by measuring the spontaneous rate of occurrence of miniature endplate potentials (MEPPs) or currents. Continuous measurements of the MEPP rate and amplitude during prolonged periods of intense secretion provide data that can be used to test the vesicle hypothesis of quantal secretion (Ceccarelli and Hurlbut, 1980a) and to characterize the kinetic properties of processes, such as vesicle recycling, that sustain high rates of quantal release. Very high MEPP rates cannot be measured by simple counting techniques because the individual MEPPs cannot be recognized, and other means must therefore be used. As the MEPPs recorded at a single junction are similar in amplitude and time course, their mean rate and amplitude can, in principle, be estimated by applying the classical procedure of shot noise analysis to the fluctuations in the membrane potential of the endplate at a vigorously secreting junction. However, serious errors occur when the classical equations (Eqns 8 and 9) are applied to the neuromuscular junction, where the shots are the MEPPs, because (a) the mean membrane potential of the endplate is affected by many factors in addition

to the summation of MEPPs, (b) the MEPPs may not occur at a stationary random rate, (c) MEPPs are not uniform in amplitude, and (d) MEPPs do not sum linearly. In recent years a series of studies have been published in which several refinements of classical noise analysis were developed, so to obtain a procedure which can be applied to endplate quantal noise even though the process under study departs under many relevant aspects from the ideal shot-noise processes.

5.3.1. *Solving the technical problems involved*

In order to apply fluctuation analysis to endplate quantal noise, four main problems must be solved: (i) the mean depolarization of the endplate in the course of an experiment is not solely due to summation of MEPPs and therefore it cannot be used straightforwardly to compute MEPP rate and amplitude by Campbell's theorem; (ii) MEPP rate generally changes with time, and such changes may be rapid (e.g. burst of MEPPs); (iii) MEPP are not uniform in amplitude, and this implies that the variance of the noise is not proportional to the square of MEPP amplitude $\langle h^2 \rangle$, but to the mean value of the squares of the amplitudes, $\langle h^2 \rangle$, so that Campbell's theorem yields biased estimates of MEPP amplitude $\langle h \rangle$ and rate of occurrence $\langle r \rangle$; (iv) MEPPs do not sum up linearly as required by Campbell's theorem.

Unreliable mean depolarization: using the skew

The first problem, unreliability of the mean depolarization, may arise, especially during prolonged recordings, from mechanical damage of the membrane due to the electrode, or from ion redistribution (e.g. chloride redistribution following transmitter-induced depolarization). However, this difficulty can be bypassed by using the extension of Campbell's theorem to higher cumulants (Rice, 1944). This is stated by Eqn 10:

$$C_n = r \cdot h^n \cdot \int w^n(t)\, dt$$

from which estimates of MEPP rate, r, and amplitude, h, can be computed by taking the ratios:

$$(C_n/I_n)^{n+1}/(C_{n+1}/I_{n+1})^n = r \qquad (27)$$

and

$$(C_{n+1}/I_{n+1})/(C_n/I_n) = h. \qquad (28)$$

Segal *et al.* (1985) used this approach to study MEPP rate and amplitude during intense quantal secretion induced by La^{3+} at the frog neuromuscular junction. They used in particular ratios between the variance ($n = 2$) and the skew ($n + 1 = 3$). The idea of using higher-order moments of a stochastic process to extract information which mean and variance cannot yield was put forward by Courtney (1978), in dealing with statistics of EPP quantal content (Section 2.2.3). Higher order moments, however, are intrinsically affected by larger random fluctuations, to the point of making them unreliable under certain conditions. Rice (1944) analyzed in detail the probability density function, $p(v)$, of the signal, v, generated by a shot-noise process and demonstrated that $p(v)$ can be expressed as an Edgeworth series:

$$p(v) = [C_2/\sigma^2 + (C_3/3!/\sigma^3) \cdot (v^3/\sigma^3 - 3 \cdot v/\sigma) + \cdots] \exp(-v^2/2\sigma^2)/(\sigma\sqrt{2\pi}) \qquad (29)$$

where σ is the standard deviation, $\sigma^2 = \mathrm{Var} = C_2$, and the contribution of each cumulant, C_n, to $p(v)$ is of order $o(C_n\sigma^{-(n+1)})$. Since the C_ns are proportional to shot rate, r, and σ to $r^{1/2}$, the contribution of each C_n to $p(v)$ is of order $o(C^n\sigma^{-(n+1)}) = o(r^{-(n-1)/2})$. As r increases, the contribution of higher cumulants decreases, and the probability distribution of the signal approaches a Gaussian distribution (central limit theorem). In particular, since the contribution of the variance, C_2, is $o(r^{-1/2})$ and that of the skew is $o(r^{-1})$, the significance of the skew vanishes as $r \to \infty$; the term involving C_3 in Eqn 29 becomes negligible with respect to the first one, $C_2/\sigma^2 = 1$, when

$$C_3/(3! \cdot \sigma^3) \approx (r \cdot h^3 \cdot I_3)/(6 \cdot r^{3/2} \cdot h^3 \cdot I_2^{3/2}) = (I_3/6/I_2^{3/2}) \cdot r^{-1/2} \ll 1.$$

For endplate recordings, I_3^2/I_2^3 ranges from $\approx 75\ s^{-1}$ (Segal *et al.*, 1985) to $\approx 200\ s^{-1}$ depending on the time course of the MEPPs under various experimental conditions. This implies that the ratio $C_3/(6 \cdot \sigma^3)$ falls below 5% for $r > 1000$ to $2500\ s^{-1}$, setting a rather low limit for the maximum MEPP rate tractable with this approach. Segal *et al.* (1985) considered a slightly different index for detectability of the skew, i.e. the ratio between

$$\int_0^\infty G(v) \cdot v^3 \cdot dv$$

and

$$\int_0^\infty D(v) \cdot v^3 \cdot dv,$$

where $G(v)$ is the Gaussian term in Eqn 29 (the first term), and $D(v)$ is the second term, representing deviation from Gaussian behaviour due to the skewness of the distribution. This ratio equals $(8 \cdot \pi \cdot r \cdot I_2^3)^{1/2}/I_3$. Segal *et al.* (1985) showed on simulated data that noise analysis of endplate recordings using variance and skew breaks down at $r > 3000\ s^{-1}$, where this ratio gets > 10, for the typical time course of a MEPP in La^{3+} 0.1 μM.

It is straightforward that the ratio I_3^2/I_2^3 is inversely related to MEPP duration, I_2 and I_3 being the equivalent durations of the squared and cubed MEPP, respectively. This implies that the upper limit for tractable MEPP rates can be elevated by shortening MEPP effective duration, e.g. by filtering the signal through a highpass filter. Segal *et al.* (1985) demonstrated that by this approach the limit in MEPP rate can be increased by a factor close to two (Fig. 9). Under most experimental conditions, where MEPP time course is 2–3 fold briefer than in La^{3+}, the upper limit for r is therefore in the order of $10^4\ s^{-1}$. This is sufficient to deal with most experimental recordings, since the maximum measured MEPP rates rarely exceed $5000\ s^{-1}$. Higher rates have been reported, but

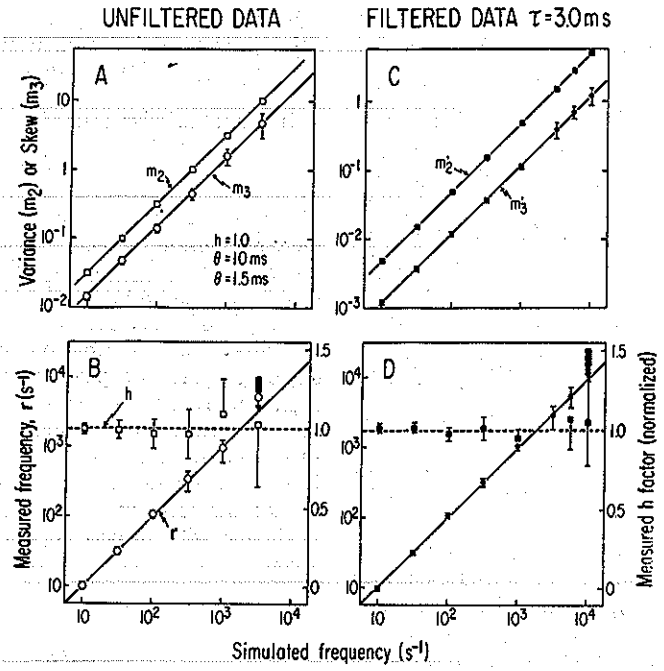

FIG. 9. Noise analysis of simulated endplate recordings. Simulated MEPP waveform = exp $(-t/10\,\text{ms}) - \exp(-t/1.5\,\text{ms})$. For different simulated MEPP-rates (abscissa), A shows variance (squares) and skew (circles) of the simulated record, and B shows estimates of amplitude (h) and rate of occurrence (r) from variance and skew. Solid and dashed lines indicate the values expected theoretically. Bars = SDs. Broad bar and downward arrow indicate that SD > mean. Panels C and D; same as A and B, respectively, using filtered data through a high-pass resistance–capacitance filter with time constant RC = 3 ms. Note good consistency in C–D for higher values of simulated MEPP rates. From Segal *et al.* (1985); reproduced from *Biophysical Journal* (1985) **47**, 183–202, by copyright permission of the Biophysical Society.

they could be sustained for brief periods only (see later).

In the first application of noise analysis to measurements of quantal secretion, Heuser and Miledi (1971) applied Campbell's theorem to the mean and variance to measure quantal secretion induced by La^{3+}, but care had to be taken that no depolarization occurred in the fiber during the experiments. The authors in the end adjudged an indirect approach more reliable: they counted which fraction of all MEPPs occurring at the neuromuscular junction (recorded intracellularly) could be detected by an extracellular electrode appropriately positioned, then they counted extracellular MEPPs during the experiment and corrected the counts by the ratio intracellular/extracellular MEPPs.

The relevance of the reliability of the mean potential can be illustrated by an example: let MEPP amplitude be 1 mV and its decay time constant be 5 ms, yielding an area under the MEPP, $A_1 \approx 5 \times 10^{-6}$ V·s. A 1 mV depolarization would correspond to $10^{-3}/(5 \cdot 10^{-6}\,\text{s}) = 200$ MEPP/s. Furthermore, let the true MEPP rate be 200/s; as the rate is estimated from the ratio mean^2/var, a 1 mV depolarization yields an apparent doubling of the mean, without affecting the variance, so that the estimated MEPP rate would be fourfold greater than its true value.

Noise analysis was applied to the mean and variance also by Simonneau *et al.* (1980), Finger (1983, 1985) and Martin and Finger (1985), at different synapses (see Section 5.4.2), and by Molenaar and Oen (1988), who studied ACh release induced by K^+ propionate. In the latter study tremendous discharges of quanta, with MEPP rates over $10^4\,s^{-1}$, were produced by transient local application of Ca^{2+} to junctions bathed in Ca^{2+}-free, isotonic K^+ propionate. Under these conditions, however, the discharge was brief and rapidly subsided as Ca^{2+} superfusion was stopped, so that the mean depolarization during the period of intense activity could be considered as exclusively due to the superposition of MEPPs and Campbell's theorem could be applied in its classical form.

Nonstationarity

Nonstationary shot rate is a quite general problem in dealing with biological shot noise processes. The approach which has become classical, in the face of nonstationary processes, is that proposed by Rice (1944).

Assuming an ensemble of records of the same process are available, time varying estimates of mean and variance are obtained by averaging over the ensemble at each value of time. If the changes in the parameters of the process (r and h) are slow compared to the time course of the single shot, then Campbell's theorem can be applied directly with small errors (Rice, 1944).

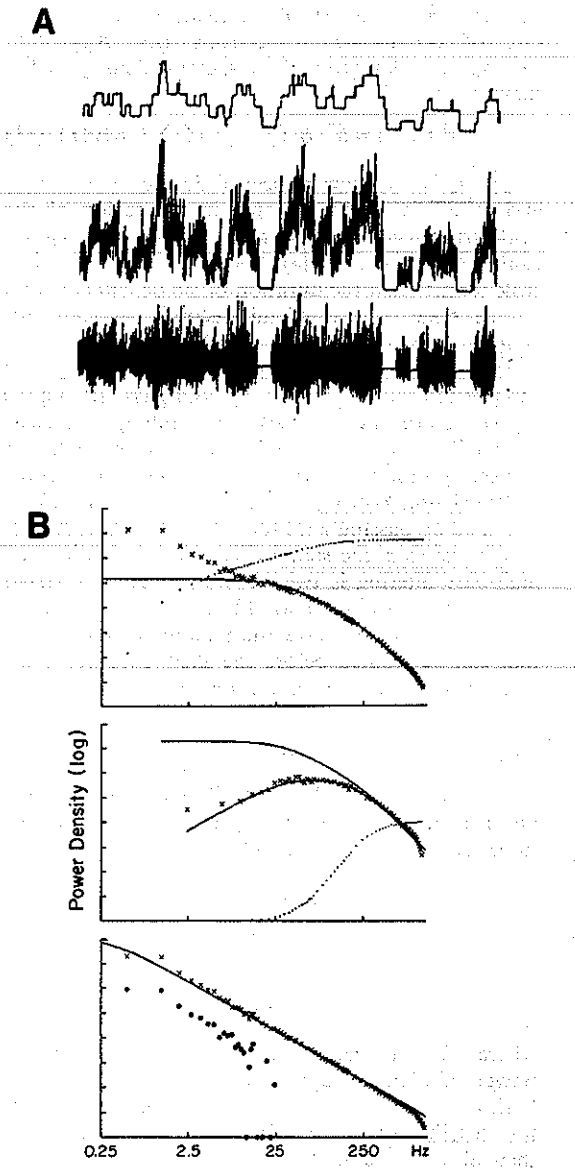

FIG. 10. A: Simulated endplate recording (10 sec) with nonstationary MEPP rate. Top trace is the rate-generating functions showing random step changes in MEPP rate produced by the superimposition of random volleys of MEPPs (volleys of 500 MEPP/s, with mean duration 0.5 s, occurring at random with mean rate 5/s). Middle trace is the endplate recording obtained by simulating this time course of MEPP rate. Bottom trace shows the high-pass filtered record (1 msec resistance–capacitance filter) at higher gain. It may be perceived that the variance of the bottom trace is proportional to MEPP rate at each value of time, which is not true for unfiltered data. B: Power spectra from records in panel A. Power densities (ordinates) in decades. Top panel: unfiltered data (×), analytical curve (solid line), and total power (dotted line, linear scale); measured variance fourfold the expected variance under stationary conditions. Middle panel: filtered data (RC = 1 ms), theoretical spectra for unfiltered and filtered data (solid lines) and total power (dotted line): the contribution of nonstationarity to the variance is almost completely obliterated, as is clearly shown by the total power plot, which does not increase significantly for frequencies below 20 Hz. For higher frequencies, the spectrum is very well fitted by the theoretical curve. Bottom panel: ×, spectrum of the top record in panel A, i.e. of $r(t)$; theoretical spectrum (solid line) for volleys occurring randomly and with random duration (mean 0.5 s); ○, spectrum of $r(t)$ as deduced from the spectrum of unfiltered data and the spectrum of the artificial MEPP through Eqn 52 (Appendix). Negative values set to zero. Notice that this reconstruction parallels the actual spectrum of $r(t)$ over about two frequency decades. The ordinate spans the range 10^{-4}–10^{4}, so that at 1 decade below half-scale, $G_n(f)/2\langle r\rangle = 0.1$ (see Appendix, Section 8.4). This shows that contributions from nonstationarity are negligible for frequencies >20 Hz. From Fesce *et al.* (1986a); reproduced from *Journal of General Physiology* (1986) **88**, 25–57, by copyright permission of the Rockefeller University Press.

Information on the shot waveform can still be obtained from the power spectrum of the noise, in general, since slow changes in the parameters of the process should introduce extra-variance limited to a narrow band in the low-frequency region of the spectrum (Rice, 1944; Schick, 1974; Sigworth, 1981; Fesce *et al.*, 1986a; see also Sections 5.2 and 8.4). This approach was introduced by Sigworth (1980, 1981a,b) to study nonstationary ion–channel noise. A different approach was used, in studying ion–channel noise at the node of Ranvier, by Conti and coworkers (1980), who measured variance and power spectra on ensembles of difference records (i.e. records obtained by subtracting the first from the second of each pair of successive recordings), thereby eliminating a priori contributions from nonstationarity. This roughly corresponds to the procedure used by Grzywacz *et al.* (1988) for computing "decompound" spectra from photoreceptor quantal noise (see Section 5.2). Although this procedure reduces to half the number of records used in the analysis (and therefore the "degrees of freedom") with concomitant increase in the random errors of the estimates, it has the advantage versus the classical procedure that the whole power spectrum is brought back to the shape expected for stationary noise.

In all these applications it was possible to obtain ensembles of records of the same process. In studying quantal secretion at the neuromuscular junction over prolonged periods of time (even hours), it is impossible to obtain a high number of records of the same process, mainly because there is no basis for assuming that the time courses of MEPP rate and amplitude at different endplates are synchronous in the time scale of milliseconds (or even seconds). In particular, ensemble averaging will not remove nonstationarity when these are related to nonPoisson distribution of intervals between MEPPs (Cohen *et al.*, 1973) or to the fast bursts (few seconds duration) of high frequency MEPPs, observed for example with spider venoms (del Castillo and Pumplin, 1975; Fesce *et al.*, 1986b). The variance, and possibly the skew, must therefore be measured by averaging over time a single recording, and will be affected by nonstationarity. Fesce *et al.* (1986a) derived the frequency composition of C_2 (power spectrum) and C_3 (skew "bispectrum") of nonstationary shot noise and demonstrated that the effects of time varying rate on these spectra can be virtually eliminated by appropriately filtering the data before analysis, as long as the deviations of

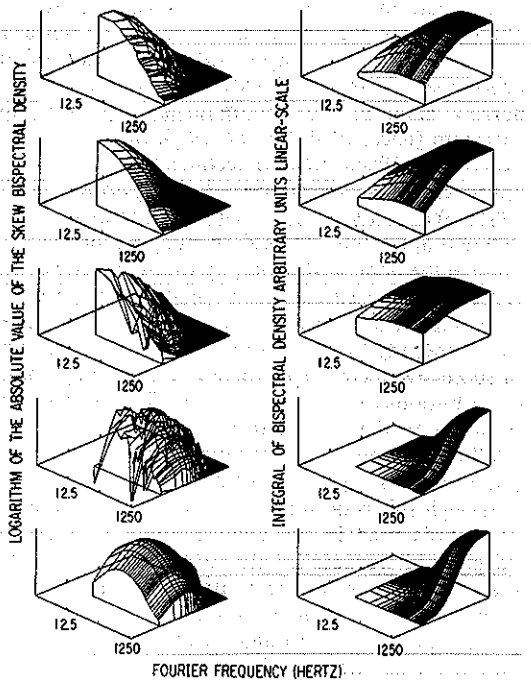

FIG. 11. Bispectral density of the skew of simulated records (left) and integrals of the same cruves (right) showing the contribution of various frequency components to the skew. Left: The two horizontal axes (X–Y) are Fourier frequencies on logarithmic scales, and the vertical axis is the bispectral density on a logarithmic scale. Positive values that would fall below the X–Y plane (i.e. densities between 0 and 1) are not plotted; negative values are plotted below the X–Y plane (negative logarithm of the absolute value). Top panel: simulated stationary record; second panel: analytical bispectrum of the simulated MEPP waveform; third panel: simulated nonstationary record (same as Fig. 10); note the deviations from the analytical shape; fourth panel: same nonstationary record, filtered through a 1-msec RC filter; fifth panel: analytical bispectrum of simulated MEPP waveform, filtered through a 1-ms RC filter. Differences are still apparent between the densities in the two bottom panels, but their contributions to the skew are negligible (right). Right: Integrals of the skew bispectra in the corresponding panels on the left. Horizontal axes as on the left. Vertical axes are linear (arbitrary units). Notice the good agreement between the two top panels (unfiltered simulated stationary record and analytical plot for stationary data), and between the two bottom panels (filtered simulated nonstationary record and analytical plot of filtered stationary data). From Fesce *et al.* (1986a); reproduced from *Journal of General Physiology* (1986) **88**, 25–57, by copyright permission of the Rockefeller University Press.

the noise spectrum from the expected stationary shape are confined to a limited region of the spectrum (Figs 10 and 11). The cumulants of the filtered records can then be used to compute h and the average value of r in successive records, $\langle r \rangle$.

The main point of this derivation is that the spectral density of the variance of nonstationary shot noise is

$$G_n(f) = h^2 \cdot G_w(f) \cdot (\langle r \rangle + G_r(f)/2) \qquad (30)$$

where $\langle r \rangle$ is the mean value of the shot rate, $r(t)$, over the record, and $G_n(f)$, $G_w(f)$ and $G_r(f)$ are the power spectral densities of the noise, the shot and the rate of occurrence, respectively (see Appendix, Section 8.4). Similarly, the bispectral density of the skew is

$$B(f_1, f_2) = h^3 \cdot B_w(f_1, f_2) \cdot (\langle r \rangle + \text{REST}) \quad (31)$$

where B_w is the skew bispectral density of the shot, and REST is significant only in the region of the bispectrum where $G_r(f_1)$ and $G_r(f_2)$ are also significant (Fesce *et al.*, 1986a). If $r(t)$ changes on a time scale longer than the duration of single shots, i.e. on a time scale of tens of milliseconds, at least, for endplate recordings, then $G_r(f)$ is significant only over a portion of the noise power spectrum (Fig. 10); this portion can be removed by high-pass filtering the signal before the analysis, so yielding a process "purged" of nonstationarity; this can be treated as stationary shot noise produced by single shots with a modified time course, $w'(t)$, which is the waveform obtained by passing $w(t)$ through the high-pass filter used to process the signal (Figs 10–11). Notice that high-pass filtering is twice useful, in using variance and skew to estimate MEPP rate and amplitude, because it also increases the maximum MEPP rate that can be studied before the skew becomes negligible (Segal *et al.*, 1985, see above).

Distributed shot amplitude

As pointed out by Rice (1944), when shots are not uniform in amplitude the cumulants of the fluctuations, are defined by Eqn 11:

$$\begin{aligned} C_n &= r \cdot \langle h^n \rangle \cdot \int w^n(t)\, dt \\ &= \langle r \rangle \cdot \langle h^n \rangle \cdot I_n \\ &= \langle r \rangle \cdot \langle h \rangle^n \cdot D_n \cdot I_n \end{aligned}$$

where $\langle h^n \rangle$ indicates the average value of the n^{th} power of MEPP amplitude over the population of MEPPs. Notice that $D_n = \langle h^n \rangle / \langle h \rangle^n$ depends only on the distribution of MEPP amplitudes, and not on their absolute values.

Using the variance and skew, C_2 and C_3, MEPP rate and amplitude are now defined by:

$$\begin{aligned} \langle r \rangle &= (D_3^2/D_2^3) \cdot (C_2/I_2)^3/(C_3/I_3)^2 \\ &= (D_3^2/D_2^3) \cdot \hat{r} \end{aligned} \qquad (32)$$

and

$$\begin{aligned} h &= (D_2/D_3^2) \cdot (C_3/I_3)/(C_2/I_2) \\ &= (D_2/D_3) \cdot \hat{h} \end{aligned} \qquad (33)$$

where $\hat{r}$ and $\hat{h}$ are the values one would obtain by applying Eqns 27 and 28 which neglect nonuniformity in MEPP amplitude.

When the distribution of MEPP amplitudes is known, the D_ns are computed and $\langle r \rangle$ and $\langle h \rangle$ are easily derived by applying in sequence Eqns 27 and 28 to obtain $\hat{r}$ and $\hat{h}$ and then Eqns 32 and 33. Note that in standard applications of Campbell's theorem, $D_1 = 1$ and $D_2 = 1 + cv^2$, where cv is the coefficient of variation of MEPP amplitudes, so that the corrections in Eqns 32 and 33, applied to mean and variance

rather than variance and skew, reduce to $(1+cv^2)$ for $\langle r \rangle$ and $(1+cv^2)^{-1}$ for h.

Fesce and colleagues (1986a) pointed out that even in the course of active secretion, when no MEPP amplitude histograms can be drawn to measure the D_ns, information on the D_ns can be extracted from higher cumulants of the noise. In particular they computed the ratio:

$$R = \frac{C_3^2 \cdot I_4 \cdot I_2}{I_3^2 \cdot C_4 \cdot C_2} = D_3^2/(D_4 \cdot D_2).$$

If the MEPP amplitude distributions are well fit by analytical distribution functions, R can be in principle determined from the parameters of the analytical function, and vice versa. In general good fit to MEPP amplitude distributions is obtained with gamma distribution functions (McLachlan, 1975; Fesce *et al.*, 1986b); these have the form

$$p_k(h) = \beta^{k+1} \cdot h^k \cdot \exp(-\beta h)/k!,$$

and constitute a quite general family of unimodal distributions, ranging from simple exponential ($k = 0$), to nearly Gaussian ($k > 10$). To each value of k corresponds one particular value of $R = (k+3)/(k+4)$, so that k can be computed from R, and the D_ns from k (Fig. 12), to correct estimated MEPP rate and amplitude for biases due to nonuniform amplitudes (Fesce *et al.*, 1986b).

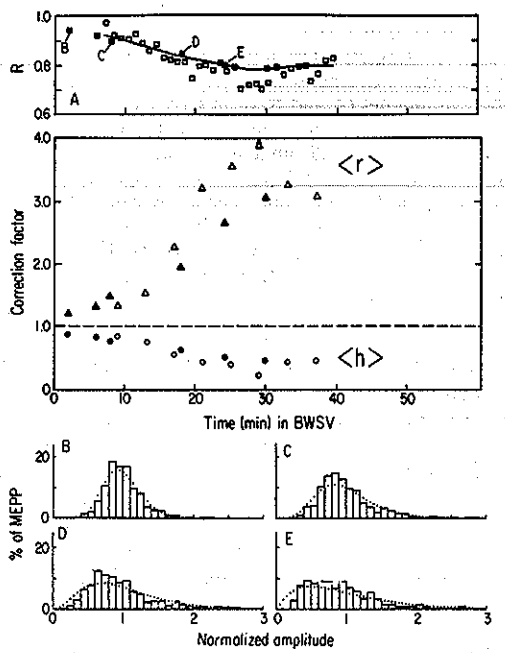

FIG. 12. Changes in the ratio R, the correction factors for $\langle r \rangle$ and $\langle h \rangle$, and the MEPP amplitude histogram during BWSV-induced secretion in Ca^{2+}-free solution. Averaged results from five experiments. (A) Ordinates: R (squares) or correction factors for rate (triangles) and amplitude (circles); solid symbols are values computed from gamma distributions fitted to the combined, normalized histograms; open symbols are values computed from the fluctuations. The latter values were computed from the averages of groups of four values of R. Abscissae: time (minutes) after adding BWSV. (B–E) Combined histograms obtained at various times in each experiment (400 to 900 MEPPs). Ordinates: fraction of MEPPs in each amplitude bin; abscissae: amplitude normalized to the mean amplitude. The dotted lines show gamma distributions computed from the mean and variance of the histograms. The k parameters (see equation in the text) were: (B) 13.3 (control); (C) 5.5; (D) 2.4; (E) 1.03. The average peak amplitudes changed from 0.48 ± 0.14 (control) to 0.45 ± 0.10 mV (end). This marked broadening of MEPP amplitude distribution is observed with BWSV only in Ca^{2+}-free solution, and reflects the occurrence of many "giant" MEPPs as the nerve terminal fatigues and approaches exhaustion of quanta and vesicles. From Fesce *et al.* (1986b); reproduced from *Journal of General Physiology* (1986) **88**, 59–81, by copyright permission of the Rockefeller University Press.

Nonlinear summation

As already discussed for EPPs (Section 2.2.2), Martin's correction factor can be used to correct for the nonlinear relation between the increases in conductance and membrane depolarization. The correction is inadequate for large EPPs (Martin, 1976; Adams, 1976; Stevens, 1976; McLachlan and Martin, 1981) because the large increases in conductance that produce EPPs also significantly reduce the time constant of the membrane during the brief period of transmitter action; however, it is appropriate for correcting small fluctuations in potential when the underlying fluctuations in conductance are too small to change the membrane time constant significantly. This is the case when skew and variance are used instead of mean and variance (Fig. 13).

Assume that conductances sum linearly and that the added endplate conductance is proportional to the MEPP rate. Suppose that quanta are secreted at an average rate, $\langle r \rangle$, such that the mean conductance of the endplate is increased 50% above its resting value. If MEPPs summed linearly, the average membrane potential, $\langle V \rangle$, would move along the initial slope, S_0 of the G–V curve to the point A in Fig. 13 and the fluctuations in the MEPP rate would cause V to fluctuate along this line. Since MEPPs sum

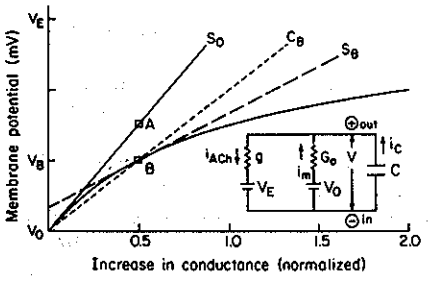

FIG. 13. Steady state voltage–conductance curve of the equivalent circuit shown in the inset. Abscissa: increase in membrane conductance, g, normalized to conductance in the absence of MEPPs; V_0 = membrane potential in the absence of MEPPs; V_E = equilibrium potential of endplate channels; C = membrane capacitance; i_{ACh} = current through acetylcholine-gated channels; i_m = current through ionic channels in the muscle fibre; i_c = current through capacitance. The cable properties of the junction are ignored. See text for further explanation. From Fesce *et al.* (1986a); reproduced from *Journal of General Physiology* (1986) **88**, 25–57, by copyright permission of the Rockefeller University Press.

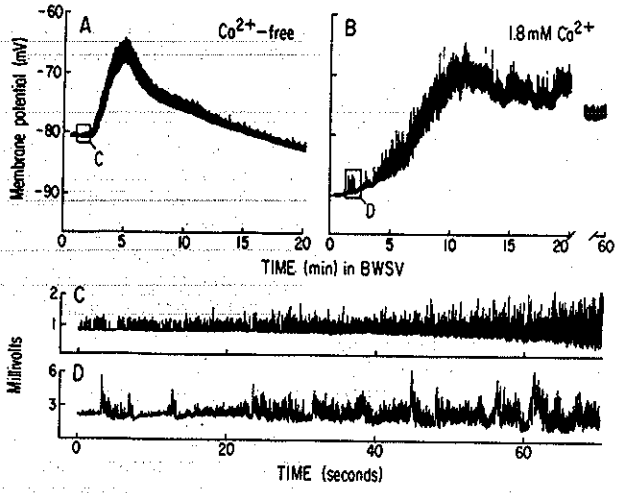

FIG. 14. Strip-chart records of the changes in membrane potential at two neuromuscular junctions after the addition of 25 μl of BWSV. (A and C) Junction in Ca^{2+}-free Ringer's solution with 4 mM Mg^{2+} and 1 mM EGTA. (B and D) Junction in Ringer's solution plus 4 mM Mg^{2+}. Ordinates: millivolts; DC recording (A and B); AC recording ($\tau \sim 1$ s; C and D). Abscissae: time in minutes (A and B) or in seconds (C and D). The membrane potential falls and the trace broadens as $\langle r \rangle$ rises at both junctions. The junction in the Ca^{2+}-free solution had recovered its original membrane potential by $\cong$25 min and $\langle r \rangle$ had subsided to low levels, but at the other junction the membrane potential remained low and $\langle r \rangle$ remained high until 60 min. (Note break in time scale of B.) C and D show the early parts of the experiments (indicated by the boxes) displayed on a faster time scale and at higher gain (AC-coupled). In C (Ca^{2+} absent), $\langle r \rangle$ rose smoothly, but it fluctuated markedly in D (Ca^{2+} present) indicating a bursting pattern of release. From Fesce *et al.* (1986b); reproduced from *Journal of General Physiology* (1986) **88**, 59–81, by copyright permission of the Rockefeller University Press.

nonlinearly, however, $\langle V \rangle$ moves along the G–V curve to point B and the fluctuations in the MEPP rate cause V to fluctuate (to a first approximation) along the slope, S_B, at point B, where $\langle V \rangle = V_B$. When $\langle r \rangle$ and the MEPP amplitude factor, **h**, are computed from the mean and variance of V, errors arise because the chord, C_B, and the slope, S_B, are not equal. These errors are avoided if C_B and S_B are corrected to the initial slope, S_0 (Wong and Knight, 1980). When the skew and variance are used, however, only the fluctuations in V about V_B are considered, and the difference among S_0, C_B, and S_B need not be corrected for. The value of **h** computed from these fluctuations is that appropriate to S_B, i.e. it is the amplitude of MEPPs occurring at membrane potential V_B. However, a second-order error arises because the G–V curve deviates slightly from the straight line, S_B. When the fluctuations in g are small, the size of this error can be estimated directly from the semi-invariants of the fluctuations (Fesce *et al.*, 1986a). The capacitance of the membrane does not affect the error because the membrane time constant remains near the value set by the average MEPP rate. Application of Martin's correction directly to the measured cumulants, rather than to the original recording, has the advantage that correction for nonlinear summation can be applied a posteriori on the cumulants of high-pass filtered data (the need for high-pass filtering was discussed earlier).

5.3.2. *Determination of the quantal store in motor nerve terminals*

The number of quanta stored at rest in a nerve terminal can be determined, in principle, by inducing massive quantal secretion under conditions where the reconstitution of quanta is impaired. Nerve terminals stop secreting quanta after a massive activation of release by black widow spider venom (BWSV) or its purified, active fraction, α-latrotoxin (α-LTx), in high doses or in the absence of extracellular calcium (Longenecker *et al.*, 1970; Hurlbut and Ceccarelli, 1979; Ceccarelli and Hurlbut, 1980b), or after stimulation with ouabain (Haimann *et al.*, 1985). Under these conditions nerve endings are depleted of synaptic vesicles when they stop secreting, indicating that vesicle recycling is impaired. The reconstitution of quanta would be consequently impeded.

The determination of the resting store of quanta is an important point under two main respects: (i) it is an important parameter for kinetic analysis of quantum turnover and for setting up a kinetic model of neurotransmitter secretion; (ii) it should be equivalent to the store of vesicles in a resting terminal if the vesicle hypothesis of quantal release is true, so that its measurement provides an indirect way of verifying the vesicle hypothesis.

The effects of BWSV, lanthanum and ouabain were studied in the presence and in the absence of Ca^{2+}, as low doses of the venom appeared to block recycling in Ca^{2+}-free solutions but not in the presence of extracellular Ca^{2+}, suggesting that calcium is necessary for vesicle recycling (Ceccarelli and Hurlbut, 1980b). This was confirmed by noise analysis of quantal release induced by BWSV (Fig. 14; Fesce *et al.*, 1986b) or by α-LTx (Fig. 15; Valtorta *et al.*, 1988). However, as appears from the data in Table 1, intense recycling appeared to occur in La^{3+} even without extracellular calcium (though it was less vigorous; Segal *et al.*, 1985) and appeared to be

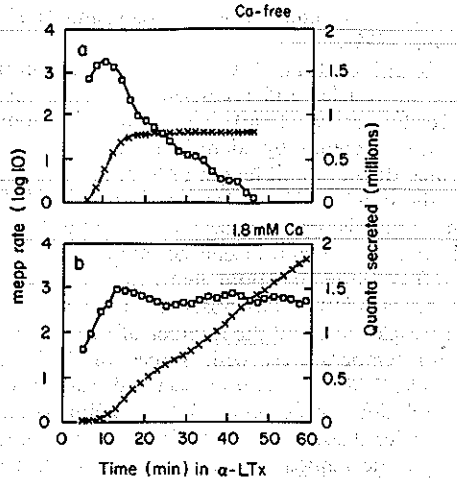

FIG. 15. Time course of MEPP rate (squares) and cumulative quantal secretion (crosses) computed from fluctuation analysis of endplate recordings during exposure to 0.2 μg/ml α-LTx in either Ca^{2+}-free or Ca^{2+}-containing Ringer's solution. Each point is the average of the corresponding values from three different experiments. MEPP rate (s^{-1}) on logarithmic scale. From Valtorta *et al.* (1988), reproduced from *Journal of Cell Biology* (1988) **107**, 2717–2727, by copyright permission of the Rockefeller University Press.

blocked by ouabain irrespective of extracellular calcium (Haimann *et al.*, 1985). In order to be sure of completely blocking endocytosis, Ceccarelli and coworkers (1988b) studied the effect of high doses of BWSV at low temperature (3°C) and obtained cumulative release comparable to those in Ca^{2+}-free solution at room temperature before the terminals became exhausted of quanta. The low temperature, however, does not seem to be sufficient *per se* to block synaptic vesicle recycling at frog neuromuscular junctions (Dekhuijzen *et al.*, 1989).

By measuring quantal secretion induced by ouabain (Haimann *et al.*, 1985) or by BWSV (Fesce *et al.*, 1986b) or α-LTx (Valtorta *et al.*, 1988) in Ca^{2+}-free solution or at low temperature (Ceccarelli *et al.*, 1988b), the upper limit for the average initial store of quanta in frog motor nerve terminals was set to $0.7–0.8 \cdot 10^6$ quanta. Molenaar and Oen (1988) counted 10^6 MEPPs secreted before rapid exhaustion of release by nerve terminals exposed to high K^+ in a chloride-free solution (with propionate) which also appears to inhibit vesicle recycling. More recently, Hurlbut *et al.* (1990), using frogs of a wide range of weights and lengths, reported average values ranging from 0.75 to 1.55×10^6 quanta for the cumulative quantal secretion induced by either BWSV or α-LTx in different batches of frogs.

5.3.3. *Quantitative ultrastructure–function correlations*

Studies with blocked vesicle recycling

The various estimates reported in the literature for the number of vesicles residing in a resting frog motor nerve terminal range from 0.25 to over $1 \cdot 10^6$ (Ceccarelli *et al.*, 1973, 1988b; Segal *et al.*, 1985; Haimann *et al.*, 1985; Torri-Tarelli *et al.*, 1987; Hurlbut *et al.*, 1990).

TABLE 1. CORRELATION BETWEEN QUANTAL RELEASE AND VESICLE LOSS AT THE FROG ENDPLATE

Experimental condition		Quanta secreted	Vesicle counts Remaining	Lost‡	Recycled	References
Electrical stimulation (2 Hz)	30 min	1330*	675 ± 225	206	1100	Ceccarelli *et al.*, 1973;
	1 hr	2500*	506 ± 131	375	2100	Torri-Tarelli *et al.*, 1987
Ouabain 0.5–1 mM	0 mM Ca, 4 mM Mg	1230*	291 ± 170	590	640	Haimann *et al.*, 1985
	1.8 mM Ca, 4 mM Mg	1470*	147 ± 106	735	740	
Lanthanum room temperature	0.1 mM no Ca	4500*	110 ± 39	718†	3800	Segal *et al.*, 1985;
	1.8 Ca	5830*	227 ± 73	601†	5200	Fesce *et al.*, 1986b
Lanthanum 3–5°C	1 mM	1100*	925 ± 875	375†	725	Dekhuijzen *et al.*, 1989
	2 mM	470*	575 ± 475	725†	<0	
BWSV 5 μg/ml $	0 mM Ca, 4 mM Mg	1170*	none	880†	290	Fesce *et al.*, 1986b;
	1.8 mM Ca, 4 mM Mg	2830*	650 ± 192	178†	2650	Torri-Tarelli *et al.*, 1987
α-LTx room temperature 0.2 μg/ml	0 Ca, 4 Mg	1380*	none	N.D.	N.D.	Valtorta *et al.*, 1988
	1.8 Ca, 4 mg	3000*	N.D.	N.D.	N.D.	
0.5 μg/ml 0 Ca, 4 Mg	5 min	370	838 ± 738	812	<0	Hurlbut *et al.*, 1990
	10 min	1100	388 ± 438	1260	<0	
	15 min	1160	275 ± 250	1375	<0	
α-LTx 1–3°C 2 μg/ml	0 Ca, 4 Mg	970*	390 ± 340	950	20	Ceccarelli *et al.*, 1988b
	1.8 Ca, 4 Mg	1180*	350 ± 312	990	190	
9–10°C 1 μg/ml 0 Ca, 4 Mg	10 min	120	1700 ± 950	650	<0	Hurlbut *et al.*, 1990
	20 min	680	1313 ± 613	1040	<0	
	40 min	1440	338 ± 175	2012	<0	
	75 min	1700	88 ± 75	2270	<0	

Notes: (‡) Vesicles lost = resting number − remaining. (†) Resting vesicle population not determined in this particular batch of frogs. (*) The length of the junction recorded from was not measured (secretion per active zone computed assuming 600 active zones per terminal). ($) Corresponding to ≈0.2 μg/ml α-LTx. N.D.: not determined.

This range of values is quite similar to the range reported for the cumulative number of quanta secreted before exhaustion in conditions where recycling is blocked (Section 5.3.2) giving indirect support to the hypothesis that the release of a quantum of acetylcholine is produced by the exocytotic fusion of one synaptic vesicle with the presynaptic membrane (Table 1).

A general impression from these experiments is that changes in MEPP amplitude are small and seem to follow variations in membrane potential rather than changes in r, as would be expected for preformed quanta that are not renewed during secretion. Broadening of MEPP amplitude distribution was generally observed towards the end of exhaustive stimulations (Fesce *et al.*, 1986b; Ceccarelli *et al.*, 1988b).

Studies with lanthanum

The cumulative release observed after exposure to 0.1 mM La^{3+} at room temperature was higher than the resting store of vesicles, indicating intense vesicle recycling under this condition, and particularly so in the presence of extracellular calcium, where the number of quanta secreted was three- to five-fold the resting store of vesicles (Segal *et al.*, 1985; Fesce *et al.*, 1986b). Even higher values of quantal release were indirectly estimated by Heuser and Miledi (1971) in 1–2 mM La^{3+} at 4–7°C. Dekhuijzen and coworkers (1989) studied the effects of various concentrations of La^{3+} at different temperatures and concluded that: (i) vesicle recycling occurs both at room and at low temperature (3–5°C); (ii) high concentrations of La^{3+} (1 mM or more) are able to block release in many nerve terminals, after the initial stimulation, as total quantal outputs measured under these conditions are comparable to the resting store of vesicles, but many terminals retain their normal complement of vesicles, and release is potentiated by removing La^{3+} after a few minutes; (iii) La^{3+} initially increases MEPP amplitude but afterwards it reduces the sensitivity of the endplate to ACh, therefore producing very small MEPPs during prolonged exposure; (iv) La^{3+} may need to enter the nerve terminals to stimulate release, and this would account for the extreme variability in the onset time of quantal discharge (1–23 min) and may explain the very low sensitivity to La^{3+} observed at some junctions, and the wide variability in the estimates of total release induced by this ion.

Further studies with black widow spider venom

Cumulative release higher than the initial store of vesicles was also reported after exposure to low doses of BWSV or α-latrotoxin in the presence of Ca^{2+} (Fesce *et al.*, 1986b; Valtorta *et al.*, 1988; Hurlbut *et al.*, 1990), so confirming the previous suggestion that vesicle recycling is blocked by BWSV in a Ca^{2+}-dependent manner (Ceccarelli and Hurlbut, 1980b). The toxin blocked recycling also in the presence of Ca^{2+}, when applied at low temperature (Ceccarelli *et al.*, 1988b), but this appears to be due to the high doses that were necessary to stimulate release at low temperature, rather than to a direct effect of the temperature on recycling (Dekhuijzen *et al.*, 1989).

Recent work has brought the correlation between loss of vesicles and secretion of quanta further on (Hurlbut *et al.*, 1990). The cumulative number of quanta secreted by identified nerve terminals was scaled down to unit length of terminal and compared to the number of vesicles remaining per unit length, in terminals fixed at several different time points during the quantal discharge induced by BWSV (or α-LTx), either at room temperature or at 9–10°C. A direct relation was observed between the number of vesicles lost and the number of quanta secreted at both temperatures, with slopes of 1.11 and 1.21 vesicles lost per quantum secreted, respectively, and correlation coefficients >0.95 (Hurlbut *et al.*, 1990).

Under these conditions of intense recycling MEPP amplitude tended to decrease more or less remarkably, but never to a major extent suggesting that refilling of vesicles is not the limiting step in quantum/vesicle recycling. With millimolar concentrations of lanthanum small MEPPs were observed due to endplate desensitization (Dekhuijzen *et al.*, 1989).

Studies with potassium

The application of noise analysis to endplate recordings obtained during exposure to elevated extracellular concentrations of K^+ (15–25 mM) disclosed an unexpected feature of K^+ effect (Ceccarelli *et al.*, 1988a): though MEPP rates attained higher peak values for higher K^+ concentrations, at the same endplate, steady state rates were usually lower for higher concentrations of K^+, indicating that some processes, either in quantal secretion or in recycling, became inactivated during prolonged depolarization by K^+.

Consistent with the idea that quantal secretion becomes partly inactivated after prolonged exposure to high K^+, the number of fusions of synaptic vesicles along the active zones of the presynaptic axolemma, observed in freeze-fracture replicas, declined with time in preparations exposed to 20 mM K^+ but not to 15 mM K^+. On the other hand, fusions in regions of the axolemma removed from the active zones began to appear by 1 min in 20 mM K^+ and predominated by 5 min, suggesting that the effect of K^+ is complex and involves (i) stimulation of release along the active zones which undergoes concentration-dependent inactivation, and (ii) delayed activation of "ectopic" exocytosis (Ceccarelli *et al.*, 1988a).

5.4. Quantal Noise at Other Synapses

Quantal noise was measured under voltage clamp conditions at invertebrate (Simonneau *et al.*, 1980) and crustacean (Crawford and McBurney, 1976; Finger and Stettmeier, 1981) synapses with the aim of determining the quantal parameters (conductance change and number of channels opened by a quantum) during activation of asynchronous quantal release by presynaptic depolarizations or during spontaneously occurring bursts of postsynaptic current noise.

Noise analysis was employed by Finger and Martin (Finger, 1983, 1985; Finger and Martin, 1987, 1988; Martin and Finger, 1988) to investigate

the secretory capability in response to several pharmacological manipulations, and the quantal store of transmitter, in both the excitatory and the inhibitory synapses at the crayfish neuromuscular junction.

5.4.1. *Estimation of quantum parameters*

Crawford and McBurney (1976) studied intra- and extracellularly recorded voltage noise (the latter corresponding to current noise) at the giant muscle fibre of the spider crab, using L-glutamate, and compared the features of the noise with quantal events produced by the endogenous transmitter. Noise could be detected only in regions of the membrane where quantal events occurred, and noise analysis yielded an apparent half-life for the channel of about 1.4 ms, in accordance with the time constant of the conductance change produced by quantal release. The authors concluded that the transmitter at this synapse is glutamate, and computed, from the ratio of the elementary voltage change (0.44 nV) to the quantal depolarization (5 μV), a quantal content of $\approx$10,000 molecules of transmitter per quantum.

Simonneau *et al.* (1980) studied quantal release of ACh at an identified neuro–neuronal synapse of *Aplysia* and determined the single channel (Cl^- permeable) conductance ($\approx$3 pS) and the miniature postsynaptic current conductance ($\approx$1.5 nS), from fluctuation analysis of ACh noise (by iontophoretic application) and of quantal noise (evoked by presynaptic depolarization). The cut-off frequency in spectra obtained under both conditions indicated a channel lifetime, $\tau \approx 10$ ms, and the authors concluded that the molecular event responsible for the noise was the same in the two situations, indicating the opening of about 500 channels by each quantum of ACh. They were not concerned with estimating the rates of quantal release, however from their pooled data the mean conductance change produced by presynaptic depolarization was in the order of $\bar{\gamma} = 1$ nA/mV $= 1\ \mu$S (Fig. 1, Simonneau *et al.*, 1980), which would yield (indicating by γ_q the quantal conductance) a quantal release rate, $r = \bar{\gamma}/(\gamma_q \cdot \tau) = 10^{-6}/(1.5 \cdot 10^{-9} \cdot 10^{-2}) \approx 6 \cdot 10^4$/s, higher than all other values reported for quantal secretion rates. Finger and Stettmeier (1981) reported a similar analysis on spontaneous bursts of inhibitory current noise at the crayfish neuromuscular junction. The noise appeared to be constituted by randomly occurring inhibitory postsynaptic currents (sIPSC) described by peak conductance (5–10 nS) about 750 times the single channel conductance (14 pS, Dudel *et al.*, 1980), and decay time constants ranging from 5–10 ms, depending on the holding potential. The rate of occurrence of sIPSC was estimated by Campbell's theorem at about 4–600/s.

5.4.2. *Asynchronous release at the crayfish neuromuscular junction*

Crayfish muscle receives both excitatory and inhibitory innervation. The excitatory transmitter at these junctions is glutamate (Takeuchi *et al.*, 1980) whereas GABA is the inhibitory one (Otsuka *et al.*, 1966).

Studies at the excitatory junction

Finger (1985) studied high rates of quantal release at the excitatory junction, evoked by the application of high concentrations of GABA. Maximum rates up to 10^4 quanta/s were attained within a few seconds, the rate declining thereafter with a time constant of 9–20 s; total releases from single terminals were in the order of 100,000 quanta. GABA-induced release was potentiated by pretreatment with serotonin, yielding up to 25,000 quanta/s and total output $\approx$200,000, and did not depend markedly on extracellular Ca^{2+} or Mg^{2+} concentrations. However, extracellular sodium was required. There is no evidence for stimulatory presynaptic GABA receptors in this system, so the author suggested that GABA-induced release is mediated by sodium uptake, coupled to amino acid transport, rather than to osmotic effects (which should not depend on extracellular sodium) or to nerve terminal depolarization by electrogenic amino acid uptake (which should induce Ca^{2+}-sensitive release). In response to 100 mM K^+, peak rates of 1–2.5 $\times$ 10^4 EPSC/s were observed in the same preparation, 200–800,000 quanta being secreted within a few minutes, before exhaustion (Martin and Finger, 1985).

In these studies quantal secretion rates were measured by Campbell's theorem. In successive studies by the same group (Finger and Martin, 1987), the response of the same junction to veratridine (an agent known to induce transmitter secretion at most synapses by activating Na^+ channels in the presynaptic membrane), was investigated by means of higher-moments noise analysis (see Section 5.3 and Segal *et al.*, 1985). Finger and Martin (1987) showed that almost 3 million quanta could be secreted by veratridine, secretion being much more prolonged in the presence of extracellular Na^+ than when Li^+ substituted for Na^+. With Li^+ high rates of release could be produced (up to 10^4 quanta/s), but release rapidly declined towards zero within a few minutes. Restoring Na^+ reactivated secretion to produce final total outputs comparable to those produced by veratridine in the presence of Na^+ during the whole experiment. Veratridine-induced secretion in the presence of Na^+ showed different sensitivity to external Ca^{2+} in two different muscles of crayfish, suggesting that, if intracellular Na^+ acts by releasing Ca^{2+} from intracellular stores, the size of such stores might be remarkably different in different nerve terminals (Finger and Martin, 1987).

Studies at the inhibitory junction

Similar studies were performed on the inhibitory junction in the same preparation. Usually, desensitizing concentrations of glutamate (the excitatory transmitter) were applied to cancel excitatory postsynaptic responses and record inhibitory quantal noise in isolation. High rates of release of inhibitory quanta were induced by glycine (Finger, 1983), by K^+ (Martin and Finger, 1985) or by veratridine (Finger and Martin, 1988; Martin and Finger, 1988).

Glycine activates with very low affinity the GABA-sensitive Cl^- channel involved in the generation of inhibitory postsynaptic currents (IPSCs), but much more effectively it elicits quantal release from the inhibitory nerve terminal (Finger, 1983), possibly by

a mechanism similar to that discussed above for GABA on excitatory terminals (Finger, 1985). Similar to the effect of GABA on excitatory release, glycine produced cumulative release in the order of 140–220,000 inhibitory quanta (Finger, 1983). Veratridine, on the other hand, could elicit an average cumulative secretion of ≈500,000 quanta, with rather large variations among fibers (up to 1.2 million quanta for a long fiber in a large crayfish; Martin and Finger, 1988). As the number of synaptic contacts per neuromuscular junction are more than 1000 in this preparation, a tentative estimate of ≈600 readily releasable quanta per single synapse was suggested (Martin and Finger, 1988).

Similar to excitatory synapses, quantal release induced by veratridine was not strictly dependent on extracellular calcium (though in low-Ca^{2+} it was reduced by ≈30% and displayed a slower time course), was potentiated by serotonin and subsided much more rapidly in Li^+-saline, with a total output only ≈10% of total output produced in Na^+-saline (Martin and Finger, 1988; Finger and Martin, 1988). Following prolonged exposure to Li^+ the nerve terminal appeared blocked and could not be induced to secrete any more quanta (Finger and Martin, 1988).

5.4.3. *Comparison among different systems*

Up to date, noise analysis techniques have been applied to asynchronous quantal secretion to estimate maximum attainable release rates and quantal stores only in few preparations.

The order of magnitude of quantal store in frog cutaneous pectoris motor nerve terminals is close to 1 million quanta (see Table 1) and wide variability has been observed among different fibres and batches of frogs, with total resting stores of quanta ranging from 0.5 to 1.5 million quanta (Haimann *et al.*, 1985; Fesce *et al.*, 1986b; Valtorta *et al.*, 1988; Ceccarelli *et al.*, 1988b; Molenaar and Oen, 1988). Hurlbut *et al.* (1990) observed a loose correlation with nerve terminal length, and estimated an average density of ≈1200 quanta/μm of nerve terminal; their secretion during exhaustive stimulation by black widow spider venom or toxin, with blocked vesicle recycling, is paralleled by an equivalent decline in vesicle store (1.1–1.2 quanta secreted per vesicle lost). This is in agreement with a previous estimate of the number of quanta per active zone (≈1200, Fesce *et al.*, 1986b), as active zones are about 1 μm apart in this preparation (Peper *et al.*, 1974). Peak secretion rates under these conditions were 2000–3000 quanta/s (Fesce *et al.*, 1986b; Valtorta *et al.*, 1988; Hurlbut *et al.*, 1990), i.e. ≈4–5 quanta/s per active zone.

Frog neuromuscular junctions can however be stimulated to secrete at rates up to 10-fold higher, according to Molenaar and Oen (1988), which suggests a maximal output rate in the order of 50 quanta/s per active zone.

At crayfish neuromuscular junctions, the maximum release rates attained were in the order of 10,000 quanta/s; this, assuming 1900 synaptic contacts, corresponds to <5 quanta/s per synapse; the readily releasable store was estimated to be about 600 quanta per inhibitory synapse, and possibly somewhat lower for excitatory synapses (Martin and Finger, 1988). However, these may be overestimates of the "initial store of quanta" as meant above, as recycling of vesicles and quantal turnover was probably not blocked in these experiments. Consistently, a total output of 600 quanta per synapse would be a few times higher than the number of synaptic vesicles counted in excitatory synapses of the crayfish (Nakajima and Reese, 1983), although the latter datum was obtained in a different muscle. It appears that the orders of magnitude of quantal store and release rates are similar for single active zones in frog and single synaptic contacts in crayfish neuromuscular junctions, although both the resting store of quanta and the maximal release rate attainable at a single frog active zone may be several-fold higher than at a single synaptic contact in crayfish.

5.4.4. *Quantal vs nonquantal release*

An interesting observation was reported by Finger and Martin (1988), in their study of the comparative effects of veratridine in Li^+ and Na^+-saline.

They estimated the quantum size from the average value of skew/variance of the noise (Eqn 28, Section 5.3.1), assuming that quantum size did not change during the experiment. Time-varying estimates of quantal release rates were obtained from the ratio [variance]/[squared amplitude]/[equivalent square duration] (corresponding to Eqn 27, Section 5.3.1), corrected for the distribution of shot amplitudes (Section 5.3.1; actually, the correction used was not precisely adequate, as D_3 was neglected in applying Eqns 32 and 33). Finally, the expected current at each value of time was computed as [rate] × [shot amplitude] × [shot duration] (Campbell's theorem). The observed current, however, was higher than this expected value, and particularly so in the initial portion of the experiment, either in Na^+ or in Li^+-saline. When the inhibitory GABA receptor is blocked by picrotoxin, veratridine induces irrelevant postsynaptic currents in this preparation, so the extra-current suggests that nonquantal release also contributes to the postsynaptic current, and particularly so at initial times of exposure to veratridine (Finger and Martin, 1988).

Nonquantal release is one of the factors that can corrupt the results of Campbell's theorem, when applied to mean and variance, as in its presence the mean is not produced exclusively by the shots that generate the process under study. On the other hand, provided that other factors that may affect the mean value of the process are not present, the use of the mean together with variance and skew offers the possibility to study two concomitant processes, i.e. both quantal and nonquantal release of neurotransmitter. This is a further indication of the usefulness of measuring and using higher moments in the study of stochastic processes, as initially proposed by Courtney (1978) as an advanced approach to the investigation of evoked quantal release.

5.5. Synaptic Activity at the Labyrinthine Cyto–neural Junction

The information reaching central vestibular neurons from the semicircular canal, i.e. the afferent

spike-firing pattern, constitutes the result of a series of signal-processing steps. Classically, the semicircular canal transfer function is investigated by studying afferent spike rates in response to rotation. By this approach, static as well as dynamic departures are observed from the predictions of the torsion-pendulum model (Steinhausen, 1931), which describes the hydrodynamic properties of the cupula-endolymph system. Static departures include asymmetry in response to excitatory or inhibitory accelerations, nonlinear intensity functions during excitation and inhibition, and rectification (transient silencing of afferent discharge). Dynamic departures from the model include adaptation in response to long-lasting velocity ramps and harmonic distortions in response to sine-wave stimuli (for a review, see Correia *et al.*, 1977).

The contributions of intermediate steps occurring in the hair cell to the overall signal processing are not clear. Information is available on the mechano-electrical transduction process: cupula displacement in the semicircular canal leads to stereocilial deflection, which in turn produces changes in hair cell membrane potential (receptor potential). The receptor potential is roughly linear with the extent of hair-tip displacement up to $\approx$400 nm, and becomes asymmetrical and nonlinear for greater deflections (Hudspeth and Corey, 1977). Receptor potential presumably activates voltage- and ion-dependent basolateral conductances (Hudspeth and Lewis, 1988), which ultimately result in regulation of transmitter release.

5.5.1. *The hair cell electrical/secretory transfer function*

In order to investigate the mechanisms that translate mechano-electrical activation of the hair cell into quantal secretion of neurotransmitter, at the cyto–neural junction, the EPSPs generated in the efferent fiber can be recorded close to the synapse, and their frequency of occurrence in response to stimulation of the hair cell can be analyzed. The EPSPs generated at the canal cyto–neural junction are recorded together with the all-or-nothing action potentials. However, spike firing can be cancelled by the external application of tetrodotoxin and EPSPs can be examined in isolation (Rossi *et al.*, 1977). Still, difficulties arise in this approach, mainly from the fact that even at rest the EPSPs occur at a considerably high rate (often over 100/s) and their frequency consistently increases during the excitatory stimulation of the canal. This leads to a high degree of overlapping of the individual EPSPs, which prevents direct counting of their numbers. In a recent study (Rossi *et al.*, 1989) the electrical signal arising from the summation of EPSPs was treated as "shot noise" and the procedure of Segal *et al.* (1985) and Fesce *et al.* (1986a), originally developed for endplate recordings (Section 5.3), was employed. Further refinements were introduced to yield continuous, time-varying estimates of EPSP amplitude, h, rate of occurrence, r, and waveform, $w(t)$.

Due to the specific recording condition, where capacitive coupling generally masked DC components, the mean value (membrane potential) was

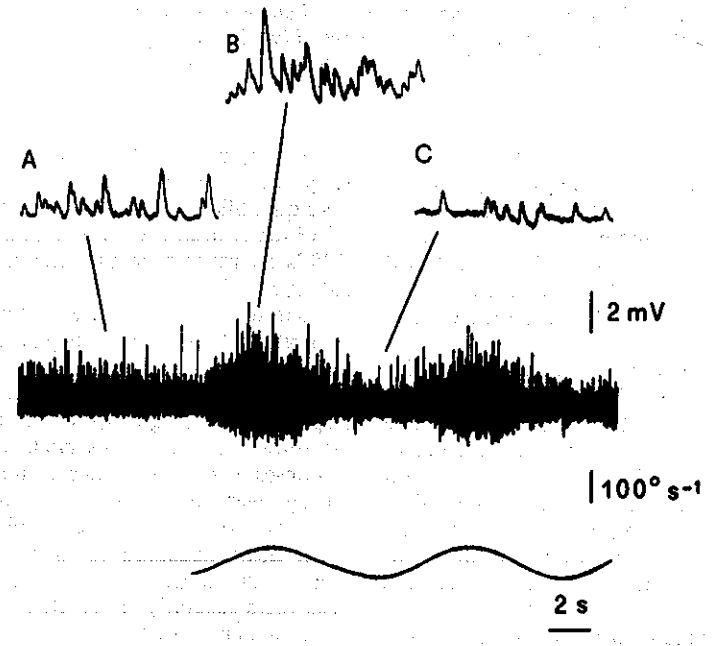

FIG. 16. Oscilloscope recordings of the fluctuations in membrane potential recorded from a posterior canal afferent axon at rest and during sinusoidal rotation at 0.1 Hz (40 deg·s^{-2} peak acceleration) in the presence of TTx. Angular velocity of the turntable is displayed below to mark the period of stimulation. Portions of the recording (100 ms) are shown with enlarged time-scale in the insets: (A) spontaneous activity, (B) excitatory acceleration, (C) inhibitory acceleration. From Rossi *et al.* (1989); reproduced from *Journal of General Physiology* (1989) **94**, 303–327, by copyright permission of the Rockefeller University Press.

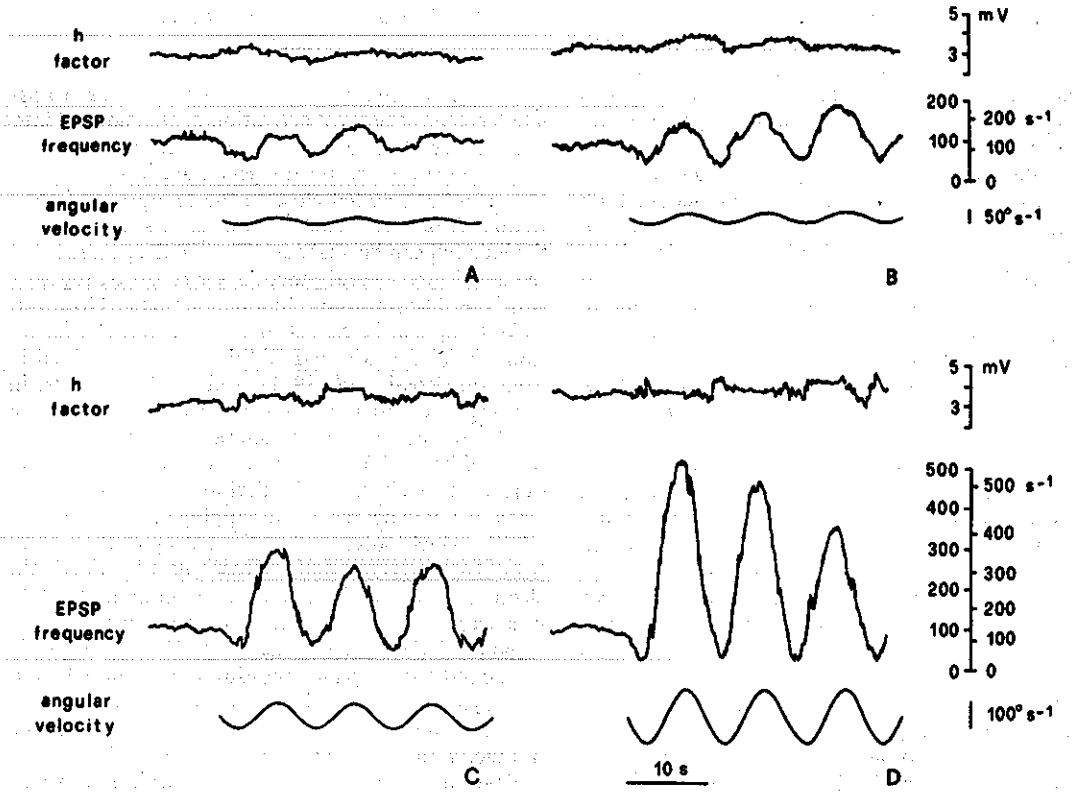

FIG. 17. Measurements of EPSP amplitude parameter h (upper traces) and rate of occurrence r (middle traces) of EPSPs from a single cyto–neural junction at rest and during sinusoidal rotation at 0.1 Hz with peak accelerations of 8 (A), 16 (B), 40 (C) and 87 (D) deg·s^{-2}. Bottom traces show the turntable angular velocity. Values of h not corrected for nonlinear summation and dispersion in amplitudes (correction factors range from 0.7 to 0.9). The two scales for r are uncorrected (left) and corrected (right) values. Note that corrections for nonlinear summation and dispersion of amplitudes roughly compensate each other. From Rossi *et al.* (1989); reproduced from *Journal of General Physiology* (1989) **94**, 303–327, by copyright permission of the Rockefeller University Press.

considered unreliable, and the extension of Campbell's theorem to the skew was employed; possible errors arising from nonstationarity, distributed amplitudes of the events, and nonlinear summation were dealt with as discussed in Section 5.3.1. The EPSP waveforms were generally well described by gamma distribution functions (as for photoreceptor bumps, see Section 5.2.1).

An important novelty in this study was that continuous estimates of variance and skew were obtained by fixing the mean value to zero by means of a brief time constant high-pass filter ($R \cdot C = 1$ ms) and then computing moving averages of the squared and cubed departure of the signal from its zero mean value. These constituted time-varying values of variance and skew, that yielded continuous estimates of EPSP amplitude and rate of occurrence, by using Eqns 27, 28, 32 and 33.

By this approach the secretory response of the hair cell to stimulation of the semicircular canal by sinusoidal rotation at 0.1 Hz (with peak accelerations ranging from 8 to 87 deg/s^2) was determined (Rossi *et al.*, 1989).

A typical response to excitatory and inhibitory rotation is illustrated in Fig. 16 and the results of noise analysis in another fiber are shown in Fig. 17. Responses to excitatory and inhibitory accelerations were quantified in terms of maximum and minimum EPSP rates, respectively, as well as total numbers of EPSPs occurring during the excitatory and inhibitory half cycles (Fig. 18).

Excitatory responses were systematically larger than inhibitory ones (asymmetry). Excitatory responses were linearly related either to peak acceleration or to its logarithm, and the same occurred for inhibitory responses. Silencing of EPSPs during inhibition (rectification) was never observed. Whereas excitatory responses displayed marked adaptation (up to 48%) during several cycles of rotation, no consistent adaptation was observed in the inhibitory response.

All fibers appeared to give responses nearly in phase with angular velocity, at 0.1 Hz, although the peak rates generally anticipated by a few degrees the peak angular velocity.

The authors concluded that asymmetry, adaptation, and at least part of the phase lead in afferent nerve response are of presynaptic origin, whereas the rectification and possible further phase lead reported for spike firing pattern (Blanks and Precht, 1976) arise at the encoder.

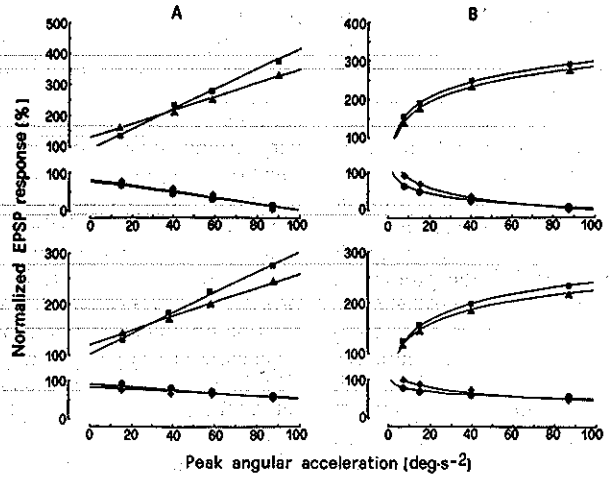

FIG. 18. Responses of EPSP rate to sinusoidal rotation at 0.1 Hz in two different units (A and B), related to the peak values of acceleration. Top: Excitatory (■ and ▲) and inhibitory (● and ◆) peaks in EPSP rate normalized to the resting levels. Bottom: Total numbers of EPSPs occurring during the excitatory and inhibitory phases, normalized to the number of EPSPs during equal periods of spontaneous activity. Asymmetry of the responses is evident. In all panels, ■ and ● refer to responses during the first cycle of stimulation, whereas ▲ and ◆ refer to average responses over several cycles. Differences between the two groups of observations reflect adaptation, which is more evident for excitatory responses. Notice that the unit illustrated in (A) responds linearly with acceleration, whereas that in (B) responds linearly with the logarithm of acceleration. Continuous lines are least-squares fits. From Rossi *et al.* (1989); reproduced from *Journal of General Physiology* (1989) **94**, 303–327, by copyright permission of the Rockefeller University Press.

5.5.2. *The properties of the spike encoder deduced from the relation between EPSP and spike rates*

The labyrinthine cyto–neural junction is a particularly interesting model synapse in that EPSPs generated by secretion of neurotransmitter (which are the result of presynaptic activity) can be recorded in conjunction with the spikes generated postsynaptically in response to the summation of EPSPs. This situation offers the possibility of studying the function of the spike firing mechanism (encoder) in response to its physiological input, i.e. a randomly fluctuating conductance and voltage signal.

An attempt at investigating this aspect was reported by Rossi *et al.* (1989). In the series of experiments discussed above (Section 5.5.1) the authors studied in some junctions both EPSP and spike rates concomitantly. In particular, spikes were counted and cancelled from the digitized recording, and fluctuation analysis was applied to the remaining portions of the record to determine EPSP amplitude and rate of occurrence. Though the analysis was limited to a small sample, interesting information arose from this approach. Spike rates were generally low; fibers with low resting spike rates showed marked rectification of the response, spikes being abolished during the whole inhibitory cycle, and a nonrectified response (though markedly asymmetrical) was exhibited by only one unit which had a resting spike frequency of ≈4/s. Furthermore, as illustrated in the example of Fig. 19, during the excitatory phase of the stimulation, while EPSP rate was rising, spike rate increased even faster (i.e. the number of spikes per 100 EPSPs also increased); the decline in spike rate generally anticipated that of EPSP rate, after the excitatory peak, so that the peak spike rate often preceded the peak EPSP rate by some 0.5 s. This apparent phase lead of spike firing was more consistently observed during the first cycle of stimulation.

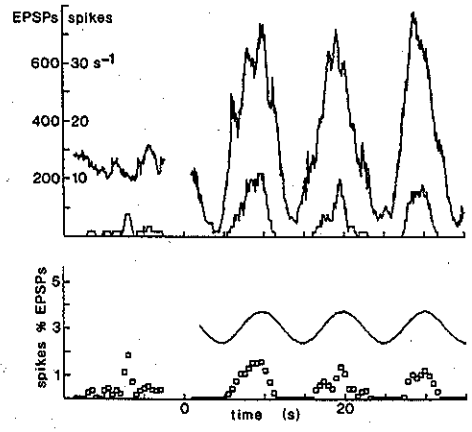

FIG. 19. Simultaneous measurement of EPSP and spike rates from a single unit at rest and during stimulation by sinusoidal rotation at 0.1 Hz with 40 deg·s^{-2} peak acceleration. Top: EPSP rate (the noisier trace) and spike rate (the trace closer to zero). The lower panel shows the number of spikes per 100 EPSPs together with the angular velocity of the turntable that marks the time scale and the period of stimulation. Notice that, as EPSP rate increases, spike rate as well as the number of spikes per 100 EPSPs rise (i.e. spike rate increases more than linearly with EPSP rate). Notice also that spike firing begins to decline prematurely with respect to EPSP rate. From Rossi *et al.* (1989); reproduced from *Journal of General Physiology* (1989) **94**, 303–327, by copyright permission of the Rockefeller University Press.

Spike rate is presumably related to the probability that the fluctuating signal generated by the summation of EPSPs reaches the threshold for firing. Therefore the relation between spike and EPSP rates is expected not to be linear, and rectification (silencing of spike firing) to occur for low EPSP rates, as observed. The nonlinearity of the relation, and the rectification by the encoder, led to amplification of the asymmetry in the spike response. Furthermore, it appears that the relation of spike rate to EPSP frequency is not static. In particular, the premature fall in spike rate indicates that the postsynaptic mechanisms implied in spike generation have complex dynamic properties. Excitatory and inhibitory peaks in EPSP rate showed a variable phase lead with respect to the peak turntable angular velocity (10–27 degrees, Rossi *et al.*, 1989), which is in agreement with the observed phase lead of spike rate (Blanks and Precht, 1976). The premature fall of spike rate during excitation may introduce an apparent further phase lead. Possible causes of this phenomenon include anticipated repolarization during excitation due to the activation of the sodium pump (Taglietti *et al.*, 1977), and partial inactivation of sodium channels.

The relation between spike and EPSP rate is now being studied under different experimental conditions of stimulation, with the aim of defining the characteristics of the transfer function of the spike encoder, i.e. the rules for the translation of the fluctuating signal generated by the summation of EPSPs occurring at random at a given frequency into a modulated spike firing rate.

6. DEALING WITH THE DEPARTURES OF BIOLOGICAL PROCESSES FROM IDEAL MODELS

Any statistical approach in the study of physical as well as biological phenomena suffers from two main limitations: (i) a series of assumptions have to be made on the basic statistical characteristics of the phenomenon, and if any one of these assumptions is false, or even slightly inexact, *bias* errors will ensue in the results of statistical analysis; (ii) the statistical approach is not an exact one, by definition, and *random* errors will necessarily affect all results of statistical analyses, due to intrinsic variability of the phenomenon under study.

Statistical tools are generally "bias-free", in that their application to phenomena that behave exactly in accord with the assumption made will yield results affected by no systematic errors; on the other hand, random errors in the output of statistical analyses, being generated by variability in the data, can theoretically be reduced to any desired size by increasing the sample size (see Appendix, Section 8.1).

Problems generally arise when the biologist turns to a sound statistical procedure in order to solve his experimental problems; in fact, mathematical models may describe physical phenomena rather accurately, but, generally, they are not quite so accurate in describing biological processes.

Quantal release (Section 2) and biological shot noise (Sections 4 and 5) are typical examples. Whereas one may well assume that emission of particles by a radioactive material gives rise to a stationary, uniform point Poisson process (shot noise as properly defined), membrane channel kinetics and "quantal" biological phenomena are generally nonstationary, nonuniform ("quanta" are such only to a very rough first approximation) and nonPoisson (memory of past events and correlations often markedly influence the course of the process). Still, once these differences between the biological process and the ideal model have been recognized, their contributions to the statistical parameters of the process can be evaluated, and unbiased results can thus be obtained. Furthermore, the adequacy of the stochastic model can be double-checked, in general. The inadequacy of the Poisson model as a general model for evoked quantal release has shown up in the inconsistencies resulting from its use in the presence of high quantal contents (Section 2.2.1), and the need for a more general model than the simple binomial one became apparent in a similar way (Section image 2.2.2–2.2.3). Similarly, more sophisticated models than a single open/shut Poisson process have had to be devised for ion channel kinetics on the basis of the accumulated results (Section 4). Stationarity, independence and uniformity of biological shot noise processes have been analyzed and either confirmed or negated for the various processes studied (Section 5). As long as the consistency of the chosen mathematical model can be verified, the reliability of the results obtained by stochastic approaches can be accurately evaluated.

7. CONCLUSIONS

In this paper the applications of stochastic approaches to several aspects of synaptic function have been reviewed. The implicit objective of this survey has been to emphasize the original contributions to our knowledge of synaptic function yielded by these approaches. However, my final ambition would be to lessen the skepticism that many biologists feel toward results obtained by means of sophisticated statistical procedures. Although it is true that biological processes depart in many relevant aspects from ideal mathematical–probabilistic models, these departures can generally be detected and studied, and their effect can be evaluated. One can simply look at the whole question as if the problem were to obtain accurate measurements with a defective instrument. As long as the defects of the instrument are fixed and known, the errors will be systematic and predictable. No one would be afraid of using a ruler with an inch scale to obtain measurements in centimeters.

In reviewing the stochastic approaches to the study of synaptic function it appears that three aspects are of particular importance in undertaking this kind of investigation: (1) The results are bound to be affected by errors due to the stochastic nature of the process under study (random errors); these errors can be reduced, in general, by increasing the number of observations, or the amount of independent data in general; (2) Incorrect assumptions and any kind of contamination of the process by nonlinearity, nonuniformity, nonstationarity and correlations yield biased estimates of the parameters under study; these

are not errors, strictly speaking; in fact, estimating and correcting for "biases" is exactly equivalent to building a more sophisticated stochastic model that incorporates the factors that generate bias in the analysis of experimental data; (3) The adequacy of the stochastic model is therefore crucial, and this points to the most important feature of any statistical procedure, the so-called "robustness". A procedure is robust when its results are correct and reliable even though the mathematical model does not describe accurately the process under study, and in general it is more robust if it requires fewer or looser assumptions (for example nonparametric tests are more robust than the analysis of variance because they do not require that the data be normally distributed). Under this respect an apparent paradox has occurred in the field of stochastic approaches to the study of synaptic function: the apparently simple and direct procedures used to extract information on the statistical properties of evoked quantal release (Section 2) may yield meaningless values for the parameters **p** and **n** of the binomial model, and it has even been questioned whether **p** and **n** have any physiological meaning at all (Barton and Cohen, 1977); on the other hand, results of noise analysis of quantal processes (Section 5) are reasonably accurate notwithstanding the greater complexity of the statistical procedures employed and the relevant departures of biological processes from ideal mathematical models. This is due in part to the high numbers of independent events that generate high frequency shot noise as opposed to the relatively few quantal responses that can be physically evoked in the same preparation under reasonably constant conditions; however, intrinsic "robustness" of power spectral analysis and of Campbell's theorem contribute to the success of noise analysis. It appears therefore that, in order to obtain meaningful, reliable and accurate results by a stochastic approach, model-independence (i.e. reliability of results even when releasing most assumptions implicit in the mathematical model used) and robustness are more important than simpleness (or "self-evidence") of the model and directness of the approach.

The problem of applying stochastic approaches to the study of biological, nonideal processes can therefore be reformulated in the following form:

(1) As for all statistical procedures, the size of random errors arising from variability in the data must be estimated, and possibly reduced by widening the size of the data sample. Residual random errors will set the limit to the accuracy of the estimates.

(2) Any possible deviation of the biological process from ideal behaviour must be considered, the systematic errors introduced by such deviations must be evaluated and corrected for to obtain unbiased estimates.

(3) The statistical procedure employed must be as robust as possible.

(4) Reliability of the results will still be limited by deviations of biological processes from ideality which are (i) undetectable, (ii) overlooked, (iii) not systematic, (iv) unpredictable. Limitations (i) and (ii) affect all results of biological (and not only such) research. Limitation (iii) is probably the most difficult to overcome, but the existence of nonsystematic, nonrandom sources of error should give rise to inconsistent results when the experiments are repeated independently, and their existence should sooner or later become evident. As regards limitation (iv), any model or interpretation of experimental data may turn out to be wrong, when previously unpredictable factors are discovered, but this is just the flavour of research.

This work is dedicated to the memory of my master and dear friend Bruno Ceccarelli, a brilliant scientist, a dedicated teacher, a fair and generous man.

8. APPENDIX: BASIC THEORETICAL PRINCIPLES

This appendix is organized on two levels: principles and concepts are illustrated with the least possible use of formalisms and equations, even though this may sometimes lead to unrigorous statements; small-print paragraphs are included where the same questions are more rigorously dealt with; these parts can be skipped without loss of continuity.

8.1. RANDOM VARIABLES AND STOCHASTIC PROCESSES

The concept of random variable is strictly interlinked to the idea of probability. Whereas a deterministic variable (e.g. the resting potential of a cell) can be expressed as a number, or as a function of some other variable(s), a random variable (e.g. the number of electrons emitted by a radioactive material in one second) has to be expressed in terms of the probability it has to take on each possible value. The accurate description of a random variable therefore requires the complete description of the probability density function $p(x)$, i.e. the probability that the variable takes on the value x, considering any possible value of x. For many purposes, however, it is convenient to describe the random variable in terms of a few parameters, e.g. mean and variance, which indicate, respectively, what will be the average value obtained measuring a great number of times the variable and the square of the departure of its value from the mean.

The stochastic processes studied in neurobiology arise from the summation of elementary events occurring at random and can therefore be considered as composite random variables, generated by the sum of elementary random variables. In dealing with such processes the most important theoretical principles regard the concept of independence and the definition of semi-invariants or cumulants.

It is well known to the scientist that the mean value of a parameter in a population is more precisely estimated if a greater sample is considered. This is because of the commonly employed relation between the standard deviation (S.D.) of single values of a variable and the standard deviation of the mean (or standard error of the mean, S.E.M.) of N randomly taken values of the same variable: $\text{S.E.M.} = \text{S.D.}/\sqrt{N}$.

This relation is but an aspect of an important general relation: it is the same as saying that the variance of the mean of N values of a variable

(S.E.M.)^2 is N times smaller than the variance of the single values (S.D.)^2. This implies that the variance of the *sum* of N values (=mean times N) is N times greater than the variance of the single values, i.e. the variance of the single values "add up" linearly to give the variance of the sum. The only condition for this general statement to hold is that the single values be *independent* from one another. Notice that also the mean of the sum of N variables equals N times the mean of the single variables. Furthermore, it can be noticed that the relation holds for the sum of many independent samples of the same variable as well as for the sum of the values of many independent variables.

The crucial principle of most stochastic analysis procedures is that certain parameters of a population, called semi-invariants or cumulants (the first of these are mean and variance), share with the variance this "additive" property, i.e. a particular cumulant of the sum of many variables is equal to the sum of the cumulants of the single variables.

In the first place it should be noticed that the first cumulant, following this definition, must be the *mean*. The second is the *variance*, i.e. the mean value of the square of the departure from the mean. It is relatively easy to show that the mean value of the cube of the departure from the mean (*skew*) is the third cumulant. Slightly more complex calculations give the higher cumulants, which all share the "additivity" property.

For the sum of N identically distributed random variables, it follows that all cumulants equal N times the corresponding cumulants of the single variables.

The characteristic function

Rigorously, let the probability density function $p(x)$ define the distribution of the random variable x, so that the probability that x takes on a value comprised between x_1 and x_2 is given by the integration of $p(x)$ in dx between x_1 and x_2; then the function

$$\Phi(u) = \int_{-\infty}^{\infty} p(x) \cdot e^{-iux}\, dx \tag{34}$$

is defined "characteristic function", or moment generating function, of the distribution, since the coefficients in its expansion as a series of powers of (iu) are the moments of x (i.e. the mean values of x^n). Notice that the probability that the sum of two variables, $z = x + y$, takes on a particular value Z, is given by the sum of the probabilities that $x = X$ and $y = Z - X$ for all possible values of X:

$$p_z(Z) = \int_{-\infty}^{\infty} p_x(X) \cdot p_y(Z - X)\, dX,$$

so that

$$\Phi_z(u) = \int_{-\infty}^{\infty} dZ\, e^{-iuZ} \cdot \int_{-\infty}^{\infty} dX p_x(X) \cdot p_y(Z - X)$$

$$= \int_{-\infty}^{\infty} dX\, e^{-iuX} \cdot p_x(X) \cdot \int_{-\infty}^{\infty} d(Z - X) e^{-iu(Z-X)}$$

$$\times p_y(Z - X) = \Phi_x(u) \cdot \Phi_y(u). \tag{35}$$

Therefore, the characteristic function of the distribution of the sum of two variables equals the product of the characteristic functions.

The cumulants of the distribution defined by $p(x)$ are the coefficients in the expansion of the *logarithm* of the characteristic function as a series of powers of (iu), and as the logarithm of a product is the sum of the logarithms, the cumulants of $z = x + y$ equal the sum of the cumulants of x and y.

Noise analysis

The most important consequence of the additive property of the cumulants, for the purpose of analysis of a stochastic process, can be expressed briefly by an example. Let the variable under study (X) be produced by the sum of many (say N) independent elementary variables. If you double the amplitude of the elementary variables the mean value of X will double also, the variance of the single variables (and of X) will become four times as big, the skew (related to the third power) will become eight times as big, and so on; on the other hand, if you double the number of independent variables (N), the mean value of X, its variance and its skew etc. will all double and nothing more.

It can be readily realized from this simple example that the use of cumulants allows recognizing whether a change in our variable X is due to a change in the size rather than in the number of the elementary constituent variables. In particular, the ratio between two cumulants, say *variance/mean*, will monitor the amplitude of the elementary variables, since it is not affected by changes in N, whereas particular ratios between powers of the cumulants can be chosen, like *mean^2/variance*, which are not affected by changes in amplitude but monitor changes in N. These principles constitute the basis of Campbell's theorem, which permits deducing the rate of occurrence and amplitude of the elementary electrical perturbations generating a noisy signal, from the mean and variance of the noise. This is the principle of noise analysis. Campbell's theorem was generalized by Rice (1944) to the higher cumulants, and to the frequency composition of the signal (see later), so extending the field of applicability of noise analysis.

8.2. Poisson and Binomial Statistics

Consider that $\mathbf{n}$ events may occur (e.g. $\mathbf{n}$ sites in a nerve terminal may release a quantum of transmitter) and that each event has the probability $\mathbf{p}$ of occurring (e.g. each site has the probability $\mathbf{p}$ of releasing a quantum following a nerve impulse). On each trial, the contribution (c) of each particular event to the composite phenomenon ($\mathbf{m}$ = number of events occurring) will be either 1, if the particular event occurs (probability = $\mathbf{p}$), or 0 if it does not (probability = $1 - \mathbf{p}$). In the average, its contribution will be $\langle c \rangle$ = [contribution when occurring] · [probability of occurring] + [contribution when not occurring] · [probability of not occurring] = $1 \cdot \mathbf{p} + 0 \cdot (1 - \mathbf{p}) = \mathbf{p}$.

Therefore if $\mathbf{n}$ events are possible, the average result, $\langle \mathbf{m} \rangle$, will equal the summed average contributions of $\mathbf{n}$ events, i.e. $\langle \mathbf{m} \rangle = \mathbf{n} \cdot c = \mathbf{n} \cdot \mathbf{p}$.

Similarly, the average square value of the contribution of each event is $\langle c^2 \rangle = 1^2 \cdot \mathbf{p} + 0^2 \cdot (1 - \mathbf{p}) = \mathbf{p}$ again; thus the variance (mean square value minus mean value squared) in c is:

$$\text{var}[c] = \langle c^2 \rangle - \langle c \rangle^2 = \mathbf{p} - \mathbf{p}^2.$$

If the events are independent, the variance in the composite phenomenon equals the sum of the variances of the events, so for **n** events we have

$$\text{var}[\mathbf{m}] = \mathbf{n}\cdot(\mathbf{p} - \mathbf{p}^2) = \mathbf{n}\cdot\mathbf{p}\cdot(1 - \mathbf{p}). \quad (36)$$

and, quite directly:

$$\mathbf{p} = 1 - \text{var}[m]/\langle m\rangle, \quad (37)$$

which is the standard equation to compute **p** for a binomial model (see del Castillo and Katz, 1954b, for the application to quantal release).

These are the classical results of binomial statistics. If the probability of occurrence is $\mathbf{p} \ll 1$ then the term containing $\mathbf{p}^2$ can be neglected and we have $\langle\mathbf{m}\rangle = \text{var}[m] = \mathbf{n}\cdot\mathbf{p}$, which is the classical result of Poisson statistics.

This condition to reduce a binomial process to Poisson statistics helps in defining whether the process under study can be dealt with Poisson statistics, where the single parameter $\mu = \langle m\rangle = \text{var}[m]$ needs be estimated, or binomial statistics, slightly more complex to handle, must be used. As discussed in Section 2.2.1, evoked quantal release may be studied using Poisson statistics when the probability of releasing a quantum is very low; similarly, Poisson statistics can be employed in the analysis of ion-channel noise only provided the number of channels is high and the probability of being open is low. If this is not the case, then the number of channels which are open is relevant, at any time, and the probability of observing further openings is lower than it would be with all channels available for opening. Accordingly, as the mean number of open channels increases, the variance increases less or even decreases, vanishing when all channels are open all the time (see Fig. 3); this is consistent with binomial statistics, where the variance is smaller than in Poisson statistics, by a factor $1 - p$.

Generalized binomial statistics

Consider that in a binomial system the **n** possible events have different probabilities of occurrence. $\{\mathbf{p_k}, \mathbf{k} = 1, 2 \ldots \mathbf{n}\}$. For example let n be the number of sites of quantal release and p_k be the probability that site k releases a quantum in response to a stimulus. Each site has probability of releasing a quantum $p_k(1) = p_k$ and probability of releasing no quanta $p_k(0) = 1 - p_k$; this yields, as above, $\text{mean}_k = p_k$ and $\text{var}_k = p_k - p_k^2$. If the events are independent, we have ($\langle\rangle$ indicates average for the n sites):

$$\langle m\rangle = \Sigma\,\text{mean}_k\{k = 1, 2, \ldots n\} = n\cdot\langle p\rangle$$

and

$$\begin{aligned}\text{var}[m] &= \Sigma\,\text{var}_k\{k = 1, 2, \ldots n\}\\ &= n\cdot\langle p\rangle - n\cdot\langle p^2\rangle\\ &= n\cdot\langle p\rangle\cdot(1 - \langle p\rangle) - n\cdot\text{var}(p). \quad (38)\end{aligned}$$

Notice that Eqn 37 now yields a biased estimate of p.

The overall mean square value will be:

$$\text{MSV} = \langle m\rangle^2 + \text{var}[m] = n\cdot\langle p\rangle + (n\cdot\langle p\rangle)^2 - n\cdot\langle p^2\rangle.$$

The probability of release may vary not only from site to site—let's call this spatial variance in p, V_s—but also among different trials—and this we call temporal variance in p, V_t. In this case the mean value will be $M = n\cdot P$, where the capital letters indicate average values over different sites and different trials. The mean square value will be:

$$\text{MSV} = n\cdot P + n^2\cdot(P^2 + V_t) - n\cdot(P^2 + V_s + V_t)$$

and the variance:

$$\text{var}[m] = \text{MSV} - M^2 = n\cdot P\cdot(1 - P) - n\cdot V_s + (n^2 - n)\cdot V_t. \quad (39)$$

As discussed in Section 2.2.3, spatial variance reduces overall variance, whereas temporal variance increases it. The relative contribution of temporal variance is bound to be more important for $n \gg 1$, unless it is very small compared to the spatial variance. Therefore, $\text{var}[m]/M$ is often greater than $(1 - P)$ and this is why Eqn 37 often underestimates p and may even yield negative values for p.

If n varies as well during successive trials, independently of p (i.e. n and p are uncorrelated in different trials) then, again indicating by capital letters averages over different trials, and letting $V_n = \text{var}[n]$:

$$\begin{aligned}M &= N\cdot P\\ \text{MSV} &= N\cdot P + (N^2 + V_n)\cdot(P^2 + V_t) - N\cdot(P^2 + V_s + V_t)\\ V &= N\cdot P(1 - P) - N\cdot V_s + (N^2 + V_n - N)\cdot V_t +\\ &\quad + P^2\cdot V_n.\end{aligned}$$

These results correspond to those of Perkel and Feldman (1979), who considered even more complex possibilities, and in particular the existence of several different classes of release sites with different statistics.

In principle, higher moments of quantal content can be used to compute the further parameters (V_s, V_t, V_n), as suggested by Courtney (1978). Here we consider the skew (third central moment and third cumulant). For the contribution of each single event (c), we saw that:

$$\langle c\rangle = p, \langle c^2\rangle = p, \text{var}[c] = p - p^2.$$

By a similar approach, as $\text{skew}[c] = E[(c - \langle c\rangle)^3] = \langle c^3\rangle - 3\cdot\langle c\rangle\cdot\langle c^2\rangle + 2\cdot\langle c\rangle^3$: $\langle c^3\rangle = 1^3\cdot p + 0^3\cdot(1 - p) = p$,

and

$$\text{skew}[c] = p - 3\cdot p^2 + 2\cdot p^3 = p\cdot(1 - p)\cdot(1 - 2p).$$

With constant p and n,

$$\text{skew}[m] = n\cdot\text{skew}[c] = n\cdot(p - p^2)\cdot(1 - 2p). \quad (40)$$

For **n** sites with average probability of release, $\langle p\rangle$, and spatial variance in p (among different sites), V_s:

$$\langle m\rangle = n\cdot\langle p\rangle, \quad \text{var}[m] = n\cdot(\langle p\rangle - \langle p\rangle^2 - V_s),$$

and

$$\begin{aligned}\text{skew}[m] = n\cdot\text{skew}[c] &= n\cdot(\langle p\rangle - 3\langle p\rangle^2 - 3\cdot V_s\\ &\quad + 2\langle p\rangle^3 + 6\langle p\rangle\cdot V_s + 2\cdot S_s)\\ &= n\cdot(\langle p\rangle - \langle p\rangle^2 - 3V_s)\cdot(1 - 2p) + 2n\cdot S_s \quad (41)\end{aligned}$$

where S_s = spatial skew in p (skew among different sites). If S_s is neglected, this equation reduces to equation 17 of Miyamoto (1986). The reasons mentioned there to neglect this term, however, are not strong, as skewness in the distribution of the ps among different sites may well be of the same order as $\langle p\rangle^3$ and $\langle p\rangle\cdot V_s$, and especially relevant for small average values of p.

When the variance in p is considered among several trials, V_t, assuming it is equal for all sites and neglecting variations

in n, we have (again indicating by capital letters the expected values over time):

$$M = n \cdot P, \text{var}[m] = n \cdot (P - P^2 - V_s + (n-1) \cdot V_t) \text{ (Eqn 39)}$$

and

$$\text{skew}[M] = n \cdot (P - P^2 - 3 \cdot [V_s - (n-1)V_t]) \cdot (1-2p) + 2n \cdot S_s + n \cdot (n-1) \cdot (n-2) \cdot S_t \quad (42)$$

where S_s and S_t represent the skewness in the spatial (among sites) and temporal (among trials) distribution of p, respectively.

Neglecting the skewness in p, and setting

$$X = V_s - (n-1) \cdot V_t,$$

Eqn 42 reduces to:

$$\text{skew}[m] = n \cdot P \cdot (1 - p - 3X/P) \cdot (1-2p), \quad (43)$$

and, substituting Eqn 39 into Eqn 43:

$$\text{skew}[m] = (1-2p) \cdot [3 \cdot \text{var}[m] - 2 \cdot M \cdot (1-p)],$$

which yields

$$(\text{skew}[m] - 3 \cdot \text{var}[m] + 2)/4M + (3/2) \cdot (\text{var}[m]/M - 1) \cdot p + p^2 = 0. \quad (44)$$

This is equation 21 of Miyamoto (1986), and can be easily solved for p, to obtain an estimate for p which is not biased by variance in p (either spatial or temporal), although residual error may occur as skewness in p and variance in n were neglected. It may be noted that Miyamoto (1986) derived this equation considering spatial variance only for p; the derivation presented here shows that his results were more general than claimed by the author. Knowing p, X can be computed from Eqns 42 and 43:

$$X = \text{skew}[m]/6M - \text{var}[m]/2M + (1-p^2)/3. \quad (45)$$

This is equivalent to equation 20 of Miyamoto (1986), where spatial variance in p, $\text{var}_s[p]$, replaced X, as temporal variance was neglected there. As mentioned above, however, temporal variance is bound to dominate the variance term, $X = \text{var}_s[p] + (n-1) \cdot \text{var}_t[p]$, in general, as $n \gg 1$. It is very likely, therefore, that negative values be found for X by this approach, which would be difficult to justify in terms of spatial variance alone, that must be >0 by the definition itself of "variance".

No experimental data have been published so far using approaches like this, employing higher moments to obtain unbiased estimates of binomial parameters in a generalized binomial model of quantal release.

8.3. Poisson Point Processes

Poisson statistics constitute the basis of random process analysis. Consider a process generated by the random occurrence of independent events, at mean rate, r. The average number of events occurring in any interval with duration Δ is $r \cdot \Delta$. If Δ is taken sufficiently small, then the probability of more than one event occurring during Δ becomes negligible, and we have:

$$p(1) = \text{probability of 1 event in } \Delta = r \cdot \Delta,$$

$$p(0) = \text{probability of no events} \approx 1 - r \cdot \Delta,$$

and

$$\{p(k), k > 1\} \approx 0.$$

If the number of events occurring in n small intervals of duration Δ is considered, we have the same situation as that described above for n sites, each with probability $p = r \cdot \Delta$ of releasing a quantum (Section 8.2), i.e. the process is binomial; the mean number of events occurring in an interval of duration τ, constituted by n small intervals each with duration Δ, will be $m = n \cdot p = n \cdot r \cdot \Delta = r \cdot \tau$. If Δ is considered very small, also $p = r \cdot \Delta$ becomes small and Poisson statistics with mean $m = r \cdot \tau$ will describe the process. Time series of this kind are called Poisson point processes.

In particular, the probability that k events occur in any interval of duration $\tau = n \cdot \Delta$ can be computed as the probability that 1 event occurs in k of the n small intervals that constitute the interval τ, and that no events occur in the remaining $n-k$ small intervals, for all combinations of k out of n (which are $n!/k!/(n-k)!$):

$$\begin{aligned} p_\tau(n) &= [n!/(n-k)!/k!] \cdot [p(1)]^k \cdot [p(0)]^{n-k} \\ &= n \cdot (n-1) \cdot \ldots \cdot (n-k+1) \cdot (r \cdot \Delta)^k \\ &\quad \times (1 - r \cdot \Delta)^{n-k}/k! \end{aligned}$$

Now consider Δ very small. As $\Delta \to 0$, $n \to \infty$ and $n-k+1 \approx n-k+2 \approx \ldots \approx n-1 \approx n$, so, remembering the analytical definition

$$e^x = \lim_{n \to \infty} (1 + x/n)^n,$$

we have:

$$\begin{aligned} p_\tau(k) &= \lim_{n \to \infty} (r \cdot \tau/n)^k \cdot n \cdot (n-1) \cdot \ldots \\ &\quad \times (n-k+1) \cdot (1 - r \cdot \tau/n)^{n-k}/k! \\ &\approx \lim_{n \to \infty} (r \cdot \tau)^k \cdot (1 - r \cdot \tau/n)^n/k! = (m^k/k!) \\ &\quad \times [\lim_{n \to \infty} (1 - m/n)^n] = m^k \cdot e^{-m}/k! \end{aligned}$$

where $m = r \cdot \tau$ = average number of events in an interval of duration τ. This is the classical probability density function of a Poisson distributed random variable, and yields the characteristic function:

$$\begin{aligned} \Phi(u) &= \sum_{k=0}^{\infty} (m^k \cdot e^{-m}/k!) \cdot e^{iuk} \\ &= e^{-m} \cdot \sum_{k=0}^{\infty} (m \cdot e^{iu})^k/k! = \exp[-m(1 - e^{iu})]. \end{aligned}$$

Notice that the logarithm of the characteristic function is:

$$\log[\Phi(u)] = m \cdot (e^{iu} - 1) = \sum_{k=1}^{\infty} m \cdot (iu)^k/k!,$$

so that *all cumulants of the distribution* (=coefficients in the expansion of $\log[\Phi(u)]$ as a series in $[iu]$) *equal m.*

Campbell's theorem

Poisson statistics describe, as we just saw, shot processes where events occur at random, independently and at a stationary mean rate (Poisson point processes). Notice that independence implies that the process has no memory, i.e. the probability of occurrence of future events is not influenced by the past history of the process.

If the signal generated by the events is considered, rather than the number of events occurring at any time, then a mean number of events, $m = r \cdot \tau$, over the interval, τ, will yield a mean value of the signal, $M = m \cdot I_1/\tau = r \cdot I_1$, where I_1 is the area under the signal generated by a single event, and a variance for the signal, $V = m \cdot I_2/\tau = r \cdot I_2$, where I_2 is the area under the square of the signal generated by a single event. This states Campbell's theorem.

If higher cumulants are considered, the same relation holds, i.e. $C_n = m \cdot I_n/\tau = r \cdot I_n$, where I_n is the area under the n^{th} power of the signal generated by a single event. This follows directly from the observation that all cumulants of a Poisson distribution equal the mean (see above), and the number of events in each time interval follows Poisson statistics, provided the events occur at random and independently. This extension of Campbell's theorem to higher cumulants is due to Rice (1944).

Generalizations

In many random processes of interest, the mean rate of the events changes with time, and/or their rate of occurrence is a function of past history. When sufficiently small intervals are considered, even under these circumstances the expectations for the occurrence of the events in the single intervals, of duration Δ, are defined by the single parameter $r(t)$: probability of one event $= p_i(1) = r(t) \cdot \Delta$ and probability of no events $= p_i(0) = 1 - r(t) \cdot \Delta$. Notice, however, that r will not be constant in this case, but will change as a defined function of time and/or of the past history of the process. If $r(t)$ can be considered constant over the small interval $\{t, t + dt\}$, then the occurrences in this interval will still be described by Poisson statistics, with mean $= r(t) \cdot dt$ and variance again $= r(t) \cdot dt$. Over a time period of longer duration, say $\{t, t + \tau\}$, the expectations of the occurrences will be:

$$\text{MEAN} = \text{VAR} = \int_t^{t+\tau} r(t) \cdot dt = \langle r \rangle \cdot \tau,$$

$\langle r \rangle$ being the average value of $r(t)$ over the interval $\{t, t + \tau\}$.

The problem is more complex for the signal generated by the process, $x(t)$, which is contributed to by all events that have occurred previously. In particular, if the function $w(t)$ describes the waveform (time course) of a single shot, then each event that occurred at a particular time, τ, will contribute $w(t - \tau)$ to the signal at time t, and $w^2(t - \tau)$ to its square. As the mean and variance of the occurrence in the small interval $\{\tau, \tau + dt\}$ are both equal to $r(\tau) \cdot dt$, we have:

$$\text{MEAN} = \int_{-\infty}^{t} r(\tau) \cdot w(t - \tau) \cdot dt$$

and

$$\text{VAR} = \int_{-\infty}^{t} r(\tau) \cdot w^2(t - \tau) \cdot dt,$$

which are equations 2.6–10 of Rice (1944) and state the extension of Campbell's theorem to nonstationary processes (see the discussion of filtering and convolution, below, and Fig. 20, for the meaning of integrals like these). Notice that the integrals in these equations are not zero only for $(t - \tau)$ smaller than the duration of a single event (see Fig. 20 for a pictorial representation). So, if $r(t)$ can be considered constant over the duration of a single event it can be taken out of the integral sign and $\text{MEAN}(t) = r(t) \cdot I_1$, $\text{VAR}(t) = r(t) \cdot I_2$. Campbell's theorem can then be applied for every single value of t, if an ensemble of records of the same time-varying process is available.

If the amplitude of the events varies with time, and we let $h(t)$ describe the height of the events as a function of their occurrence time, then the above equations become:

$$\text{MEAN}(t) = \int_{-\infty}^{t} r(\tau) \cdot h(\tau) \cdot w(t - \tau) \cdot dt \quad (46)$$

and

$$\text{VAR}(t) = \int_{-\infty}^{t} r(\tau) \cdot h^2(\tau) \cdot w^2(t - \tau) \cdot dt, \quad (47)$$

which are the equations used by Grzywacz *et al.* (1988) to deduce shot rate of occurrence and height during the fast transients that follow exposure of *Limulus* photoreceptors to brief flashes of light (Section 5.2.2).

8.4. Fourier Analysis and Power Spectra

It can be mathematically demonstrated that a time varying signal can be expressed as the sum of an infinite number of sinusoids at different frequencies, each with particular amplitude and phase delay (see, e.g. Bendat and Piersol, 1971). These sinusoids can be considered as pure frequency components of the signal, and the amplitude of each frequency component can be measured, in principle, by filtering through a narrow band filter adjusted on the frequency under study and measuring the power dissipated through a unitary resistor (1 Ohm) by the remaining signal, from which all the other frequencies have been eliminated. This was in fact the usual procedure before fast digital computers became available, and through this procedure a power density function, or *power spectrum* could be defined. Amplitude and phase of the frequency components can also be computed by means of Fourier transforms of the original signal, which is done by the computer.

An electrical event, like a miniature endplate potential or the current through an ion channel, can be described in terms of its frequency composition (or its spectral density). It is important to our purpose here to study what will be the frequency composition of the signal arising from the summation of many such events. Assume that the single event is fed through a narrow bandpass filter centered at the frequency f: its component at frequency f is obtained; if the composite signal is now input, only the component of frequency f from each event will contribute to the output. If the events occur independently and at random, the additivity of the variance of independent random variables can be advocated to predict that the variance of the output (power at frequency f of the composite signal) will be given by the sum of the energies of the components of frequency f of the single events. Therefore the power density (in any frequency band) of a signal generated by N/sec events occurring at random will be N times the energy density of the single event, so that *the frequency composition of a composite signal is the same, in relative terms, as that of the elementary events that generate it.* This statement can be rigorously demonstrated (see Rice, 1944), and illustrates the important information contained in the power spectrum of a stochastic process: it permits deducing the frequency composition of the underlying elementary events

(at least under certain constraints which will be discussed later). This in turn gives information on the waveform of the events, which in some cases can even be fully reconstructed from the power spectrum of the process (see Section 8.5, and Wong and Knight, 1980).

Power spectrum of stationary shot noise

Consider the product of a time-varying signal, $x(t)$, and a complex sinusoid, $e^{-2\pi ft i}$. The average value over a finite time period of duration, T, of this product is:

$$X(f)/T = (1/T)\cdot\int_0^T dt x(t)\cdot e^{-2\pi ft i}$$

where $X(f)$ is known as the finite Fourier transform of $x(t)$ in f, and is meaningful only for values of f that equal integer multiples of $1/T$. The true Fourier transform is theoretically obtained for T infinite, and becomes therefore meaningful for any value of f.

We just saw that a time varying signal can be considered as the sum of many sinusoids, each with different period, amplitude and phase. Let therefore:

$$x(t) = \sum a_k\cdot\exp(2\pi f_k ti + \Phi_k i)\cdot\Delta f\ \{k = -\infty, \infty\}, \quad (48)$$

where

$$f_k = k\cdot\Delta f \quad \text{and} \quad \Delta f = 1/T \to 0.$$

We have:

$$\begin{aligned} X(f) &= \int_0^T dt\, e^{-2\pi ft i}\cdot\sum a_k\cdot\exp(2\pi f_k ti + \Phi_k i)\cdot\Delta f \\ &\quad \{k = -\infty,\infty\} \\ &= \sum a_k\cdot\int_0^T dt\, e^{-2\pi ft i}\cdot\exp(2\pi f_k ti + \Phi_k i)/T \\ &\quad \{k = -\infty,\infty\} \\ &= \sum a_k\cdot\int_0^T dt\, e^{-2\pi(f-f_k)ti + \Phi_k i}/T \quad \{k = -\infty,\infty\}. \end{aligned}$$

The integral at the right hand side of this equation equals zero for all values of f_k, except for $f_k = f$, where its value is $e^{\Phi_k i}$. Therefore:

$$X(f_k) = a_k\cdot e^{+\Phi_k i}, \text{ and} \quad (49)$$

the frequency components of $x(t)$ have amplitude and phase equal to the amplitude and phase of the Fourier transform of $x(t)$. This is the basis for the mathematical computation of frequency components and power spectra, which is rapidly performed by digital computers. In particular the *estimated* power *density* of $x(t)$ at frequency f, $\hat{S}_x(f)$, equals the square module of the Fourier transform of $x(t)$, for frequency f, divided by the frequency bandwidth over which the transform was computed ($\Delta f = 1/T$); if only positive values are considered for f, the estimated power spectrum becomes:

$$\hat{G}_x(f) = \hat{S}_x(f) + \hat{S}_x(-f) = 2/T\cdot|X(f)|^2.$$

The true power spectrum equals the *expected value* of this estimate.

The signal generated by shot noise at any time, $x(t)$, is contributed to by all events occurred at previous times; if $n(\tau)$ events actually occurred in the small interval $(\tau, \tau + d t)$, and the function $w(t)$ describes shot waveform then:

$$x(t) = \int_{-\infty}^{t} n(\tau)\cdot w(t-\tau)\cdot d\tau = \int_0^{\infty} n(t-\tau)\cdot w(\tau)\cdot d\tau$$

(see Fig. 20 for the interpretation of integrals of this kind). Under these conditions the power spectrum of the signal equals the product of the spectra of shot occurrence, $n(t)$, and shot waveform, $w(t)$. In particular, $G_x(f) = G_w(f)\cdot G_n(f)/2$.

In fact:

$$\begin{aligned} \hat{G}_x(f) &= \frac{2}{T}\cdot\left|\int_0^T\int_0^{\infty} n(t-\tau)\cdot w(\tau)\cdot d\tau\cdot e^{-2\pi ft i}\right|^2 \\ &= \frac{2}{T}\cdot\left|\int_0^{\infty} d\tau\cdot w(\tau)\cdot e^{-2\pi ft i}\cdot\int_{-\tau}^{T-\tau} du\cdot n(u)\right. \\ &\quad \left.\times e^{-2\pi fui}\right|^2 \quad \{u = t-\tau\} \\ &\approx \frac{2}{T}\cdot|N(f)\cdot W(f)|^2 = \hat{G}_n(f)\cdot G_w(f)/2 \end{aligned} \quad (50)$$

where

$$\hat{G}_n(f) = \frac{2}{T}\cdot|N(f)|^2$$

is the estimated power spectrum of the shot occurrence rate, $n(t)$, and $G_w(f) = 2\cdot|W(f)|^2$ is the energy density function of shot waveform $w(t)$.

It is of interest to consider the power spectrum of the Poisson point process, $n(t)$:

$$\begin{aligned} \hat{G}_n(f) &= \frac{2}{T}\cdot\int_0^T dt\cdot n(t)\cdot e^{-2\pi ft i}\cdot\int_0^T du\cdot n(u)\cdot e^{2\pi fui} \\ &= \frac{2}{T}\cdot\int_0^T dt\cdot\int_0^T du\cdot e^{-2\pi f(t-u)i}\cdot[n(t)n(u)]. \end{aligned}$$

Let's consider the expected value of this expression, $G_n(f) = E[\hat{G}_n(f)]$. For $t \neq u$, $n(t)$ and $n(u)$ are uncorrelated and

$$\begin{aligned} E[n(t)\,dt\cdot n(u)\,du] &= E[n(t)\,dt]\cdot E[n(u)\,du] \\ &= r(t)dt\cdot r(u)du; \end{aligned}$$

for $t = u$,

$$\begin{aligned} E[n^2(t)\,dt\,du] &= E[n(t)]^2\,dt\,du + \mathrm{var}[n(t)\,dt] \\ &= r^2(t)\,dt\,du + r(t)\,dt. \end{aligned}$$

Therefore:

$$G_n(f) = \frac{2}{T}\int_0^T dt\cdot\int_0^T du\cdot e^{-2\pi f(t-u)i}\cdot r(t)r(u) + \frac{2}{T}\int_0^T dt r(t).$$

Thus:

The power spectrum of shot (actual) occurrences equals

$$G_n(f) = G_r(f) + 2\cdot\langle r\rangle. \quad (51)$$

where $G_r(f)$ is the power spectrum of the expected rate of occurrence as a function of time, $r(t)$, and $\langle r\rangle$ is the mean shot rate. In conclusion we have:

$$G_x(f) = G_w(f)\cdot[G_r(f)/2 + \langle r\rangle]. \quad (52)$$

For stationary processes, $r(t) = \langle r\rangle = \text{constant}$, so $G_r(f) = 0$ for any $f \neq 0$, and Eqn 52 reduces to $G_x(f) = \langle r\rangle\cdot G_w(f)$, i.e. the power spectrum of the noise is $\langle r\rangle$ times the power spectrum of the single shot for all frequencies other than zero. For $f = 0$,

$G(f)$ is the square of the DC component of the signal, and thus $G(0) = (\langle r \rangle \cdot I_1)^2$ = the square of the mean signal.

Power spectrum of nonstationary shot noise

The power spectra of signals generated by nonstationary random processes, or processes where the parameters of the shots are correlated, have been studied in several theoretical and experimental papers (Rice, 1944; Schick, 1974; Heiden, 1969; Wong and Knight, 1980; Sigworth, 1980, 1981a; Fesce *et al.*, 1986a). Many complex derivations have been published, each of them concerned with some particular aspects of the problem. A general feature is however present in all these analyses, which has a rational basis in the analysis of generalized point Poisson processes presented above (Section 8.3).

If the rate of occurrence of the events, $r(t)$, and/or their height, $h(t)$, or even their waveform, $w(t)$, change as deterministic functions of time, or as functions of the previous history of the process, still one feature remains general, namely that the random variable in the process is the number of events occurring in any small time interval, i.e. the "instantaneous rate of occurrence". This random variable obeys Poisson statistics, in the sense that the mean and variance of the number of events occurring in any small time intervals are both and solely determined by $r(t)$, the expected rate at the particular time considered. Therefore the term $\langle r \rangle \cdot G_w(f)$, discussed above in Eqn 52, will always be present in the noise power spectrum, $G_x(f)$.

For nonstationary rate of occurrence, the power spectrum is (Eqn 52) $G_x(f) = [G_r(f)/2 + \langle r \rangle] \cdot G_w(f)$. At all frequencies an extra term $G_r(f) \cdot G_w(f)/2$ is present, and the spectrum of the noise will have a different shape from that of the single event for all frequencies where $G_r(f)/2$ is significant with respect to $\langle r \rangle$. Generally shot rate changes more slowly, with time, than the signal generated by a single shot, and $G_r(f)$ will therefore be significant over only a part (at the low frequencies) of the single shot spectrum $G_w(f)$. This permits fitting the noise spectrum to the shape of $G_w(f)$, limited to the high frequency region, to extract from the noise information on the waveform of the single shot, $w(t)$, as discussed in Section 5.2 (see Wong and Knight, 1980; Fesce *et al.*, 1986a).

However, if the average value of the signal over an ensemble of recordings is subtracted at each time point from the single records, before the spectrum is computed, or the spectrum of the ensemble average is subtracted from the spectrum of each record, then the resulting power spectra, "decompound spectra", will be purged of contributions arising from time-dependent changes in $r(t)$ and will reduce to the "stationary" shape, $G_x(f) = \langle r \rangle \cdot G_w(f)$ (Conti *et al.*, 1980; Sigworth, 1981; Grzywacz *et al.*, 1988).

Similar arguments can be developed to show that variations in shot amplitude with time also contribute extra-factors to the power spectra, which become negligible in the high-frequency region, provided these changes are slower than the time course of a single shot (Wong and Knight, 1980); again, the "decompound spectrum", which can be computed if an ensemble of recordings of the same process is available, will be purged of these contributions and display the "stationary" shape (Grzywacz *et al.*, 1988).

Even correlations among the parameters of the shot (occurrence, height, duration, waveform) do not cancel the "stationary component" of the noise spectrum, $\langle r \rangle \cdot G_w(f)$, but just add (or subtract for negative correlations) components in the region of the power spectrum correspondent to the time-scale of the correlations (Heiden, 1969; Wong and Knight, 1980).

A general argument was developed by Fesce and colleagues (1986a) to show that the behaviour of the frequency composition of higher semi-invariants, in the presence of nonstationarity or correlations, follows the same rules. The authors concluded that the removal of the frequency bands where contributions from these factors are significant yields back a signal which can be dealt with as if it were generated by uncorrelated shots occurring at random with stationary rate. This removal of frequency bands can be performed by appropriately filtering the signal. The resulting process can then be analyzed using Campbell's theorem, and, if necessary, its extension to higher cumulants, even though only one recording of the process may be available (Fesce *et al.*, 1986a,b; Rossi *et al.*, 1989).

Finally, notice that once the uncontaminated region of the noise power spectrum is fit to the shape of the shot spectrum, the departures in the contaminated region yield information on the magnitude and time-scale of the contaminating process. For example, the general time course of changes in shot rate can be estimated to study fast bursting patterns in shot occurrence (Fesce *et al.*, 1986a,b), as illustrated in Fig. 10 (bottom panel), where the power spectrum of $r(t)$ is recovered from the signal spectrum, $G_x(f)$ and the shot spectrum appropriately scaled, $\langle r \rangle \cdot G_w(f)$, by rearranging Eqn 52: $G_r(f) = 2 \cdot [G_x(f)/\langle r \rangle G_w(f) - 1]$; similarly, the magnitude of the reduction in variance due to negative correlation among shot heights, and the time-scale of such correlation, can be evaluated (Wong and Knight, 1980), as illustrated in Figs 7–8.

8.5. MINIMUM PHASE ANALYSIS

The minimum phase property is often possessed by shot waveforms in biological noise and can be exploited to deduce shot waveform directly from the power spectrum of the noise when shots cannot be examined in isolation (Wong and Knight, 1980; Rossi *et al.*, 1989). It is of interest to try and define this property in some detail.

Any function of time can be considered as the sum of many sinusoids. Each sinusoid (frequency component) is defined by a frequency of oscillation, an amplitude (module) and a delay on the time axis (phase angle). The power density equals, for each frequency, the square of the amplitude of the sinusoid at that frequency. No information on the phases of the frequency components is retained in the power spectrum. The power spectrum of stationary shot noise has the same shape as the energy density function of the single shot, and the amplitudes of the

frequency components that constitute the shot waveform, $w(t)$, can therefore be easily derived. However, no information is obtained on the phases of the frequency components of $w(t)$.

If $w(t)$ is generated by a physical system that behaves as a stable filter (for example is generated by the resistance + capacitance of a physical membrane in response to an impulse), then it will have the property of "minimum phase", i.e. the phases of its frequency components will be univocally determined by the amplitudes. It directly follows that the unknown phases can be derived from the known amplitudes (from the power spectrum) when $w(t)$ can be assumed (or shown) to be a "minimum phase" function. Once both the amplitude and phase of each frequency component of $w(t)$ are known, the waveform is easily reconstructed by efficient algorithms such as the "fast Fourier transform".

As many biologists may be puzzled by the expression "a physical system that behaves as a stable filter", a few remarks on filters and filtering theory follow.

A physical system (for example the cell membrane) produces specific output signals (e.g. MEPPs) in response to specific inputs (e.g. MEPCurrents). The output signal, $y(t)$, is obviously determined by past values only of the input (a physical system cannot predict the future), and can therefore be represented, in general as a function of past values, or *moving average*, of the input, $x(t)$:

$$y(t) = \int_{-\infty}^{t} d\tau x(\tau) \cdot w(t-\tau); \qquad (53)$$

$w(t)$ is the weighting function for the moving average, and can be seen as an averaging window that moves on $x(t)$ along the time axis to yield $y(t)$. Figure 20 is a pictorial representation of Eqn 53 and gives a geometrical interpretation of the process of filtering as a moving average. The physical system can be considered as a *filter*, and $w(t)$ is the filter transfer function. We consider here only linear systems; however, in the presence of nonlinear gain, the output can often be "linearized" to bypass the problem (see for example the correction factor for nonlinear summation of EPPs; Martin, 1955, 1976).

The output of the system (filter) is a weighted average of the past values of the input, and the weights given to each past value are determined by the filter transfer function, $w(t)$: for example, the value the input had 2.5 seconds before will be weighted by $w(2.5)$, the value τ seconds before by $w(\tau)$ and so on; quite obviously, any value the input will assume in the future is not considered, thus the value the input will have at any time, τ, in the future will be weighted by $w(-\tau) = 0$. The filter is *causal* (as it only reacts to past inputs) and its transfer function

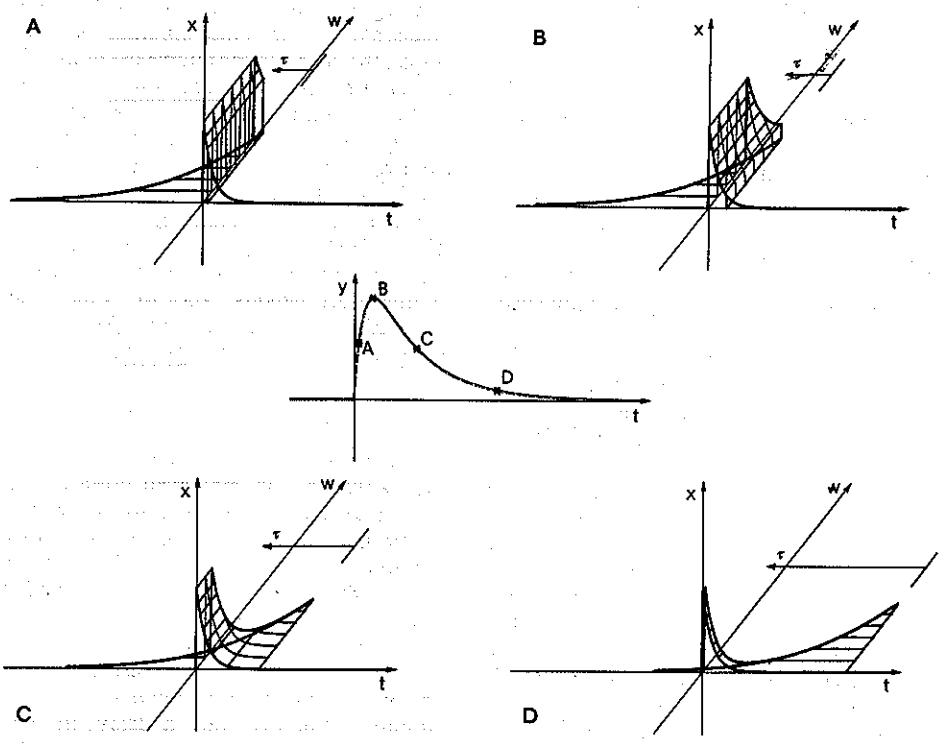

FIG. 20. Geometrical representation of filtering and convolution. The input function, $x(t)$ is represented in panels A–D on the vertical plane. The filter transfer function (weighting function), $w(\tau)$, is represented on the horizontal plane. The output function, $y(t)$, shown in the centre panel, is determined, at each value of time, by shifting the weighting function on the time axis and considering the volume of the solid generated by the product $x(t-\tau) \cdot w(\tau)$; this is illustrated in panels A–D for 4 different values of time (asterisks in the centre panel).

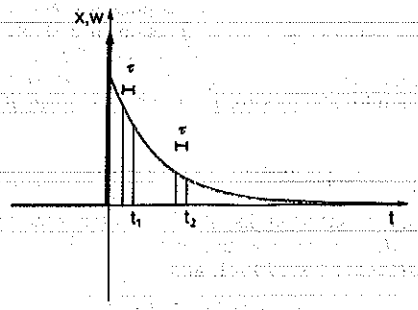

FIG. 21. Response of a filter to an impulsive input, represented by the upward arrow at zero time. In computing the output, $y(t)$, as the weighted average of past values of the input, at each value of time t the weight for the only nonzero value of the input is $w(t)$. Therefore $y(t)$ just equals the weighting function of the filter, $w(t)$. Note that for the particular form of $w(t)$ here represented (a single exponential), each value of $w(t)$ is easily expressed in autoregressive terms, i.e. as a function of its own previous values. For example, the time interval required for the exponential to fall by 20% (τ) is indicated in the figure, and it can be observed that $w(t_1) = 0.8 \cdot w(t_1 - \tau)$, $w(t_2) = 0.8 \cdot w(t_2 - \tau)$, and in general $w(t)$ can be predicted as 0.8 times the value $w(t)$ had τ seconds before.

w(t) *is also said to be causal*, which simply implies w(t) = 0 *for all negative values of t*.

Autoregression

Assume for example the filter weighting function is a single exponential: $w(t) = (1/\Theta) \cdot e^{-t/\Theta}$, and consider the response of the filter to an impulse input (Fig. 21). If the input to the system is just a unit-area impulse at zero time, the output will be $y(t) = w(t)$, as the only input value to average is 1, for zero time, and in determining the output of the system, at each value of time (τ), it will be weighted by $w(\tau)$ to yield the output $y(\tau) = w(\tau)$. It may be observed that, except at zero-time, where there is input to the system, the output of the filter can be easily predicted from previous values of the output itself: the output at time (t) just equals the output at time ($t - \tau$) multiplied by $e^{-\tau/\Theta}$:

$$y(t) = (1/\Theta) \cdot e^{-t/\Theta} = (1/\Theta) \cdot e^{-(t-\tau)/\Theta} \cdot e^{-\tau/\Theta} = y(t-\tau) \cdot e^{-\tau/\Theta}.$$

This is a general feature of stable filters: in the absence of input, the output of a stable system is a function of its state and its past history, and it is possible to predict the output as a function of past values only of the output itself. This constitutes the autoregressive approach (the signal behaving as a moving average of itself). The weighting function for the autoregression, $\alpha(t)$, can be defined and interpreted exactly as the filter weighting function, $w(t)$, was defined and interpreted above. The only differences are: (i) $\alpha(t)$ operates on past values of the output itself rather than of the input to the system; (ii) the output can be determined, at least in part, by the *present* value of the input, so $w(0)$ may be different from zero, whereas, in predicting the output (at the present time) as a function of its own past values, its present value cannot be considered, and therefore $\alpha(t)$ must be zero for $t = 0$ (the present time) as well as for negative values of t (future times). For our example, $\alpha(t)$ is just a single point, i.e. always zero except for the arbitrarily chosen value τ where $\alpha(\tau) = e^{-\tau/\Theta}$.

For a stable system, thus, with no input the value of the output, $y(t)$, equals the weighted average of its own past values, using $\alpha(t)$ as the weighting function. It directly follows that, if a weighting function $a(t) = -\alpha(t)$ is used instead, $-y(t)$ is obtained, and if a further weight is added, $a(0) = 1$, we obtained $y(t) \cdot a(0) - y(t) = 0$. In conclusion, an autoregressive weighting function, $a(\tau)$ $\{= 1$ for $\tau = 0$, and $= -\alpha(\tau)$ for $\tau > 0\}$, exists for a stable filter, such that the weighted average of the output of the filter, in the absence of input, using $a(\tau)$ as the weighting function, is always zero. As the transfer function of the filter, $w(t)$, equals its output to an impulse input (Fig. 21), what we just saw for $y(t)$ holds for $w(t)$ as well: the weighted average of the past values of $w(t)$ using the autoregressive function $a(t)$ as the weighting function is always zero; this is not true at time = 0, where an input is present, previous values are all zero, and we just have $w(0)$. For our example, $a(t) = 1$ for $t = 0$, $a(t) = -\alpha(t) = -e^{-\tau/\Theta}$ for $t = \tau$, $a(t) = 0$ for all other values of t; thus the weighted average of $y(t)$ with weights $a(t)$ equals

$$y(t) \cdot a(0) + y(t-\tau) \cdot a(\tau) = (1/\Theta) \cdot e^{-t/\Theta} - e^{-(t-\tau)/\Theta} \cdot e^{-\tau/\Theta} = 0;$$

for $t = 0$, however, $y(t - \tau) = 0$ and we have $y(0) \cdot a(0) + 0 \cdot a(\tau) = y(0) = w(0)$.

This relation between $w(t)$ and $a(t)$ has been derived from $w(t)$ being the transfer function of a *causal* filter (a physical system that does not predict the future) and of a *stable* filter (whose output in the absence of input is determined by the past history of the system only). This same relation defines the filter transfer function, $w(t)$, as a "*minimum phase*" function, which makes it possible to determine the phases of its frequency components from their amplitudes. This permits the direct reconstruction of the shot waveform from noise power spectra (yielding information only on amplitudes of frequency components), provided the shot waveform can be considered as the output of a stable causal filter to an impulse input.

Waveform reconstruction

The expression at the right hand side of Eqn 53 is defined as the convolution of $x(t)$ with $w(t)$, and convolution is generally indicated by the operator $*$:

$$y(t) = \int_{-\infty}^{t} d\tau x(\tau) \cdot w(t-\tau) = x(t) * w(t). \qquad (53a)$$

If Fourier transforms are considered, it can be shown that the Fourier transform of the *convolution* of two functions equals the *product of the Fourier transforms* of the two functions (see Section 8.4 and Eqn 50 in particular). Therefore, if we indicate by $\supset$ Fourier transformation, we have:

$$x(t) \supset X(f); \quad y(t) \supset Y(f); \quad w(t) \supset W(f);$$
$$y(t) = x(t) * w(t) \supset X(f) \cdot W(f). \qquad (53b)$$

Now let the input to the system be a unit amplitude impulse at time, $t = 0$: $x(t) = \delta(t)$, $\delta(t)$ being Dirac's delta

function, such that $\delta(t)dt$ $\{= 0$ for $t \neq 0$, $= 1$ for $t = 0\}$. It is easily shown that the Fourier transform of an impulse is a constant ($=1$ for a unit area impulse), so that $x(t) \supset X(f) = 1$, and:

$$y(t) = x(t) * w(t) = \delta(t) * w(t) \supset 1 \cdot W(f) = W(f) \subset w(t). \tag{54}$$

As we saw, $w(t)$ is zero for all times before zero ($t < 0$) and is therefore *causal*. Consider now (Fig. 22) the symmetric function $r(t) = w(|t|)/2$ and the antisymmetric function $j(t) = r(t) \cdot \text{sign}(t)$ $\{= w(t)/2$ for $t > 0$, $= -w(|t|)/2$ for $t < 0\}$, and observe that $r(t) + j(t) = w(t)$. When taking Fourier transforms, as $e^{-2\pi fti} = \cos(2\pi ft) - i \cdot \sin(2\pi ft)$, the symmetrical part of $w(t)$ will generate the real part, $R(f)$, of its transform (cosine is symmetrical), whereas its antisymmetrical part will generate the imaginary part, $J(f)$ (sinus is antisymmetrical):

$$w(t) = r(t) + j(t) \supset R(f) + J(f) = W(f).$$

As $r(t)$ and $j(t)$ are strictly related, the real and imaginary part of the transform of $w(t)$ are also strictly related to each other: in particular, as $j(t) = r(t) \cdot \text{sign}(t)$ and the Fourier transform of sign(t) is just $1/(\pi fi)$:

$$j(t) = r(t) \cdot \text{sign}(t) \supset R(f) * 1/(\pi fi), \text{ and} \tag{55}$$

$$W(f) = R(f) + J(f) = R(f) + R(f) * 1/(\pi fi). \tag{55a}$$

This equation states that the imaginary part of the Fourier transform of a causal function can be deduced from its real part by convolution with $1/(\pi fi)$ (Kramers–Kronig method).

Now let's recall the observations presented above on the autoregression of the transfer function of a stable causal filter: we saw that the weighted average of past values of $w(t)$, using the autoregressive function $a(t)$ as the weights, equals zero for all times except at zero time, where it equals $\delta(t)$:

$$\int_{-\infty}^{t} d\tau w(t-\tau) \cdot a(\tau) = \delta(t).$$

Note that the left-hand side of this equation is the convolution of $a(t)$ and $w(t)$ so that taking Fourier transforms: $w(t) * a(t) \supset A(f) \cdot W(f) = 1$, and

$$a(t) \supset A(f) = 1/W(f). \tag{56}$$

Both $a(t)$ and $w(t)$ are causal, as we saw, and also causal is the function $t \cdot w(t)$, as it also equals zero for all negative values of t; the Fourier transform of $t \cdot w(t)$ is

$$\frac{d}{df} W(f).$$

We therefore have:

$$\begin{aligned} \int_{-\infty}^{t} d\tau a(t-\tau) \cdot \tau \cdot w(\tau) &= t \cdot \phi(t) \\ &= a(t) * [t \cdot w(t)] \supset A(f) \cdot \frac{d}{df} W(f) \\ &= 1/W(f) \cdot \frac{d}{df} W(f) \\ &= \frac{d}{df} \log[W(f)]. \end{aligned} \tag{57}$$

As $w(t)$ is causal, the expresion in the integral in Eqn 57 equals zero for $\tau < 0$; as $a(t)$ is also causal, $a(t-\tau) = 0$ for

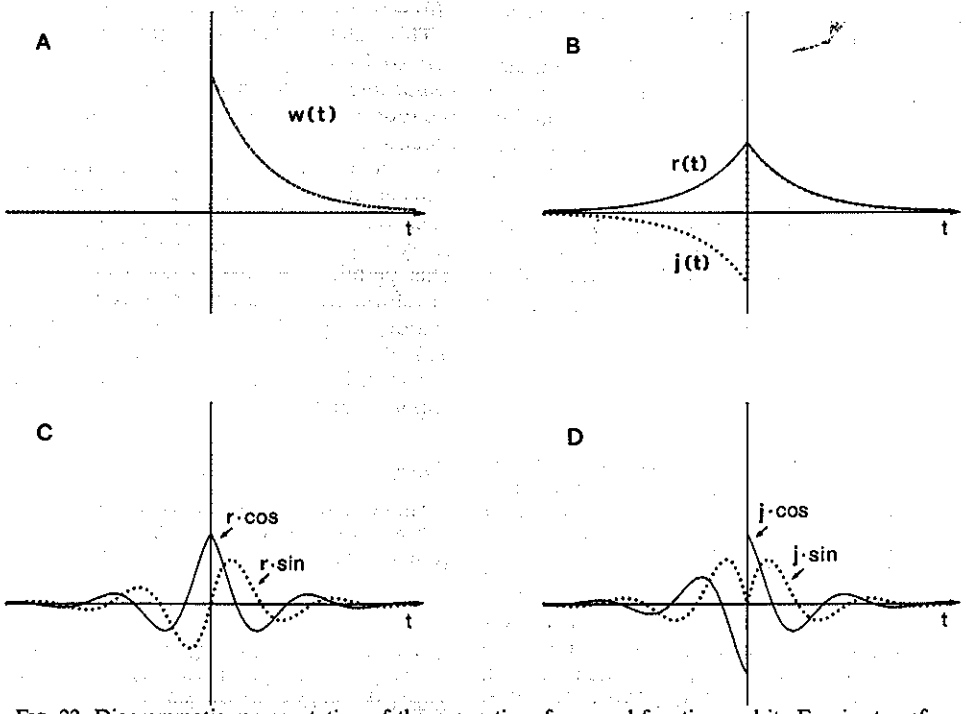

FIG. 22. Diagrammatic representation of the properties of a causal function and its Fourier transform. The causal function $w(t)$ is represented in panel A. The symmetrical function $r(t)$ (solid line) and the antisymmetrical function $j(t)$ (dotted line) are represented in panel B; note that their sum yields $w(t)$. Panel C shows the products $r(t) \cdot \cos 2\pi ft$ (solid line) and $r(t) \cdot \sin 2\pi ft$ (dotted line). The areas under these curves represent the real and imaginary part, respectively, of the Fourier transform of $r(t)$; note that the area under $r(t) \cdot \sin 2\pi ft$ is zero as this function is antisymmetric, so yielding a zero imaginary part for the Fourier transform of $r(t)$. Panel D shows the product $j(t) \cdot \cos 2\pi ft$ (solid line) and $j(t) \cdot \sin 2\pi ft$ (dotted line); note that in this case the *real* part of the transform is zero, as the area under the solid line is zero.

$\tau > t$. Therefore, if $t < 0$, either $\tau < 0$ or $\tau > t$, and the integral in Eqn 57 is null, i.e. $t \cdot \phi(t) = 0$, and $\phi(t) = 0$. Thus $\phi(t)$ is also causal. But $\phi(t)$ transforms to log $W(f)$, and the imaginary part of its transform, imag[log $W(f)$] = the phase of $W(f)$, can be deduced from its real part, real[log $W(f)$] = the logarithm of the module of $W(f)$, by convolving with $1/(\pi fi)$.

This permits the complete reconstruction of $w(t)$ from the power spectrum (square module of $W(f)$). This procedure was used by Wong and Knight (1980) to deduce the shot waveform, $w(t)$, in photoreceptor noise from the power spectrum: the phase of the transform was derived from its module (=square root of the power spectrum, $G(f) = \langle r \rangle \cdot |W(f)|^2$, a part from a constant factor $\langle r \rangle$, see Sections 5.1 and 8.4), by taking the logarithm and deducing its imaginary part (=phase of $W(f)$) from the real part (=log $|W(f)|$).

Instead of convolving with $1/(\pi fi)$, as in Eqn 55, they used a "time domain" approach (Peterson and Knight, 1973) based on the principles used above to derive Eqn 55 (Fig. 22). The inverse Fourier transform of log[$|W(f)|$] = real[log $W(f)$] is symmetrical. Multiplication by sign(t) (i.e. inversion of the function of $t < 0$) yields an antisymmetrical function whose Fourier transform is imag[log $W(f)$] = Phase[$W(f)$]. The conditions that $W(f) = 1/A(f)$ is never zero (and therefore log $W(f)$ is meaningful), $w(t)$ is causal and the inverse Fourier transform of log[$W(f)$] is also causal, define $w(t)$ as a "minimum phase" function.

This same approach was used by Rossi and colleagues (1989) in dealing with postsynaptic noise at the labyrinthine cyto–neural junction.

The conditions discussed here may not be necessary for $w(t)$ to be causal and "minimum phase" (this problem is of little interest here); however, it is sufficient that $w(t)$ be a function of time which can be produced as the output of a stable physical filter in response to an impulsive input, to endow $w(t)$ with the properties of causality and minimum phase.

The autoregressive approach permits an alternative computation of $w(t)$, as the autoregressive weights, $\alpha(t)$, can be computed directly from the autocorrelation, or autocovariance, of the output of the system in response to white noise input (e.g. a Poisson point process). This procedure, based on Yule–Walker's equation (see e.g. Kay and Marple, 1981), is particularly efficient when few values of $\alpha(t)$ are sufficient to describe $w(t)$ in autoregressive terms. For example, for a low-pass resistance–capacitance network (RC-filter), $w(t) = e^{-t/RC}/RC$, and $w(t) = w(t-\tau) \cdot e^{-\tau/RC}$, i.e. a single autoregressive coefficient, $\alpha(\tau) = e^{-\tau/RC}$ and $\alpha(t \neq \tau) = 0$, is sufficient to describe the filter. In these cases, where $w(t)$ is a low order autoregressive function, this approach has the advantage that an analytical function with few parameters is obtained to fully describe $w(t)$, and in general this function will be smoother than fits obtained either with the Kramers–Kronig method (see above), with its impressive computational burden, or with the more tractable method of Wong and Knight (1980) described above.

Acknowledgement—I thank Mrs Serenella Avogadro for her skilful and patient work in typing the manuscript.

REFERENCES

ADAMS, P. R. (1977) Voltage jump analysis of procaine action at frog endplate. *J. Physiol.* **268,** 291–318.

ADAMS, P. R. and SAKMANN, B. (1978) Decamethonium both opens and blocks endplate channels. *Proc. natn. Acad. Sci. U.S.A.* **75,** 2994–2998.

ADAMS, W. B. (1976) Upper and lower bounds on the non-linearity of summation of end-plate potentials. *J. theor. Biol.* **63,** 217–224.

ADOLPH, A. (1964) Spontaneous slow potential fluctuation in the *Limulus* photoreceptor. *J. gen. Physiol.* **48,** 297–322.

ANDERSON, C. F. and STEVENS, C. F. (1973) Voltage clamp analysis of acetylcholine produced end-plate current fluctuations at frog neuromuscular junction. *J. Physiol.* **235,** 655–691.

ANDERSON, C. F., CULL-CANDY, S. G. and MILEDI, R. (1976) Glutamate and quisqualate noise in voltage-clamped locust muscle fibres. *Nature* **261,** 151–153.

AUERBACH, A. and SACHS, F. (1983) Flickering of a nicotinic ion channel to a subconductance state. *Biophys. J.* **42,** 1–10.

BARTON, S. B. and COHEN, I. S. (1977) Are transmitter statistics meaningful? *Nature* **268,** 267–268.

BENDAT, J. S. and PIERSOL, A. G. (1971) *Random Data: Analysis and Measurement.* 471 pp. John Wiley & Sons: New York.

BENHAM, C. D. and TSIEN, R. W. (1987) A novel receptor-operated calcium-permeable channel activated by ATP in smooth muscle. *Nature* **328,** 275–278.

BETZ, W. J. (1970) Depression of transmitter release at the neuromuscular junction of the frog. *J. Physiol.* **206,** 629–644.

BHATNAGAR, S. P. and MACINTOSH, F. C. (1960) Acetylcholine content of striated muscle. *Proc. Can. Fedn Biol. Sci.* **3,** 12–13.

BIRKS, R., HUXLEY, H. E. and KATZ, B. (1960) The fine structure of the neuromuscular junction in frog. *J. Physiol.* **150,** 134–144.

BLANKS, R. H. I. and PRECHT, W. (1976) Functional characterization of primary vestibular afferents in the frog. *Expl Brain Res.* **25,** 369–390.

BORSELLINO, A. and FUORTES, M. G. (1968) Responses to single photons in visual cells of *Limulus*. *J. Physiol.* **196,** 507–539.

BOYD, I. A. and MARTIN, A. R. (1956) The end-plate potential in mammalian muscle. *J. Physiol.* **132,** 74–91.

BROWN, T. H., PERKEL, D. H. and FELDMAN, M. W. (1976) Evoked neurotransmitter release: statistical effects of nonuniformity and nonstationarity. *Proc. natn. Acad. Sci. U.S.A.* **73,** 2913–2917.

CAMPBELL, N. (1909) The study of discontinuous phenomena. *Proc. Camb. phil. Soc.* **15,** 117–136.

CECCARELLI, B. and HURLBUT, W. P. (1980a) The vesicle hypothesis of the release of quanta of acetylcholine. *Physiol. Rev.* **60,** 396–441.

CECCARELLI, B. and HURLBUT, W. P. (1980b) Ca^{2+}-Dependent recycling of synaptic vesicles at the frog neuromuscular junction. *J. Cell Biol.* **87,** 297–303.

CECCARELLI, B., HURLBUT, W. P. and MAURO, A. (1972) Depletion of vesicles from frog neuromuscular junctions by prolonged tetanic stimulation. *J. Cell Biol.* **54,** 30–38.

CECCARELLI, B., HURLBUT, W. P. and MAURO, A. (1973) Turnover of transmitter and synaptic vesicles at the frog neuromuscular junction. *J. Cell Biol.* **57,** 499–524.

CECCARELLI, B., FESCE, R., GROHOVAZ, F. and HAIMANN, C. (1988a) The effect of potassium on exocytosis of transmitter at the frog neuromuscular junction. *J. Physiol.* **401,** 163–183.

CECCARELLI, B., HURLBUT, W. P. and IEZZI, N. (1988b) Effect of alpha-Latrotoxin on the frog neuromuscular junction at low temperature. *J. Physiol.* **402,** 195–217.

CHANGEUX, J. P., GIRAUDAT, J. and DENNIS, M. (1987) The nicotinic acetylcholine receptor: molecular architecture of a ligand-regulated ion channel. *Trends Pharmac. Sci.* **8,** 459–465.

CHRISTENSEN, B. N. and MARTIN, A. R. (1970) Estimates of probability of transmitter release at the mammalian neuromuscular junction. *J. Physiol.* **210,** 933–945.

CLEMENTI, F., GOTTI, C. and SHER, E. (Eds) (1988) *Nicotinic Acetylcholine Receptors in the Nervous System,* NATO ASI Series Vol. H25. Springer-Verlag: Berlin.

COHEN, I. and VAN DER KLOOT, W. (1985) Calcium and transmitter release. *Int. Rev. Neurobiol.* **27,** 299–336.

COHEN, I., KITA, H. and VAN DER KLOOT, W. (1973) The intervals between miniature endplate potentials in the frog are unlikely to be independent or exponentially distributed. *J. Physiol.* **236,** 327–339.

COLQUHOUN, D. and HAWKES, A. G. (1977) Relaxation and fluctuations of membrane currents that flow through drug-operated channels. *Proc. R. Soc. Lond. B* **199,** 231–262.

COLQUHOUN, D. and HAWKES, A. G. (1981) On the stochastic properties of single ion channels. *Proc. R. Soc. Lond. B* **211,** 205–235.

COLQUHOUN, D. and OGDEN, D. C. (1986) States of the nicotinic acetylcholine receptor: enumeration, characteristics and structure. In: *Nicotinic Acetylcholine Receptor. Structure and Function,* NATO ASI Series Vol.H3, pp. 197–218. Ed. A. MAELICKE. Springer-Verlag: Berlin.

COLQUHOUN, D. and SAKMANN, B. (1981) Fluctuations in the microsecond time range of the current through single acetylcholine receptor ion channels. *Nature* **294,** 464–466.

COLQUHOUN, D. and SAKMANN, B. (1985) Fast events in single-channel currents activated by acetylcholine and its analogues at the frog muscle end-plate. *J. Physiol.* **369,** 501–557.

COLQUHOUN, D., DIONNE, V. E., STEINBACH, J. H. and STEVENS, C. F. (1975) Conductance of channels opened by acetylcholine-like drugs in muscle endplate. *Nature* **253,** 204–206.

COLQUHOUN, D., LARGE, W. A. and RANG, H. P. (1977) An analysis of the action of a false transmitter at the neuromuscular junction. *J. Physiol.* **266,** 361–395.

COLQUHOUN, D., OGDEN, D. and MATHIE, A. (1987) Nicotinic acetylcholine receptors of nerve and muscle: functional aspects. *Trends Pharmac. Sci.* **8,** 465–472.

CONNOR, E. A. and PARSONS, R. L. (1983) Analysis of fast excitatory postsynaptic currents in bullfrog. *J. Neurosci.* **3,** 2164–2171.

CONTI, F. and WANKE, E. (1975) Channel noise in nerve membranes and lipid bilayers. *Q. Rev. Biophys.* **8,** 451–506.

CONTI, F., NEUMCKE, B., NONNER, W. and STÄMPFLI, R. (1980) Conductance fluctuations from the inactivation process of sodium channels in myelinated nerve fibres. *J. Physiol.* **308,** 217–239.

CONTI, F., HILLE, B. and NONNER, W. (1984) Non-stationary fluctuations of the potassium conductance at the node of Ranvier of the frog. *J. Physiol.* **353,** 199–230.

CORREIA, M. J., LANDOLT, J. P., MI, M. D., EDEN, A. R. and RAE, J. L. (1977) A species comparison of linear and nonlinear transfer characteristics of primary afferents innervating the semicircular canal. In: *The Vestibular System: Function and Morphology,* pp. 280–316. Ed. T. GUALTIEROTTI. Springer Verlag: New York.

COURTNEY, K. R. (1978) Extended moment analysis for binomial parameters of transmitter release. *J. theor. Biol.* **73,** 285–292.

COUTEAUX, R. and PÉCOT-DÉCHAVASSINE, M. (1970) Vésicles synaptiques et poches au niveau des zones actives de la jonction neuromusculaire. *C. r. Acad. Sci.* **D271,** 2346–2349.

CRAWFORD, A. C. and MCBURNEY, R. N. (1976) On the elementary conductance event produced by L-glutamate and quanta of the natural transmitter at the neuromuscular junction of *Maia squinado*. *J. Physiol.* **258,** 105–225.

CULL-CANDY, S. G. (1986) Miniature and evoked inhibitory junctional currents and gamma-aminobutyric acid-activated current noise in locust muscle fibres. *J. Physiol.* **374,** 179–200.

DE FELICE, L. J. (1977) Fluctuation analysis in neurobiology. *Int. Rev. Neurobiol.* **20,** 169–208.

DEKHUIJZEN, A. J., IEZZI, N. and HURLBUT, W. P. (1989) A re-examination of the effects of lanthanum on the frog neuromuscular junction. *Pflügers Arch.* **414,** 683–689.

DEL CASTILLO, J. and KATZ, B. (1954a) The effect of magnesium on the activity of motor nerve endings. *J. Physiol.* **124,** 553–559.

DEL CASTILLO, J. and KATZ, B. (1954b) Quantal components of the endplate potential. *J. Physiol.* **124,** 560–573.

DEL CASTILLO, J. and KATZ, B. (1954c) The membrane change produced by the neuromuscular transmitter. *J. Physiol.* **125,** 546–565.

DEL CASTILLO, J. and KATZ, B. (1956) Localization of active spots within the neuromuscular junction of the frog. *J. Physiol.* **132,** 630–649.

DEL CASTILLO, J. and PUMPLIN, D. W. (1975) Discrete and discontinuous action of brown widow spider venom on the presynaptic nerve terminals of frog muscle. *J. Physiol.* **252,** 491–508.

DERKACH, V. A., SELYANKO, A. A. and SKOK, V. I. (1983) Acetylcholine-induced current fluctuations and fast excitatory post-synaptic currents in rabbit sympathetic neurones. *J. Physiol.* **336,** 511–526.

DERKACH, V., SURPRENANT, A. and NORTH, R. A. (1989) 5-HT_3 receptors are membrane ion channels. *Nature* **339,** 706–709.

DE ROBERTIS, E. D. P. and BENNET, H. S. (1954) Submicroscopic vesicular component in the synapse. *Fedn Proc.* **13,** 35.

DIONNE, V. E. and RUFF, R. L. (1977) Endplate current fluctuations reveal only one channel type at frog neuromuscular junction. *Nature* **266,** 163–265.

DODGE, F. A., KNIGHT, B. W. and TOYODA, J. (1968) Voltage noise in *Limulus* visual cells. *Science* **160,** 88–90.

DODGE, F. A. JR and RAHAMIMOFF, R. (1967) Cooperative action of Ca ions in the transmitter release at the neuromuscular junction. *J. Physiol.* **193,** 419–432.

DREYER, F., WALTHER, C. and PEPER, K. (1976) Junctional and extra-junctional acetylcholine receptors in normal and denervated frog muscle fibres: noise analysis experiments with different agonists. *Pflügers Arch.* **366,** 1–9.

DUDEL, J. and KUFFLER, S. W. (1961) The quantal nature of transmission and spontaneous miniature potentials at the crayfish neuromuscular junction. *J. Physiol.* **155,** 514–529.

DUDEL, J., FINGER, W. and STETTMEIER, H. (1980) Inhibitory synaptic channels activated by gamma-aminobutyric acid (GABA) in crayfish muscle. *Pflügers Arch.* **387,** 143–151.

EDWARDS, C., DOLEZAL, V., TUCEK, S., ZEMKOVA, H. and VYSKOCYL, F. (1985) Is an acetylcholine transport system responsible for nonquantal release of acetylcholine at the rodent myoneural junction? *Proc. natn. Acad. Sci. U.S.A.* **82,** 3514–3518.

EDWARDS, F. A., KONNERTH, A., SAKMANN, B. and TAKAHASHI, T. (1989) A thin slice preparation for patch clamp recordings from neurones of the mammalian central nervous system. *Pflügers Arch.* **414,** 600–612.

ELMQVIST, D. and QUASTEL, D. M. J. (1965) A quantitative study of end-plate potentials in isolated human muscle. *J. Physiol.* **178,** 505–529.

FATT, P. and KATZ, B. (1950) Some observations on biological noise. *Nature* **166,** 597–598.

FATT, P. and KATZ, B. (1951) An analysis of the end-plate potential recorded with an intracellular electrode. *J. Physiol.* **115,** 320–370.

FATT, P. and KATZ, B. (1952) Spontaneous subthreshold activity at motor nerve endings. *J. Physiol.* **117,** 109–128.

FESCE, R., SEGAL, J. R. and HURLBUT, W. P. (1986a) Fluctuation analysis of nonideal shot noise. Application to the neuromuscular junction. *J. gen. Physiol.* **88,** 25–58.

FESCE, R., SEGAL, J. R., CECCARELLI, B. and HURLBUT, W. P. (1986b) Effect of black widow spider venom and Ca on quantal secretion at the frog neuromuscular junction. *J. gen. Physiol.* **88,** 59–81.

FINGER, W. (1983) Effects of glycine on the crayfish neuromuscular junction. II. Release of inhibitory transmitter activated by glycine. *Pflügers Arch.* **397,** 128–134.

FINGER, W. (1985) Excitatory transmitter release induced by high concentrations of gamma-aminobutyric acid (GABA) in crayfish neuromuscular junctions. *Pflügers Arch.* **405,** 265–273.

FINGER, W. and MARTIN, C. (1987) Differential effect of intraterminal sodium on spontaneous quantal release of transmitter in two neuromuscular junctions of crayfish. *Neurosci. Lett.* **75,** 293–298.

FINGER, W. and MARTIN, C. (1988) Effect of lithium on veratridine-induced quantal and non-quantal release from inhibitory nerve terminals in crayfish muscle. *Pflügers Arch.* **411,** 362–364.

FINGER, W. and STETTMEIER, H. (1981) Analysis of miniature spontaneous inhibitory postsynaptic currents (sIPSCs) from current noise in crayfish opener muscle. *Pflügers Arch.* **392,** 157–162.

FLETCHER, P. and FORRESTER, T. (1975) The effect of curare on the release of acetylcholine from mammalian motor nerve terminals and an estimate of quantum content. *J. Physiol.* **251,** 131–144.

FUORTES, M. G. F. and YEANDLE, S. (1964) Probability of occurrence of discrete potential waves in the eye of *Limulus*. *J. gen. Physiol.* **47,** 443–463.

GIBB, A. J. and MARSHALL, I. G. (1984) Pre- and post-junctional effects of tubocurarine and other nicotinic antagonists during repetitive stimulation in the rat. *J. Physiol.* **351,** 275–297.

GINSBORG, B. L. and JENKINSON, D. H. (1976) Transmission of impulses from nerve to muscle. In: *Neuromuscular Junction. Handbook of Experimental Pharmacology*, **42,** pp. 229–364. Ed. E. ZAIMIS. Springer-Verlag: Berlin.

GORIO, A., HURLBUT, W. P. and CECCARELLI, B. (1978) Acetylcholine compartments in mouse diaphragm: a comparison of the effects of black widow spider venom, electrical stimulation and high concentrations of potassium. *J. Cell Biol.* **78,** 716–733.

GRZYWACZ, N. M., HILLMAN, P. and KNIGHT, B. W. (1988) The quantal source of area supralinearity of flash responses in *Limulus* photoreceptors. *J. gen. Physiol.* **91,** 659–684.

HAIMANN, C., TORRI-TARELLI, F., FESCE, R. and CECCARELLI, B. (1985) Measurement of quantal secretion induced by ouabain and its correlation with depletion of synaptic vesicles. *J. Cell Biol.* **101,** 1953–1965.

HARDIE, R. C. (1989) A histamine-activated chloride channel involved in neurotransmission at a photoreceptor synapse. *Nature* **339,** 704–706.

HATT, H. and SMITH, D. O. (1976) Non-uniform probabilities of quantal release at the crayfish neuromuscular junction. *J. Physiol.* **259,** 395–404.

HEBB, C. O., KRNJEVIĆ, K. and SILVER, A. (1964) Acetylcholine and cholinacetyltransferase in the diaphragm of the rat. *J. Physiol.* **171,** 504–513.

HEIDEN, D. (1969) Power spectrum of stochastic pulse sequences with correlation between the pulse parameters. *Phys. Rev.* **188,** 319–326.

HEUSER, J. E. and MILEDI, R. (1971) Effect of lanthanum ions on function and structure of frog neuromuscular junction. *Proc. R. Soc. Lond. B* **179,** 247–260.

HEUSER, J. E. and REESE, T. S. (1973) Evidence for recycling of synaptic vesicle membrane during transmitter release at the frog neuromuscular junction. *J. Cell Biol.* **57,** 315–344.

HEUSER, J. E., REESE, T. S., DENNIS, M., JAN, Y., JAN, L. and EVANS, L. (1979) Synaptic vesicle exocytosis captured by quick-freezing and correlated with quantal transmitter release. *J. Cell Biol.* **81,** 275–300.

HILLE, B. (1984) *Ionic Channels of Excitable Membranes.* 426 pp. Sinauer: Sunderland, MA.

HUBBARD, J. I. (1973) Microphysiology of vertebrate neuromuscular transmission. *Physiol. Rev.* **53,** 674–723.

HUDSPETH, A. J. and COREY, D. P. (1977) Sensitivity, polarity and conductance change in the response of vertebrate hair cells to controlled mechanical stimuli. *Proc. natn. Acad. Sci. U.S.A.* **74,** 2407–2411.

HUDSPETH, A. J. and LEWIS, R. S. (1988) Kinetic analysis of voltage- and ion-dependent conductances in saccular hair cells of the bull-frog. *Rana catesbeiana. J. Physiol.* **400,** 237–274.

HURLBUT, W. P. and CECCARELLI, C. (1979) The use of black widow spider venom to study the release of neurotransmitter. *Adv. Cytopharmac.* **3,** 87–115.

HURLBUT, W. P., IEZZI, N., FESCE, R. and CECCARELLI, B. (1990) Correlation between quantal secretion and vesicle loss at the frog neuromuscular junction. *J. Physiol.*, **425,** 501–526.

ISRAEL, M., GAUTRON, I. and LESBATS, B. (1970) Fractionnement de l'organe electrique de la Torpille: localisation subcellulaire de l'acetylcholine. *J. Neurochem.* **17,** 1441–1450.

KARLIN, A., KAO, P. N. and DI PAOLA, M. (1986) Molecular pharmacology of the nicotinic acetylcholine receptor. *Trends Pharmac. Sci.* **7,** 304.

KATZ, B. (1962) The transmission of impulses from nerve to muscle, and the subcellular unit of synaptic action. *Proc. R. Soc. Lond. B* **155,** 455–477.

KATZ, B. (1966) *Nerve, Muscle and Synapse.* McGraw-Hill: New York.

KATZ, B. (1969) *The Release of Neural Transmitter Substances.* University Press: Liverpool.

KATZ, B. and MILEDI, R. (1963) A study of spontaneous miniature potentials in spinal motoneurones. *J. Physiol.* **168,** 389–422.

KATZ, B. and MILEDI, R. (1965) The effect of calcium on acetylcholine release from motor nerve terminals. *Proc. R. Soc. Lond. B* **161,** 496–503.

KATZ, B. and MILEDI, R. (1970) Membrane noise produced by acetylcholine. *Nature* **226,** 962–963.

KATZ, B. and MILEDI, R. (1972) The statistical nature of the acetylcholine potential and its molecular components. *J. Physiol.* **224,** 665–699.

KATZ, B. and MILEDI, R. (1973a) The characteristics of "end-plate" noise produced by different depolarizing drugs. *J. Physiol.* **230,** 707–717.

KATZ, B. and MILEDI, R. (1973b) The binding of acetylcholine to the receptors and its removal from the synaptic cleft. *J. Physiol.* **231,** 549–574.

KATZ, B. and MILEDI, R. (1977) Transmitter leakage from motor nerve endings. *Proc. R. Soc. Lond. B* **196,** 59–72.

KATZ, B. and MILEDI, R. (1978) A re-examination of curare action at the motor endplate. *Proc. R. Soc. Lond. B* **203,** 114–133.

KAY, S. M. and MARPLE, S. L. JR (1981) Spectrum analysis—A modern perspective. *Proc. IEEE* **69,** 1380–1419.

KORN, H. and FABER, D. S. (1987) Regulation and significance of probabilistic release mechanisms at central synapses. In: *Synaptic Function*, pp. 57–108. Eds. G. M. EDELMAN, W. E. GALL and W. M. COWAN. John Wiley & Sons: New York.

KRNJEVIĆ, K. (1974) Chemical nature of synaptic transmission in vertebrates. *Physiol. Rev.* **54,** 418–540.

KUFFLER, S. W. and YOSHIKAMI, D. (1975) The number of transmitter molecules in a quantum: an estimate from

iontophoretic application of acetylcholine at the neuromuscular synapse. *J. Physiol.* **240,** 465–482.

KUNO, M. (1964) Quantal components of excitatory synaptic potentials in spinal motoneurones. *J. Physiol.* **175,** 81–99.

KUNO, M. (1971) Quantum aspects of central and ganglionic synaptic transmission in vertebrates. *Physiol. Rev.* **51,** 647–672.

LANGOSCH, D., THOMAS, L. and BETZ, H. (1988) Conserved quaternary structure of ligand-gated ion channels: the postsynaptic glycine receptor is a pentamer. *Proc. natn. Acad. Sci. U.S.A.* **85,** 7394–7398.

LILEY, A. W. (1956a) An investigation of spontaneous activity at the neuromuscular junction of the rat. *J. Physiol.* **132,** 650–666.

LILEY, A. W. (1956b) Quantal components of the mammalian endplate potential. *J. Physiol.* **133,** 561–587.

LILEY, A. W. and NORTH, K. A. K. (1953) An electrical investigation of effects of repetitive stimulation on mammalian neuromuscular junction. *J. Neurophysiol.* **16,** 509–527.

LONGENECKER, H. B., HURLBUT, W. P., MAURO, A. and CLARK, A. W. (1970) Effects of black widow spider venom on the frog neuromuscular junction. *Nature* **225,** 701–705.

MADSEN, B. W. and EDESON, R. O. (1988) Nicotinic receptors and the elusive beta. *Trends Pharmac. Sci.* **9,** 315–316.

MAELICKE, A. (Ed.) (1986) *Nicotinic Acetylcholine Receptor. Structure and Function*, NATO ASI Series Vol. H3. Springer-Verlag: Berlin.

MAGLEBY, K. L. (1979) Facilitation, augmentation and potentiation of transmitter release. In: *The Cholinergic Synapse*. Progr. Br. Res. **49,** 175–182. Ed. S. TUCEK. Elsevier: Amsterdam.

MAGLEBY, K. L. and STEVENS, C. F. (1972a) The effect of voltage on the time course of end-plate currents. *J. Physiol.* **223,** 151–171.

MAGLEBY, K. L. and STEVENS, C. F. (1972b) A quantitative description of end-plate currents. *J. Physiol.* **223,** 173–197.

MAGLEBY, K. L. and TERRAR, D. (1975) Factors affecting the time course of decay of endplate currents: a possible cooperative action of acetylcholine on receptors at the frog neuromuscular junction. *J. Physiol.* **244,** 467–495.

MALLART, A. and MARTIN, A. R. (1967) An analysis of facilitation of transmitter release at the neuromuscular junction of the frog. *J. Physiol.* **193,** 679–694.

MALLART, A. and MOLGO, J. (1978) The effects of pH and curare on the time course of endplate currents at the neuromuscular junction of the frog. *J. Physiol.* **276,** 343–352.

MARTIN, A. R. (1955) A further study of the statistical composition of the endplate potential. *J. Physiol.* **130,** 114–122.

MARTIN, A. R. (1966) Quantal nature of synaptic transmission. *Physiol. Rev.* **46,** 51–66.

MARTIN, A. R. (1976) The effect of membrane capacitance on non-linear summation of synaptic potentials. *J. theor. Biol.* **59,** 179–187.

MARTIN, C. and FINGER, W. (1985) Tonic depolarization of excitatory nerve terminals in crayfish muscle by high concentrations of extracellular potassium. *Neurosci. Lett.* **53,** 309–314.

MARTIN, C. and FINGER, W. (1988) Veratridine-induced high-frequency asynchronous release of inhibitory transmitter quanta in crayfish nerve–muscle synapses superfused with normal and low-calcium saline. *Pflügers Arch.* **411,** 469–477.

MCLACHLAN, E. M. (1975) An analysis of the release of acetylcholine from preganglionic nerve terminals. *J. Physiol.* **245,** 447–466.

MCLACHLAN, E. M. (1978) The statistics of transmitter release at chemical synapses. *Int. Rev. Physiol. Neurophysiol. III* **17,** 49–117.

MCLACHLAN, E. M. and MARTIN, A. R. (1981) Non-linear summation of end-plate potentials in the frog and mouse. *J. Physiol.* **311,** 307–324.

MILEDI, R., MOLENAAR, P. C. and POLAK, R. L. (1982) Free and bound acetylcholine in frog muscle. *J. Physiol.* **333,** 189–199.

MILNE, R. K., EDESON, R. O. and MADSEN, B. W. (1986) Stochastic modelling of a single ion channel: interdependence of burst length and number of openings per burst. *Proc. R. Soc. Lond B* **227,** 83–102.

MISHINA, M., TAKAI, T., IMOTO, K., NODA, M., TAKAHASHI, T. and NUMA, S. (1986) Molecular distinction between fetal and adult forms of muscle acetylcholine receptor. *Nature* **321,** 406–411.

MITCHELL, J. F. and SILVER, A. (1963) The spontaneous release of acetylcholine from the denervated hemidiaphragm of the rat. *J. Physiol.* **165,** 117–129.

MIYAMOTO, M. D. (1986) Probability of quantal transmitter release from nerve terminals: theoretical considerations in the determination of spatial variation. *J. theor. Biol.* **123,** 289–304.

MOLENAAR, P. C. and OEN, B. S. (1988) Analysis of quantal acetylcholine noise at end-plate of frog muscle during rapid transmitter secretion. *J. Physiol.* **400,** 335–348.

NAKAJIMA, Y. and REESE, T. S. (1983) Inhibitory and excitatory synapses in crayfish receptor organs studied with direct rapid-freezing substitution. *J. comp. Neurol.* **213,** 66–73.

NEHER, E. and SAKMANN, B. (1976a) Single-channel currents recorded from membrane of denervated frog muscle fibres. *Nature* **260,** 799–802.

NEHER, E. and SAKMANN, B. (1976b) Noise analysis of drug induced voltage clamp currents in denervated frog muscle fibres. *J. Physiol.* **258,** 705–729.

NEHER, E. and STEINBACH, J. H. (1978) Local anesthetics transiently block currents through single ACh-receptor channels. *J. Physiol.* **277,** 153–176.

NEHER, E. and STEVENS, C. F. (1977) Conductance fluctuation and ionic pores in membranes. *A. Rev. Biophys. Bioengng* **6,** 345–381.

OLSEN, R. W., BUREAU, M., RANSOM, R. W., DEND, L., DILBER, A., SMITH, G., KRESTCHATISKY, M. and TOBIN, A. J. (1988) The GABA receptor–chloride ion channel protein complex. *Adv. exp. med. Biol.* **236,** 1–14.

OTSUKA, M., IVERSEN, L. L., HALL, Z. W. and KRAVITZ, E. A. (1966) Release of gamma-aminobutyric acid from inhibitory nerves of lobster. *Proc. natn. Acad. Sci. U.S.A.* **56,** 1110–1115.

PARNAS, H. and SEGEL, L. A. (1989) Facilitation as a tool to study the entry of calcium and the mechanism of neurotransmitter release. *Prog. Neurobiol.* **32,** 1–9.

PATON, W. D. M. and ZEIMIS, E. (1952) The methonium compounds. *Pharmac. Rev.* **4,** 219–253.

PEPER, K., DREYER, F., SANDRI, C., AKERT, K. and MOOR, H. (1974) Structure and ultrastructure of the frog motor endplate. A freeze-etching study. *Cell Tissue Res.* **149,** 437–455.

PERKEL, D. H. and FELDMAN, M. W. (1979) Neurotransmitter release statistics: moment estimates for inhomogeneous Bernoulli trials. *J. math. Biol.* **7,** 31–40.

PETERSON, C. W. and KNIGHT, B. W. (1973) Causality calculations in the time domain: An efficient alternative to the Kramers–Kronig method. *J. opt. Soc. Am.* **63,** 1238–1242.

RICE, S. O. (1944) Mathematical analysis of random noise. *Bell Syst. Tech. J.* **23,** 282–332. (Reprinted in *Noise and Stochastic Processes*. Ed. N. WAX. Dover, New York, 1954.)

ROSSI, M. L., VALLI, P. and CASELLA, C. (1977) Post-synaptic potentials recorded from afferent nerve fibres of the posterior semicircular canal in the frog. *Brain Res.* **135,** 67–75.

ROSSI, M. L., BONIFAZZI, C., MARTINI, M. and FESCE, R. (1989) Static and dynamic properties of synaptic trans-

mission at the cyto–neural junction of frog labyrinth posterior canal. *J. gen. Physiol.* **94,** 303–327.

RUFF, R. L. (1977) A quantitative analysis of local anesthetic alteration of miniature endplate currents and endplate current fluctuations. *J. Physiol.* **264,** 89–124.

RUFF, R. L. (1986) Ionic channels: II. Voltage and agonist-gated and agonist-modified channel properties and structure. *Muscle and Nerve* **9,** 767–786.

RUSHTON, W. A. H. (1961) The intensity factor in vision. In: *Light and Life*, pp. 706–722. Eds. W. D. MCELROY and H. B. GLASS. Johns Hopkins University Press: Baltimore.

SACCHI, O. and PERRI, V. (1971) Quantal release of acetylcholine from the nerve endings of the guinea-pig superior cervical ganglion. *Pflügers. Arch.* **329,** 207–219.

SAKMANN, B. and BRENNER, H. R. (1978) Change in synaptic channel gating during neuromuscular development. *Nature* **276,** 401–402.

SAKMANN, B., PATLAK, J. and NEHER, E. (1980) Single acetylcholine-activated channels show burst-kinetics in presence of desensitizing concentrations of agonist. *Nature* **286,** 71–73.

SAKMANN, B., METHFESSEL, C., MISHINA, M., TAKAHASHI, T., TAKAI, T., KURASAKI, M., FUKUDA, K. and NUMA, S. (1985) Role of acetylcholine receptor subunits in gating the channel. *Nature* **318,** 538–543.

SALPETER, M. M. and ELDEFRAWI, M. E. (1973) Sizes of endplate compartments, densities of acetylcholine receptor and other quantitative aspects of neuromuscular transmission. *J. Histochem. Cytochem.* **21,** 769–778.

SCHICK, K. L. (1974) Power spectra of pulse sequences and implications for membrane fluctuations. *Acta biotheor.* **23,** 1–17.

SCHOFIELD, P. R., DARLISON, M. G., FUJITA, N., BURT, D. R., STEPHENSON, F. A., RODRIGUEZ, H., RHEE, L. M., RAMARCHANDRAN, J., REALE, V. and GLENCORSE, T. A. (1987) Sequence and functional expression of the $GABA_A$ receptor shows a ligand-gated receptor superfamily. *Nature* **328,** 221–227.

SCHUETZE, S. M. and ROLE, L. W. (1987) Developmental regulation of nicotinic acetylcholine receptors. *A. Rev. Neurosci.* **10,** 403–457.

SCHWARTZ, R. D. (1988) The $GABA_A$ receptor-gated ion channel: biochemical and pharmacological studies of structure and function. *Biochem. Pharmac.* **37,** 3369–3375.

SEGAL, J. R., CECCARELLI, B., FESCE, R. and HURLBUT, W. P. (1985) Miniature endplate potential frequency and amplitude determined by an extension of Campbell's theorem. *Biophys. J.* **47,** 183–202.

SIEGHART, W. (1989) Multiplicity of $GABA_A$-benzodiazepine receptors. *Trends Pharmac. Sci.* **10,** 407–411.

SIGWORTH, F. J. (1980) The variance of sodium current fluctuations at the node of Ranvier. *J. Physiol.* **307,** 97–129.

SIGWORTH, F. J. (1981a) Covariance of nonstationary sodium current fluctuations of the node of Ranvier. *Biophys. J.* **34,** 111–133.

SIGWORTH, F. J. (1981b) Interpreting power spectra from nonstationary membrane current fluctuations. *Biophys. J.* **35,** 289–300.

SILINSKY, E. M. (1985) The biophysical pharmacology of calcium-dependent acetylcholine secretion. *Pharmac. Rev.* **37,** 81–132.

SIMONNEAU, J., TAUC, L. and BAUX, G. (1980) Quantal release of acetylcholine examined by current fluctuation analysis of an identified neuro-neuronal synapse of *Aplysia*. *Proc. natn. Acad. Sci. U.S.A.* **77,** 1661–1665.

STEINHAUSEN, A. (1931) Über den Nachweis der Bewegung der Cupula in der intakten Bogengaengsampulle des Labyrinths bei der natuerlichen rotatorischen and calorischen Reizug. *Pflügers Arch.* **228,** 322–328.

STEPHENSON, F. A. (1987) Progress towards the understanding of the $GABA_A$ receptor structure. *J. Recept. Res.* **7,** 43–54.

STEVENS, C. F. (1976) A comment on Martin's relation. *Biophys. J.* **16,** 891–895.

TAGLIETTI, V., ROSSI, M. L. and CASELLA, C. (1977) Adaptive distortions in the generator potential of semicircular canal sensory afferents. *Brain Res.* **123,** 41–57.

TAKEUCHI, A. and TAKEUCHI, N. (1960) On the permeability of end-plate membrane during the action of transmitter. *J. Physiol.* **154,** 52–67.

TAKEUCHI, A., ONODERA, K. and KAWAGOE, R. (1980) Release of endogenous glutamate from the nueromuscular junction of the crayfish. *Proc. Jap. Acad.* **56,** 246–249.

TAUC, L. (1967) Transmission in invertebrate and vertebrate ganglia. *Physiol. Rev.* **47,** 521–593.

THIES, R. E. (1965) Neuromuscular depression and apparent depletion of transmitter in mammalian muscle. *J. Neurophysiol.* **28,** 427–442.

TORRI-TARELLI, F., HAIMANN, C. and CECCARELLI, B. (1987) Coated vesicles and pits during enhanced quantal release of acetylcholine at the neuromuscular junction. *J. Neurocytol.* **16,** 205–214.

VALTORTA, F., JAHN, R., FESCE, R., GREENGARD, P. and CECCARELLI, B. (1988) Synaptophysin (p38) at the frog neuromuscular junction: its incorporation into the axolemma and recycling after intense quantal secretion. *J. Cell Biol.* **107,** 2717–2727.

VERE-JONES, D. (1966) Simple stochastic models for the release of quanta of transmitter from a nerve terminal. *Aust. J. Stat.* **8,** 53–63.

VYSKOCIL, F., NIKOLSKY, E. and EDWARDS, C. (1983) An analysis of the mechanisms underlying the non-quantal release of acetylcholine at the mouse neuromuscular junction. *Neuroscience* **9,** 429–435.

WALMSLEY, B., EDWARDS, F. R. and TRACEY, D. J. (1987) The probabilistic nature of synaptic transmission at a mammalian excitatory central synapse. *J. Neurosci.* **7,** 1037–1046.

WESSLER, I. (1989) Control of transmitter release from the motor nerve by presynaptic nicotinic and muscarinic autoreceptors. *Trends Pharmac. Sci.* **10,** 110–114.

WHITTAKER, V. P., ESSMAN, W. B. and DOWE, G. H. C. (1972) The isolation of pure cholinergic synaptic vesicles from the electric organs of elasmobranch fish of the family *Torpedinidae*. *Biochem. J.* **128,** 833–846.

WONG, F. and KNIGHT, B. W. (1980) Adapting-bump model for eccentric cells of *Limulus*. *J. gen. Physiol.* **76,** 539–557.

ZEIMIS, E. (1953) Motor endplate differences as a determining factor in the mode of action of neuromuscular blocking substances. *J. Physiol.* **122,** 238–251.

ZIMMERMAN, H. (1979) Commentary: vesicle recycling and transmitter release. *Neuroscience* **4,** 1773–1803.

ZUCKER, R. S. (1973) Changes in the statistics of transmitter release during facilitation. *J. Physiol.* **229,** 787–810.